N O T I C E

THIS DOCUMENT HAS BEEN REPRODUCED FROM
MICROFICHE. ALTHOUGH IT IS RECOGNIZED THAT
CERTAIN PORTIONS ARE ILLEGIBLE, IT IS BEING RELEASED
IN THE INTEREST OF MAKING AVAILABLE AS MUCH
INFORMATION AS POSSIBLE

ANALYTICAL METHODOLOGY FOR
DETERMINATION OF HELICOPTER IFR
PRECISION APPROACH REQUIREMENTS

Anil V. Phatak

Analytical Mechanics Associates, Inc.
Mountain View, California

July 1980

Prepared for:

Ames Research Center
National Aeronautics and Space Administration
Moffett Field, California

ANALYTICAL METHODOLOGY FOR

DETERMINATION OF HELICOPTER IFR

PRECISION APPROACH REQUIREMENTS

By

Anil V. Phatak

July 1980

Distribution of this report is provided in the interest of information
exchange. Responsibility for the contents resides
in the author or organization that prepared it.

Prepared under Contract No. NAS2-10291 by
ANALYTICAL MECHANICS ASSOCIATES, INC.
Mountain View, California

for

AMES RESEARCH CENTER
NATIONAL AERONAUTICS AND SPACE ADMINISTRATION
Moffett Field, California

PREFACE

Page intentionally left blank

ABSTRACT

A systematic analytical approach to the determination of helicopter IFR precision approach requirements is formulated. The approach is based upon the hypothesis that pilot acceptance level or opinion rating of a given system is inversely related to the degree of pilot involvement in the control task. A nonlinear simulation of the helicopter approach to landing task incorporating appropriate models for the UH-1H aircraft, the environmental disturbances and the human pilot was developed as a tool for evaluating the pilot acceptance hypothesis. The simulated pilot model is generic in nature and includes analytical representation of the human information acquisition, processing, and control strategies. Simulation analyses in the flight director mode indicate that the pilot model used is reasonable. Results of the simulation are used to identify candidate pilot workload metrics and to test the well known performance-workload relationship. A pilot acceptance analytical methodology is formulated as a basis for further investigation, development and validation.

Page intentionally left blank

TABLE OF CONTENTS

Page intentionally left blank

LIST OF FIGURES

INTRODUCTION

Background

It is safe to state that helicopter operations are expected to grow rapidly over the next two decades [1]. This optimistic forecast for expanded potential markets is predicated upon the assumption of an established capability for all-weather rotorcraft operations, and the ensuing advantages of reduced direct operating costs. However, at the present time, helicopters under Instrument Meterological conditions (IMC) are forced to operate as though they were a fixed-wing aircraft and must abide by the standard Instrument Flight Rules (IFR) regulations and weather minima. This approach does not give any credit to the helicopters most unique and distinguishing characteristic - its ability to make steep decelerating approaches to a hover and touchdown into confined landing sites. The pilot workload demand for a decelerated approach to a hover is extremely high or not acceptable because of the generally poor handling qualities of the basic helicopter in low speed flight. Consequently, some minimum level of control and display sophistication in the form of a stability and control augmentation system (SCAS) and/or flight director guidance is, essential for acceptable IMC precision decelerating approaches.

There are a number of factors which impact upon the pilot acceptance of a helicopter decelerating steep approach and landing (DSAL) task under IMC. Clearly, the most important, though obvious, factor is the severity of the weather conditions as prescribed by the slant visibility and cloud ceiling at the landing site. Typically, weather minimums are given in terms of the runway visual range (RVR) and decision height (DH) associated with the standard ILS approach trajectory. However, the helicopter is uniquely qualified to perform steep precision approaches with glide slope angles as high as 12 degrees. Hence, more realistic approach weather minimums, specifically tailored to helicopter IFR approaches to a hover over a prescribed landing area (as opposed to a runway), need to be defined.

Depending upon the flight path glideslope angle γ_{ref} and weather minima, some degree of deceleration under IMC conditions may prove necessary. For example, helicopter straight-in approaches to a helipad under IMC to a DH of 50 ft would provide a horizontal distance to the landing site of. approximately, 1000 ft for a 3° approach (DH/tan γ_{ref} for a γ_{ref} approach and decision height DH) in which to decelerate from breakout (IFR/VFR transition) speed to hover. Results of a flight investigation of visual approaches to a hover, conducted by NASA-LaRc [2], show that the pilot chooses to decelerate in two phases - 1) a slow deceleration, starting at a range of 3000 ft, from an initial groundspeed of 50, 80 or 100 knots to, approximately, 45 knots at a range of 1000 ft, followed by 2) a more rapid deceleration to a hover on the prescribed landing pad. No such data exists for the helicopter IFR approach to a hover task. However, the VFR flight test data does provide some indication of the close relationship between aircraft groundspeed and distance-to-go from the landing pad. Thus, the need for deceleration under IMC conditions would depend upon the glideslope angle of the approach profile and the prescribed decision height for IFR/VFR transition. Pilot acceptance would be contingent upon his being able to perform the landing task with satisfactory performance and within reasonable workload demands.

The objective of helicopter IFR operations is to try and reduce the weather minimums to as low a level as possible (zero visibility/zero ceiling). For given weather minimums and aircrew manning level, the acceptability of a helicopter for IFR approach to a landing pad would depend upon the quality or sophistication of the guidance, navigation, control, and display components of the overall system. At the present time, the acceptance of a given helicopter with its inherent dynamics, flight control system and display avionics is based upon subjective flight evaluation by the examining pilot on an individual basis. A pilot/ aircraft system is accepted for a given IFR approach scenario if it can meet prescribed performance standards while keeping crew pilot workload levels within reasonable bounds. Such an approach is intuitive in nature and provides little insight into the rationale for the examining pilots acceptance criteria. Therefore, there is a clear need to develop a

2

rigorous structured approach towards the evaluation and, if possible, specification of aircraft system requirements (i.e., crew, displays, flight control, navigation and guidance) for helicopter IFR precision approach and landing operations.

Objectives

The NASA Ames Research Center has initiated a long-term program aimed towards the development of a technology base for improved helicopter all-weather capability. A step in pursuit of this goal was to conduct systematic helicopter piloted simulation experiments for a precision decelerating approach to a hover for various levels of flight-control and display sophistication. The goal of these experiments (referred to as the single-pilot IFR or SPIFR simulation) was to provide an adequate data base for:

1. the experimental evaluation of minimum guidance, control, and display requirements for various weather minima; and

2. the formulation of a systematic analytical methodology directed towards the establishment of minimum guidance, control and display requirements for acceptable, single-pilot, helicopter precision landing approaches, under IMC.

A description of the SPIFR simulation including the analysis of the experimental data is given in reference 3. The objective of this research effort is to use data acquired in the previous fixed base simulation investigation of helicopter SPIFR requirements towards the formulation of an analytical methodology for determining pilot acceptance. The overall approach is discussed in the following paragraphs.

Technical Approach

The current state-of-the-art for assessing competing aircraft system configurations is fundamentally empirical. The level of acceptance or

3

satisfaction is usually expressed in terms of a pilot opinion rating (POR) scale [4,5] such as the Cooper-Harper handling qualities scale. For lack of a better alternative the POR approach is the most frequently used method for evaluating the relative merits of candidate aircraft system configurations.

The degree of pilot acceptance expressed as a pilot opinion rating depends upon a number of factors which can broadly be put into two categories - system performance and pilot workload. In axiomatic terms, a system A would be rated better than system B, if for a given acceptable level of system performance, system A requires less pilot workload than system B. Clearly, a tradeoff between the two attributes of system performance and pilot workload is involved in arriving at an aggregate measure such as an opinion rating of pilot acceptability.

Further quantification requires the development of analytical measures for system performance and pilot workload. This constitutes the fundamental step and stumbling block in the formulation of an analytical methodology for determining the level of pilot acceptance or opinion rating. The problem is complicated further by virtue of the fact that in most realistic conditions, system performance is a vector quantity and that pilot workload may also depend upon many individual factors. However, the system performance vector

$$s = (s_1, s_2, \ldots, s_n)^T \tag{1}$$

is relatively easier to quantify in terms of objective or physical attributes, given adequate knowledge and background of the particular phase of the piloting task. Thus, for a helicopter precision hover task, the system performance vector may be selected to be

$$s = (\sigma_x, \sigma_q, \sigma_y, \sigma_p, \sigma_z, \sigma_{\dot{z}}) \tag{2}$$

where σ_i represents the root mean squared (rms) deviation of variables $(x,q,y,p,z,\dot{z})$ from nominal, namely $(x_0,0,y_0,0,z_0,0)$. This representa-

4

tion for the system performance vector is not unique, and could include standard deviation of additional variables such as sideslip β and yaw rate r. Depending upon the task, the pilot must somehow combine the individual components of the system performance vector to formulate an aggregate scalar metric, J, for total system performance; thus

$$J = g(s) \tag{3}$$

The functional g is internal to the human pilot and must be inferred using systematic methods: for example - pilot questionnaire, multiattribute utility analysis, stepwise regression analysis and others. Typically, the functional g is chosen in an ad-hoc manner based upon subjective judgement and pilot comments, and has the additive structure:

$$J = \alpha_1 s_1 + \alpha_2 s_2 + \ . \ . \ + \alpha_n s_n \tag{4}$$

with the $\{\alpha_i\}$ specified by the analyst. Nevertheless, inspite of the arbitrariness of this procedure, it is conceivable in terms of physical attributes such as standard deviations of key variables and hence amenable to systematic analysis.

On the other hand, finding the elements of the vector workload metric and the manner in which they contribute to an aggregate measure or index for pilot workload is even less obvious. The term workload has various connotations in the human factors literature. Typically workload has been partitioned into three categories: (1) scanning or information acquisition workload, (2) central information processing or decision workload, and (3) motor or control workload. Three approaches have been presented in the literature for quantifying pilot-workload. They are (1) subjective opinion ratings, (2) reserve attention capacity as measured by secondary task performance, for fixed main task performance, and (3) physiological indicators such as galvanic skin resistance, pupil dilation, heart-rate, electroencephalogram (eeg) features and others. However, these techniques are not useful as analytical measures of workload. As a consequuence, techniques based on an analytical representation or model of the human pilot's information acquisition, processing and control strategy have been sought over the past three decades.

5

Model-based measures by definition assume that an input-output mathematical model for the pilots control strategy exists and can be determined. Given that a pilot model can be found, the following axioms are used implicitly in the formulation of workload metrics:

1) For a given task, it is hypothesized that there exists a nominal pilot strategy (for information acquisition, processing, and utilization) characterized by a nominal set of parameters which corresponds to minimum workload for a given acceptable level of performance,

2) Workload increases for deviation of the pilot's strategy from nominal or, in other words, with the deviation of the model parameter values from nominal, and

3) Workload is related to the sensitivity of the system performance to perturbations of the model parameters from nominal values.

Thus, analogous to the earlier discussion on system performance, pilot workload can be represented as a vector quantity

$$\theta = (\theta_1, \theta_2, \ldots, \theta_m)^T \tag{5}$$

where the components $\{\theta_i\}$ represent the parameters corresponding to the particular pilot strategy model parameterization. The aggregate scalar workload metric W is assumed to be some function of θ; thus,

$$W = h(\theta) \tag{6}$$

where $h(\theta)$ could be some linear or nonlinear function on θ.

Assuming that suitable scalar metrics for system performance J and pilot workload W have been developed, the pilot-opinion rating, R, can be formulated as

$$R = f(J,W) \tag{7}$$

6

As discussed earlier, some sort of tradeoff between performance J and work-load W is essential in evaluating the relative merits of competing system configurations and arriving at a preferance in terms of an opinion rating R. A plausible relationship between J, W and R is illustrated in Figure 1, where iso-rating curves are drawn on a J versus W plot. The figure shows three constant rating curves R_1, R_2, and R_3 corresponding to low (e.g., 3), medium (e.g., 5) and high (e.g., 7) pilot opinion ratings, respectively. Pilot workload is bounded by W_{max} on the high side and W_{min} representing minimum value or open loop control. Similarly the system performance has a minimum value J_{min} corresponding to maximum pilot workload levels and a maximum value that culminates with instability of the pilot aircraft closed-loop system and subsequent loss of control.
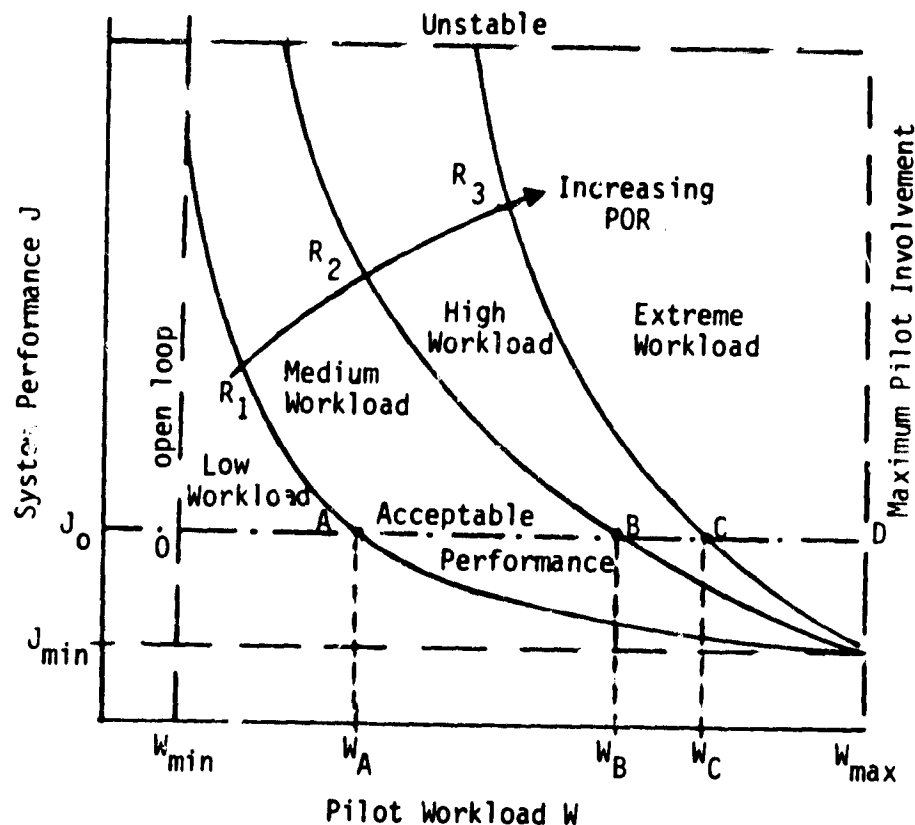
Figure 1. Performance - Workload Iso-Rating Contours - Illustrative Example

Thus 4 regions of pilot workload from low to extreme are obtained. For a given level of acceptable performance $J = J_o$, the horizontal line OABC defines different levels of pilot acceptance or option rating. Thus, if the three rating curves R_1, R_2, and R_3 correspond to three different aircraft configurations under evaluation then system 1 would be preferred over system 2 which in turn is chosen over system 3. Points A, B and C define the rating or preference level in terms of the workload levels W_A, W_b and W_C required to maintain the prescribed level of performance J_o. Figure 2 shows the plot of ratings versus pilot workload metric W for various constant levels of performance J.

Figure 2. Pilot Rating versus Pilot Workload
Iso-Performance Curves

8

For a given acceptable level of system performance J, the pilot opinion ratings may thus be obtained from Figure 2 as a function of the workload.

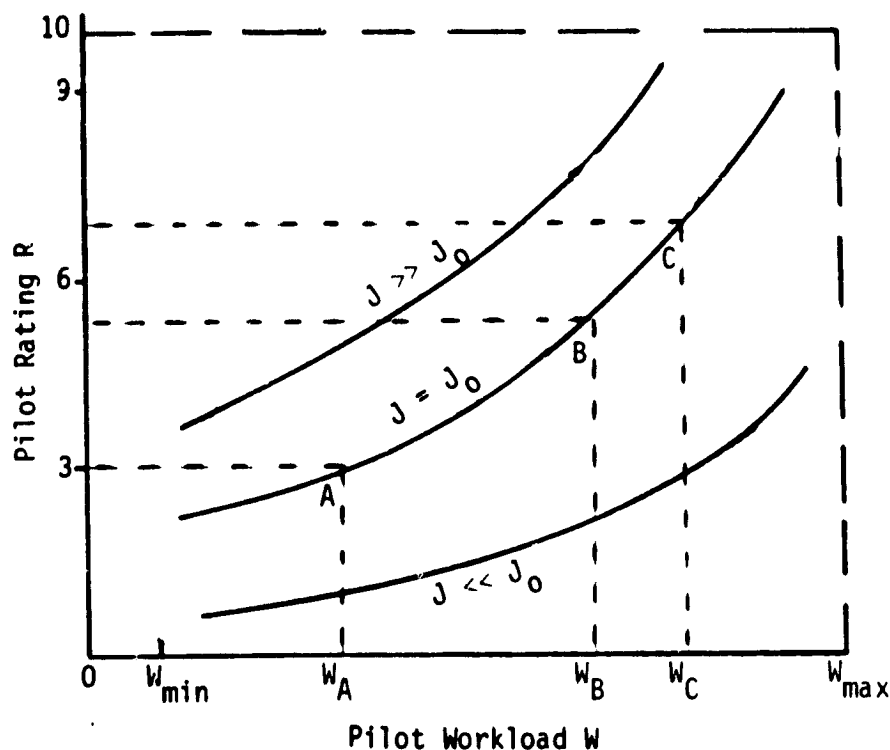A generic description of a systematic methodology for determining pilot acceptance level or rating for competing system configurations has been presented. Formulation of the above pilot acceptance analytical methodology is based upon one fundamental assumption - the existence of a suitable mathematical model describing the human pilot's information processing and control strategy and an acceptable parameterization of the system performance and pilot workload metrics.

Task Outline

The purpose of this research effort is to formulate an appropriate dynamic model for the pilot in the helicopter precision approach to hover task and evaluate the suitability of candidate model-based system performance and workload metrics using available SPIFR data. The ultimate goal is to use the analytical measures for system performance and pilot workload in formulating an assessment methodology for determining the level of pilot acceptance for any given system configuration.

The helicopter IFR approach to landing task is a complex piloting task requiring nonlinear and time varying control laws on behalf of the human pilot. Thus, the use of two existing UH-1H approach and landing simulation programs was stipulated at the beginning of this study. The two programs are: (1) a UH-1H nonlinear simulation of the approach and landing task, and (2) a generic linear time varying covariance propagation program useful for the propagation of helicopter approach path dispersions during the precision landing task.

The overall approach consists of four tasks, as follows:

9

Task 1. Automatic Mode Validation:

The objective of this task is to validate the approach performance predictions of the existing nonlinear simulation and linear time varying covariance propagation programs by comparison with ensemble statistics data for the automatic mode acquired from the SPIFR simulation.

Task 2. Manual Mode Validation:

The purpose of this task is to validate the two existing programs using SPIFR data for the manual flight director mode of operation. Representative pilot model structures are to be used in the flight director mode validation.   Configurations involving raw data are outside the scope of this preliminary effort.

Task 3. Evaluate Candidate Pilot Model Based Workload Metrics:

The purpose of this task is to identify via simulation the existence of any plausible metrics for pilot workload and their relationship to system performance and pilot opinion rating.

Task 4. Formulate Pilot Acceptance Analytical Methodology:

Here the experienced gained from Tasks 1 - 3 above is to be assimilated to propose a systematic analytical approach towards determining pilot acceptance levels or opinion ratings.

The above task delineation served the general purpose of providing a framework for this study effort. The approach followed this outline with some minor modifications dictated by the problems encountered during the course of this investigation.

PILOTED SIMULATION EXPERIMENTS

Facility Description

The SPIFR experiments were conducted on the NASA-Ames V/STOLAND fixed
base UH-1H simulator, shown in Figure 3, and involved the participation
of three pilots (2 NASA and 1 Army). Details on the V/STOLAND digital
avionics system may be obtained from reference 6. A six degree of freedom
mathematical model of a UH-1H helicopter [7] at a gross weight of 6158 lbs
was used to drive the real time simulation.

Figure 4   shows a schematic of the UH-1H simulator cockpit display
panel. The instruments are arranged in a standard "T" format except for
the CRT multifunction display which was not used in the simulation.   In
addition, engine power indicator instruments (torque-meter and dual tacho-
meter) and the inclinometer (turn and slip indicator) were not operational
during the experiments.
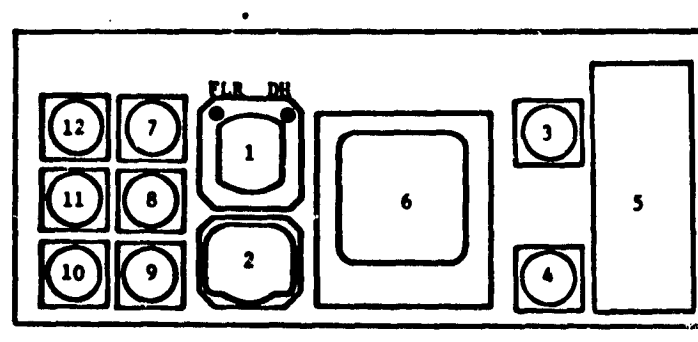
1. Attitude Director
   Indicator (ADI)

2. Horizontal Situation
   Indicator (HSI)

3. Barometric Altimeter

4. Radio Altimeter

5. Mode Select Panel

6. Multifunction
   Display (MFD)

7. True Airspeed

8. Barometric Altitude

9. Vertical Speed
   Indicator (IVSI)

10. Torquemeter

11. Dual Tachometer

12. Clock

FLR: Flare Annunicator - Green
DH :   Decision Height Annunicator - Amber

Figure 4.   V/STOLAND Cockpit Displays

11

Figure 3. NASA-Ames V/STOLAND UH-1H Simulator

12

The helicopter controls consisted of cyclic stick, collective stick and directional pedals. The controls travels are limited to $\pm$ 6.3 in for the longitudinal cyclic, $\pm$ 6.3 in for the lateral cyclic, $\pm$ 3.45 in for the pedals and 11 in for the collective lever. Adjustable friction on the collective lever and artificial force-feel characteristics for the cyclic stick and directional pedals are also provided.

Piloting Task

The pilots were instructed to follow the commanded flight path shown in Figure 5. The piloting task consisted of the following six phases: 1) localizer capture, 2) tracking at cruise altitude h_0 and constant speed V_0, 3) constant speed glide slope capture, 4) constant speed glide slope tracking until initiation of deceleration or flare at X_{FLR}, 5) IFR deceleration to velocity V_{DH}, at decision height, DH, and 6) VFR deceleration following breakout at DH to a hover 10 ft above the prescribed 125 ft diameter landing pad.
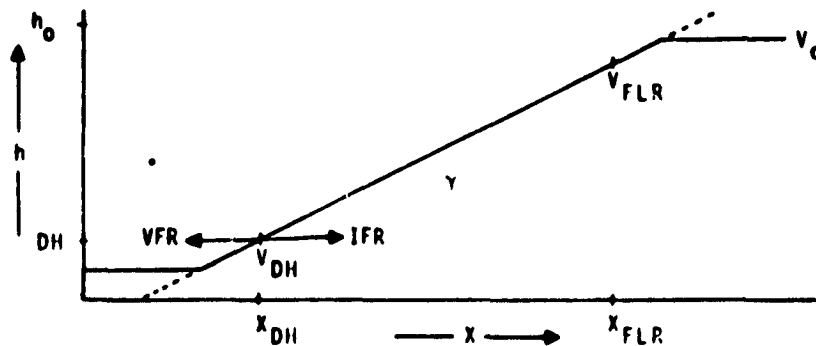

Figure 5. Flight Path Geometry

Constant attitude deceleration guidance [3,8] was used to compute the commanded velocity profile during the flare maneuver. Decision heights (DH) of 100 ft, 50 ft and 0 ft were flown. The aircraft velocity at decision height, V_{DH} was adjusted downward with decreasing decision height to 45 knots (76 ft/s), 31 knots (52 ft/s), and 0 knots corresponding to the three decision heights of 100 ft, 50 ft and 0 ft respectively. This downward adjustment of V_{DH} with reduced DH was necessary to allow for the shorter distance available for an acceptable visual deceleration profile.

A simplified Dryden wind model in each of the three aircraft body axes was used. A stationary model was selected through presimulation pilot comments since it is more amenable to analytical investigation as required in this study, and because of the pilot comments indicating no noticable differences between a non-stationary wind model and the chosen stationary representation.

Control and Display Configurations

Four control augmentation levels were simulated as follows:

1. Basic UH-1H with stabilizer bar (WSB)

2. UH-1H (WSB) with control stick steering (CSS)

3. UH-1H (WSB) with CSS and automatic collective axis

4. UH-1H (WSB) with CSS and fully automatic control system.

The Control Stick Steering (CSS) mode incorporates a first order attitude SCAS in pitch and roll axis, first order vertical velocity command control system (i.e., first order $\theta/\theta c$, $\phi/\phi c$ and $\dot{h}/\dot{h}c$ systems), and a fully automatic directional (or pedals) control system. The CSS mode with automatic collective leaves only the pitch and roll axes under the pilot's control. The 4 axes, fully automatic system commands the aircraft to fly down the prescribed trajectory of Figure 5 to a hover following a constant attitude deceleration profile (CADP).

14

Two display configurations were simulated: (1) a raw data (RD) mode where the pilot had to use the standard cockpit instruments in Figure 4 and (2) a 3-cue flight director (FD) mode for the pitch, roll and vertical axes. The pitch and roll flight director signals drive the standard horizontal and vertical bars on the attitude director indicator (ADI) shown in Figure 6, and are configured to provide a rate command/attitude hold system (i.e., k/s) between the pilots stick output and corresponding flight director display. The vertical flight director signal is displayed as a "fly-to" symbol (except for pilot number 2 who preferred an error command) on the left side of the ADI. Two discrete signals on the ADI (see Fig. 6) are provided to aid the pilot - a green light to indicate the initiation of deceleration or flare and an amber signal to display the occurence of IFR/VFR transition at decision height. In the raw data display mode the pilot must use the standard glide slope and localizer information for flight path tracking; IFR deceleration command is missing and the pilot must use the raw data on altitude (radio altimeter) and airspeed on cue from the green light to arrive at the desired velocity at decision height. Note that the absence of a ground speed or range rate indicator on the cockpit panel forces the pilot to use airspeed and subjective estimates of the wind turbulence for internally generating the deceleration velocity command.

Experimental Test Matrix

A total of 6 configurations corresponding to three levels of control augmentation and two types of displays were simulated. A fully automated system was also simulated to serve as a benchmark for evaluating competing piloted configurations and for validating the off-line UH-1H simulation programs

Details of the specific system configurations tested are given in Table 1. Approximately 12 runs per configuration were conducted to provide an adequate data base for statistical evaluation of the results and subsequent use in the formulation of a pilot acceptance analytical methodology.
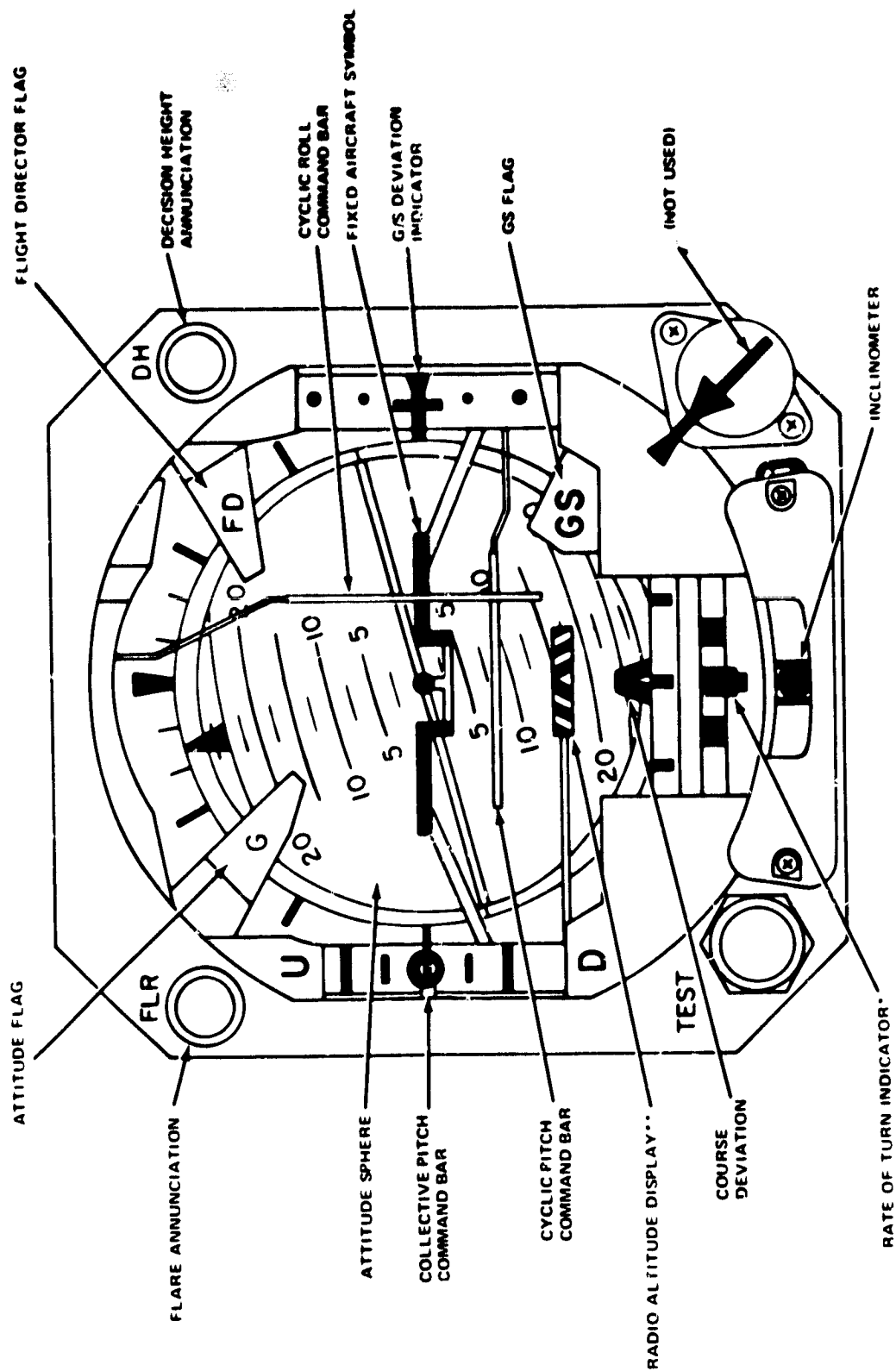
15

Figure 6. Attitude Director Indicator

16

Data Summary

Four types of data were obtained: (1) strip-chart recordings, (2)
line-printer data, (3) digital tape recordings (run dum), and (4) pilot
opinion ratings including responses to a questionnaire. 40 variables
were recorded on digital tape at a sampling period of 55 ms. Some of
the key variables include: aircraft attitude and angular velocities,
airspeed, groundspeed, altitude, sink rate, cross-track error and error-
rate, aircraft control positions, flight director commands, distance to
helipad and longitudinal and normal accelerations.

Cooper-harper ratings for the IFR portion alone, VFR portion alone
and the entire IFR/VFR task were obtained. In addition, pilot ratings
of the workload demands were also solicited. Details on the rating
scales used may be found in reference 3.

The raw data for the individual runs were used to generate ensemble
statistics (using time or distance to go as the independent variable) for
24 of the 40 recorded vraiables. These ensemble mean and standard devia-
tion data provide the data base for validating the off-line nonlinear
simulation and linear time-varying covariance propagation programs.

Table 1. SPIFR Experimental Matrix

Configuration / Pilot	Basic Helicopter (BH)				Control Stick Steering (CSS)							CSS Auto IFR/Man. VFR		
	Raw Data (RD)		Flt. Director (FD)		Raw Data (RD)				Flt. Director (FD)					
					Man. Coll. (MC)		Auto. Coll. (AC)		Man. Coll. (MC)		Auto. Coll. (AC)			
	DH100	DH50	DH100	DH50	DH100	DH50	DH100	DH50	DH50	DH0	DH50	DH100	DH50	DH0
1	12*	5	12	3	12	3	11	3	14	10	12	20	18	16
2	10	4	10	3	12	3	13	4	12	-	12	-	-	-
3	6	3	3	4	12	4	12	3	4	-	4	-	-	-

* Number of runs

18

VALIDATION OF UH-1H APPROACH AND
LANDING SIMULATION PROGRAMS

A first step in the pursuit of an analytical methodology for determining pilot acceptance is the development and validation of offline computer simulation programs capable of mimicking automatic as well as manual flight director approach and landing controls strategies and closed-loop pilot-aircraft system performance. The use of two existing UH-1H approach and landing simulation programs resident on the NASA-Ames IBM 360 computer was stipulated at the initiation of this research effort. They are:

1) A UH-1H nonlinear simulation program for the Monte-Carlo simulation of the approach and landing task - hereafter referred to as the Nonlinear Covariance Computation (NCC) program; and

2) a linear time varying simulation program for the propagation of approach path dispersions (i.e., mean and standard deviation) during the approach and landing task - hereafter called the Linear Time-Varying Covariance Progagation (LTVCP) program.

Therefore, the first two tasks in this study effort were to validate the approach performance prediction capability of the existing NCC and LTVCP simulation programs using data from the previously completed SPIFR experiments. The NCC program validation is discussed first followed by an analysis of the LTVCP program.

Nonlinear Covariance Computation (NCC)
Program Validation

Description. The NCC program provides a closed loop simulation of the UH-1H approach and landing task. The 6 degree of freedom aircraft equations of motion for the UH-1H as given in reference 7 are used to simulate the basic helicopter nonlinear dynamics and are incorporated into a larger and general IBM 360 program existing at NASA/Ames, called "UNCLE". Four

different control options are provided corresponding to:

1) Basic helicopter (WSB) with 3-cue flight director and raw
    data for the directional axis (BH/FD),

2) Basic helicopter (WSB) with CSS, 3 cue flight director and
    automatic directional axis (CSS/FD),

3) Basic helicopter with CSS, 2 cue flight director, and automatic
    vertical and directional axis (CSS/FD/AC),

4) Basic helicopter with CSS, 3 cue flight director and fully
    automated system (CSS/Auto).

The control stick steering configuration consists of pitch, roll and ver-
tical SCAS and an automated directional control system. Block diagrams
for the longitudinal, vertical, lateral and directional systems are
shown in Figures 7-10, respectively. Details on the design of the CSS
augmentation and flight director may be found in reference 3.

A velocity command, V_c, corresponding to the constant attitude de-
celeration profile is simulated to allow for decision heights of 100 ft,
50 ft and 0 ft respectively. The velocity command is generated by solving
an implicit algebraic equation between command velocity and distance to
go.

A Dryden model as shown in Figure 11 is used to simulate the three
orthogonal turbulence components u_g, v_g and w_g in aircraft body axes. A
root mean square value of 1.7 ft/s is used for each of the three wind gust
standard deviations. Mean winds or shears were not implemented in the off-
line program.

A plotting routine (PLOTTA/DISSPL) is used to allow plotting SPIFR
data from digital tape and NCC program outputs on the same page (e.g.,
Beta or UCC plots). This permits direct visual evaluation of the quality
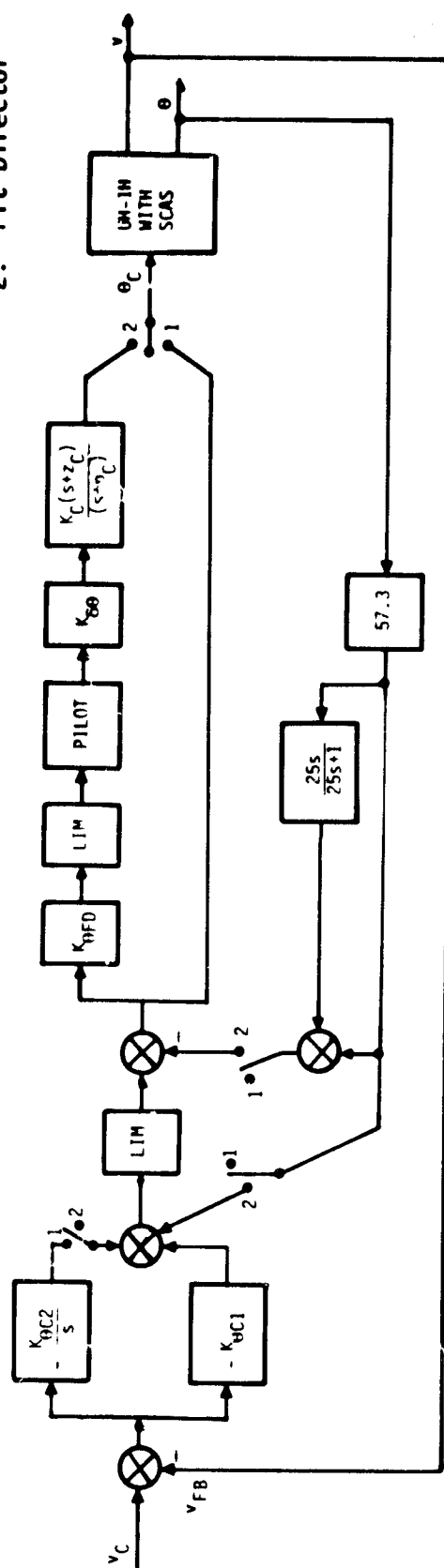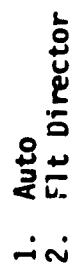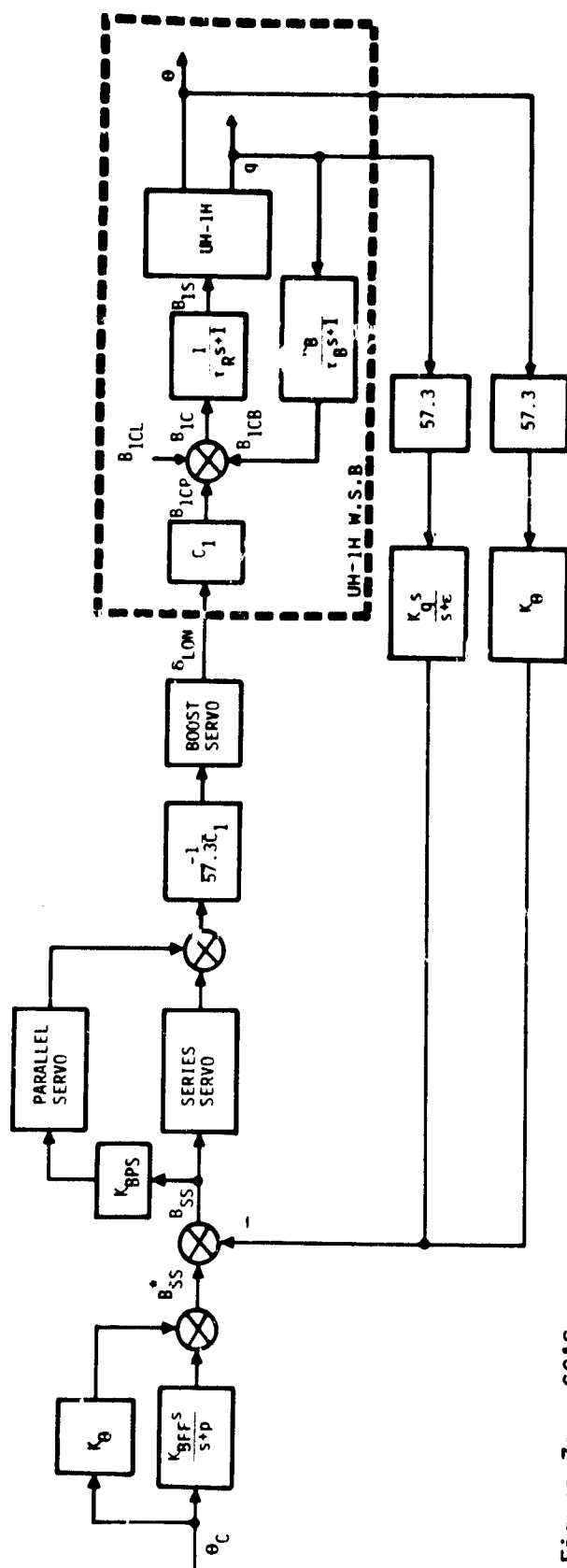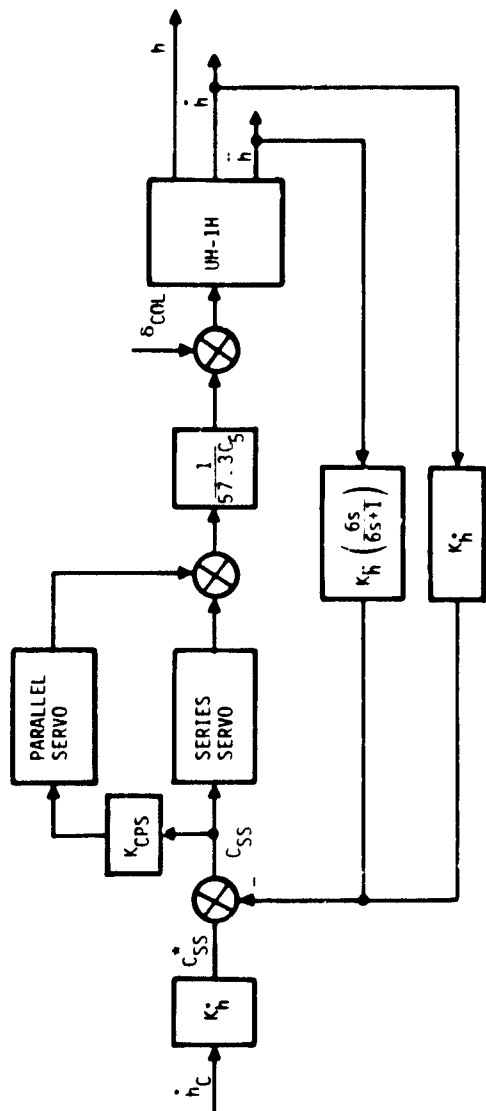of fit between NCC program outputs and piloted simulation data.

Figure 7a. SCAS

1. Auto
2. Flt Director

Figure 7b. Automatic and Flight Director Guidance

Figure 7. Longitudinal System

Figure 8a. SCAS
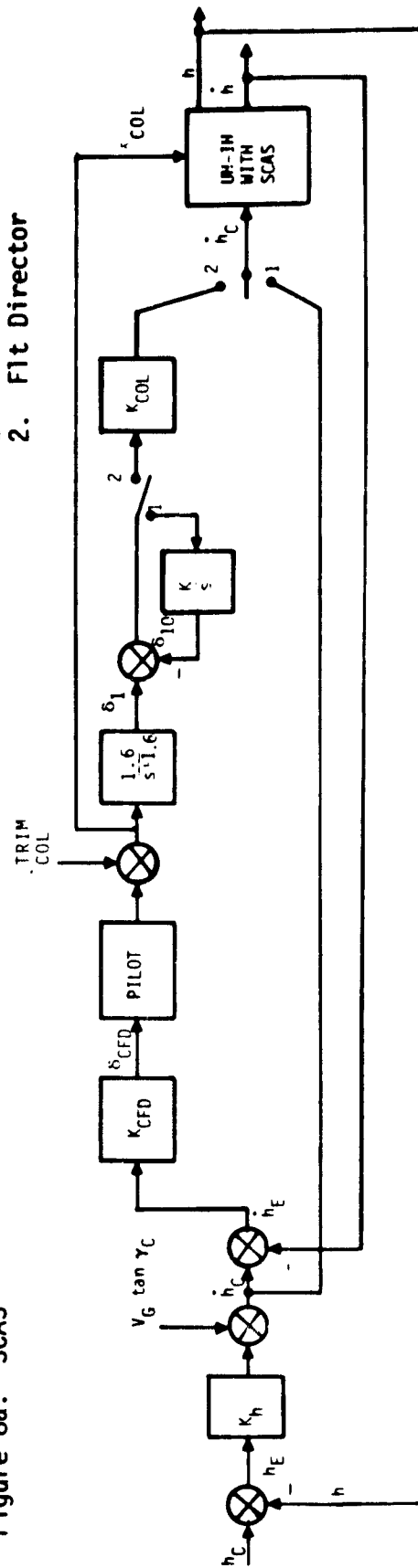
Figure 8b. Automatic and Flight Director Guidance

1. Auto
2. Flt Director

Figure 8. Vertical System
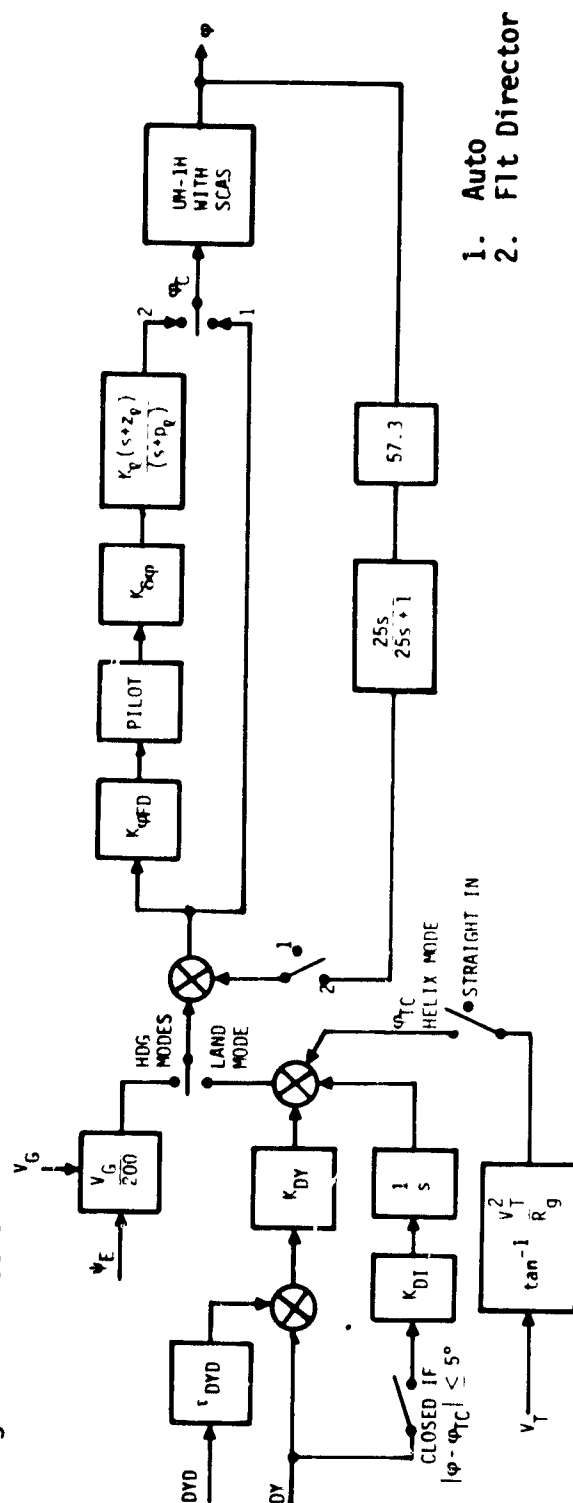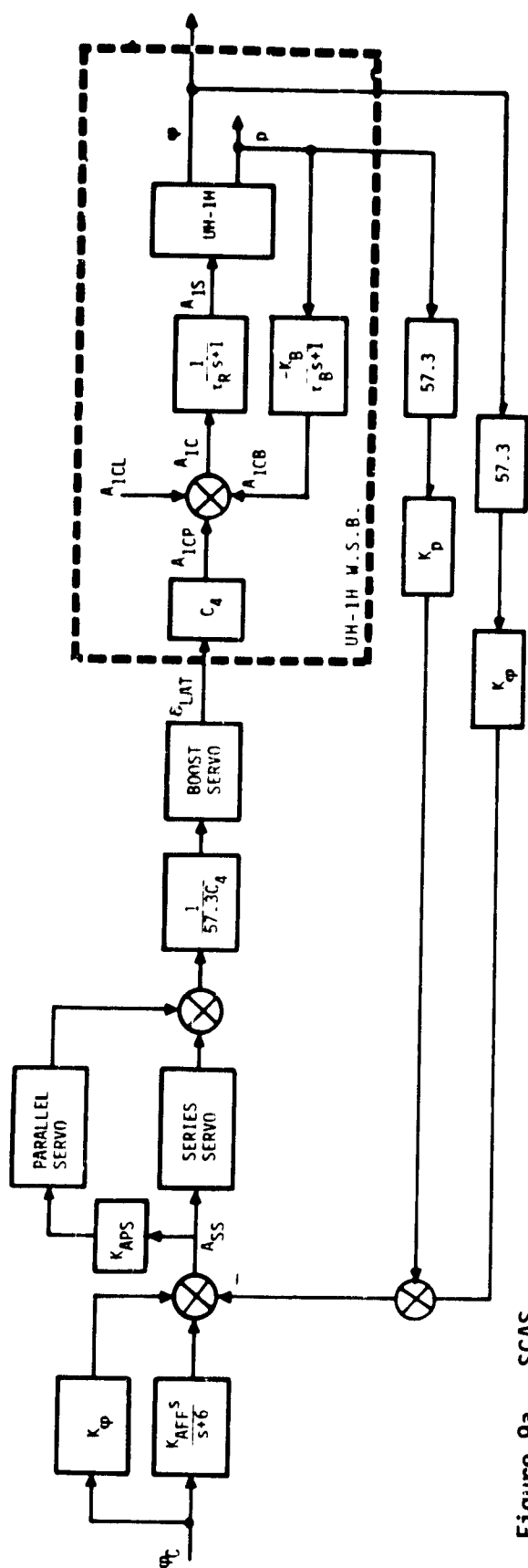
22

Figure 9a. SCAS

Figure 9b. Automatic and Flight Director Guidance

1. Auto
2. Flt Director

Figure 9. Lateral System
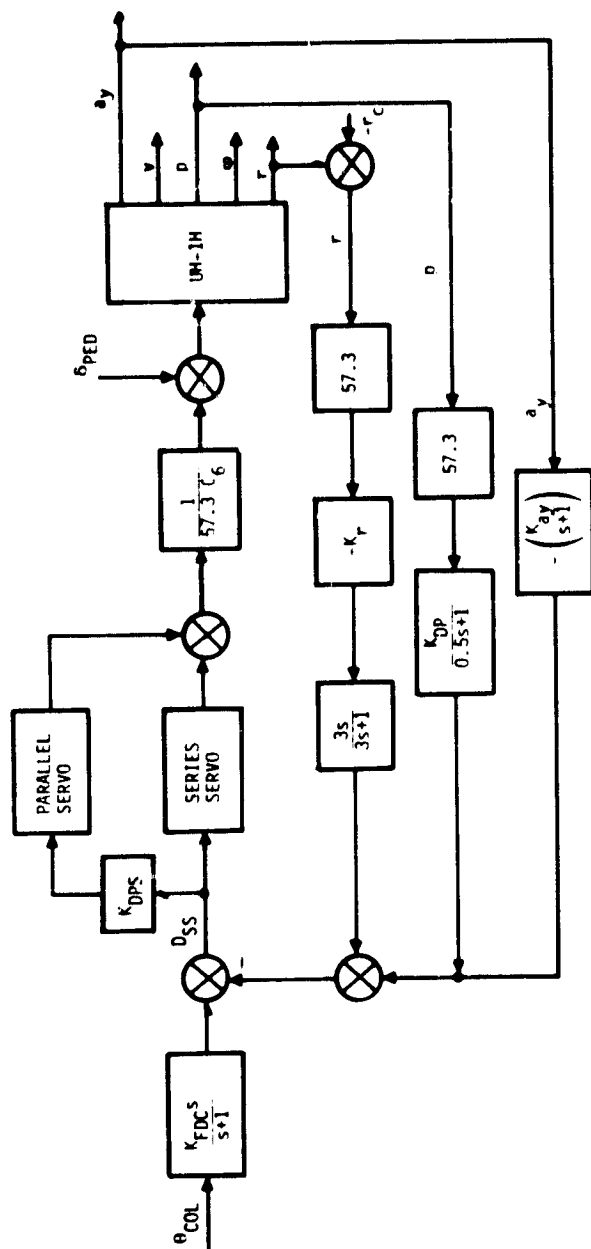
Figure 10a. SCAS: Turn Coordination Mode
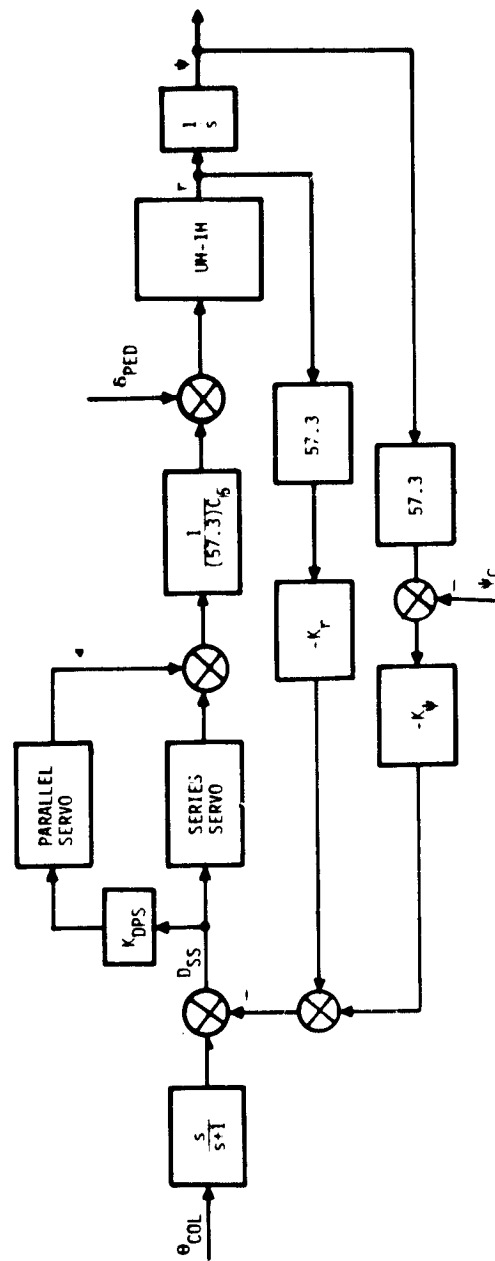
Figure 10b. SCAS: Heading Hold Mode

Figure 10. Directional System

24

$$\eta \cong \underline{N(0.1)} \longrightarrow \boxed{\frac{\sigma_x \sqrt{2\alpha_x}}{\alpha_x s + 1}} \longrightarrow x \ (u_g, v_g, w_g)$$

$$\alpha_x = \frac{L_x}{V} \ , \quad L_x = \text{scale length}$$

$$V = \text{airspeed}$$

$$\sigma_x = \text{R M S value of } x$$

$$\sigma_{u_g} = \sigma_{v_g} = \sigma_{w_g} = 1.7 \text{ ft/s}$$

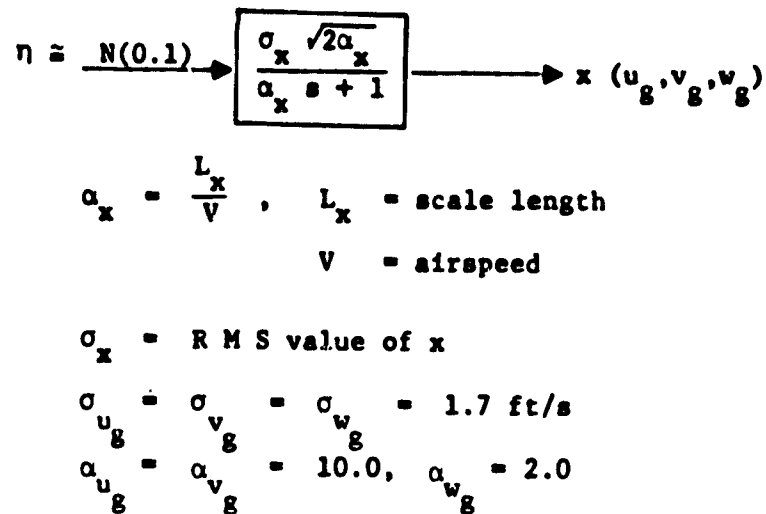$$\alpha_{u_g} = \alpha_{v_g} = 10.0, \quad \alpha_{w_g} = 2.0$$

Figure 11. Dryden Turbulence Models

Some of the above options were not available on the existing IBM 360 program and were added to make realistic comparison to experimental data feasible. The NCC program was then exercised to match experimental data in the automatic mode and the CSS/FD mode. A single-input/single-output describing function model of the form shown in Figure 12 was implemented in each of the three flight director axes. In this model, k is the pilot gain, -z is the zero, -p is the pole and τ is the effective time delay.

$$FD_i \longrightarrow \boxed{\frac{k \ (s + z)}{(s + p)} e^{-\tau s}} \longrightarrow u_i$$

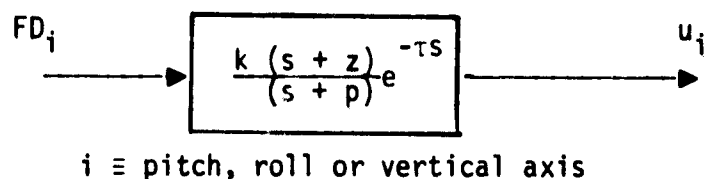$$i \equiv \text{pitch, roll or vertical axis}$$

Figure 12. Input/Output Describing Function Pilot Model

The selection of this simple model was merely for the purpose of initial verification of the flight director mode. More realistic representation of the pilot's decision making and control behavior would be essential in order to reproduce some of the finer details of human operator response data.

However, the existing NCC program has several problems associated with it; the most significant being the lack of adequate documentation for the UNCLE program that is used to represent the UH-1H nonlinear equations of motion. This made it very difficult to comprehend, analyze or modify overall NCC program operations. In addition, the program is inefficient for use in the Monte Carlo mode. For example, a single 120 s run using the NCC program on the IBM 360 takes, approximately, 170 CPU seconds (CSS/Auto mode) to complete at an integration step size DTP of 0.1 s. The flight director mode takes 10 ~ 20 per cent longer. An ensemble calculation using 10 runs would take approximately 30 minutes CPU time on the IBM 360. This amount of time is prohibitive for routine use. Two options were considered: (a) convert the existing UH-1H nonlinear simulation program (UNCLE version of the NCC) to the CDC 7600, or (b) start from scratch and develop a separate IBM 360 UH-1H nonlinear simulation program using only those parts of the UNCLE program that are useful for this study. The first option was not seriously entertained in view of the dearth of documentation on the existing UNCLE program and the inefficient nature of the overall code. Instead, it was decided to develop a separate NCC program on the IBM 360 computer using only those elements of the overall UNCLE program (i.e., the UH-1H equations of motion) that were needed for the intended simulation. This program was developed and response time history results are indistinguishable from the original NCC outputs. However, the new version takes 35 CPU seconds at a step size DTP or 0.1 s, for a single 120 s CSS/Auto run. This is at least five times more efficient than the original version of the NCC program for the IBM 360 computer. Additional cost savings may be obtained by conversion to the CDC 7600 computer.

Simulation Results

The new version of the NCC program was exercised for the CSS/Auto, CSS/FD and CSS/FD/AC configurations. Figures 13 - 14 show a comparison of the NCC program outputs (i.e., ensemble mean and standard deviation) with experimental data for the CSS/Auto/DH = 0 ft mode for the no wind (IWIND = 0) and wind (IWIND = 1) conditions. A total of 11 flight variables are displayed with standard nomenclature used to label each output. The following observations are worth noting:

1. The mean response comparisons show an excellent fit between the NCC program outputs and the SPIFR data.

26
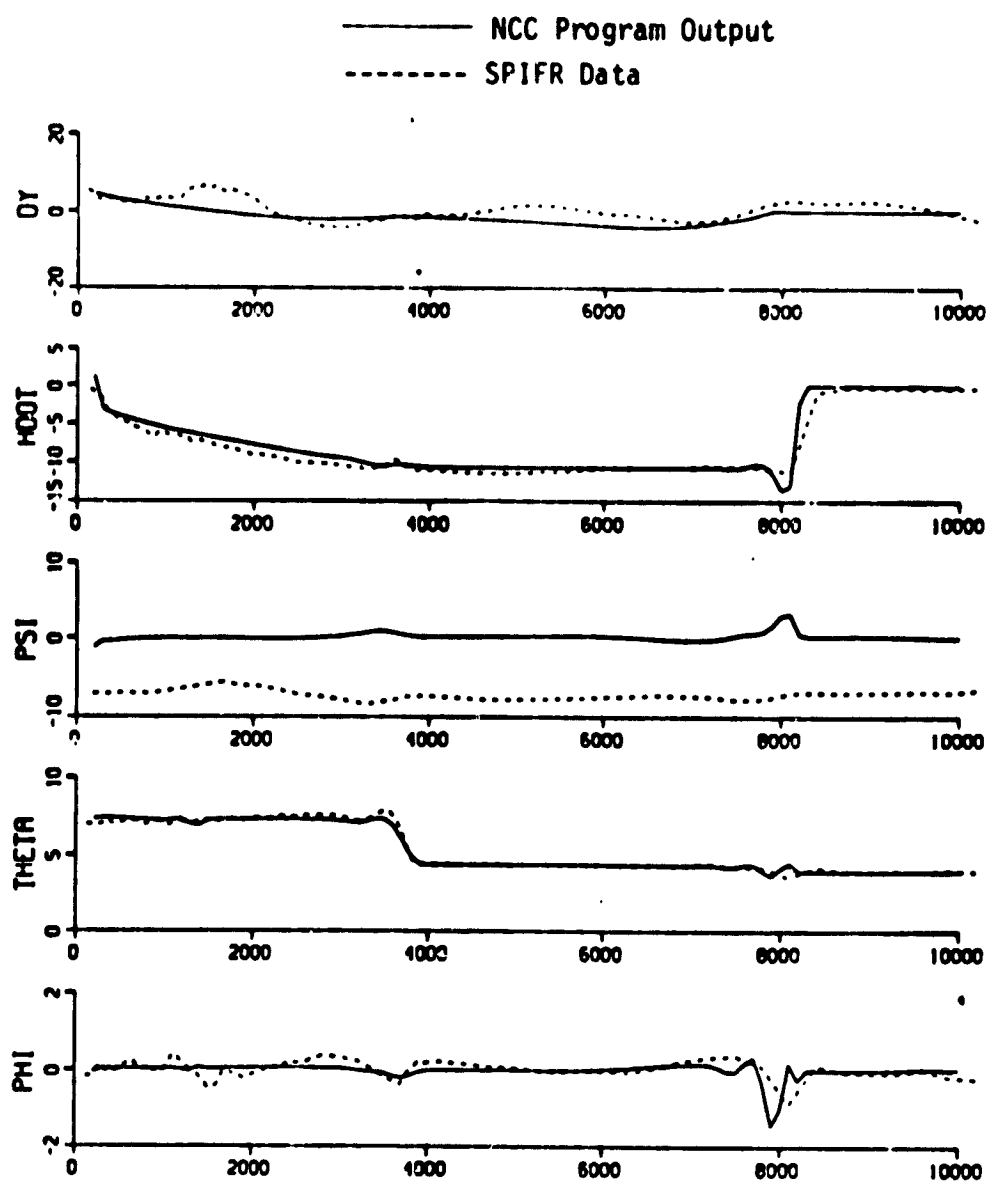
a.) Mean

Figure 13. NCC Program Simulation Results: CSS/AP/NO WIND/DH = 0 ft, 10 runs

27

Figure 13. NCC Program Simulation Results: CSS/AP/NO WIND/DH = 0 ft, 10 runs
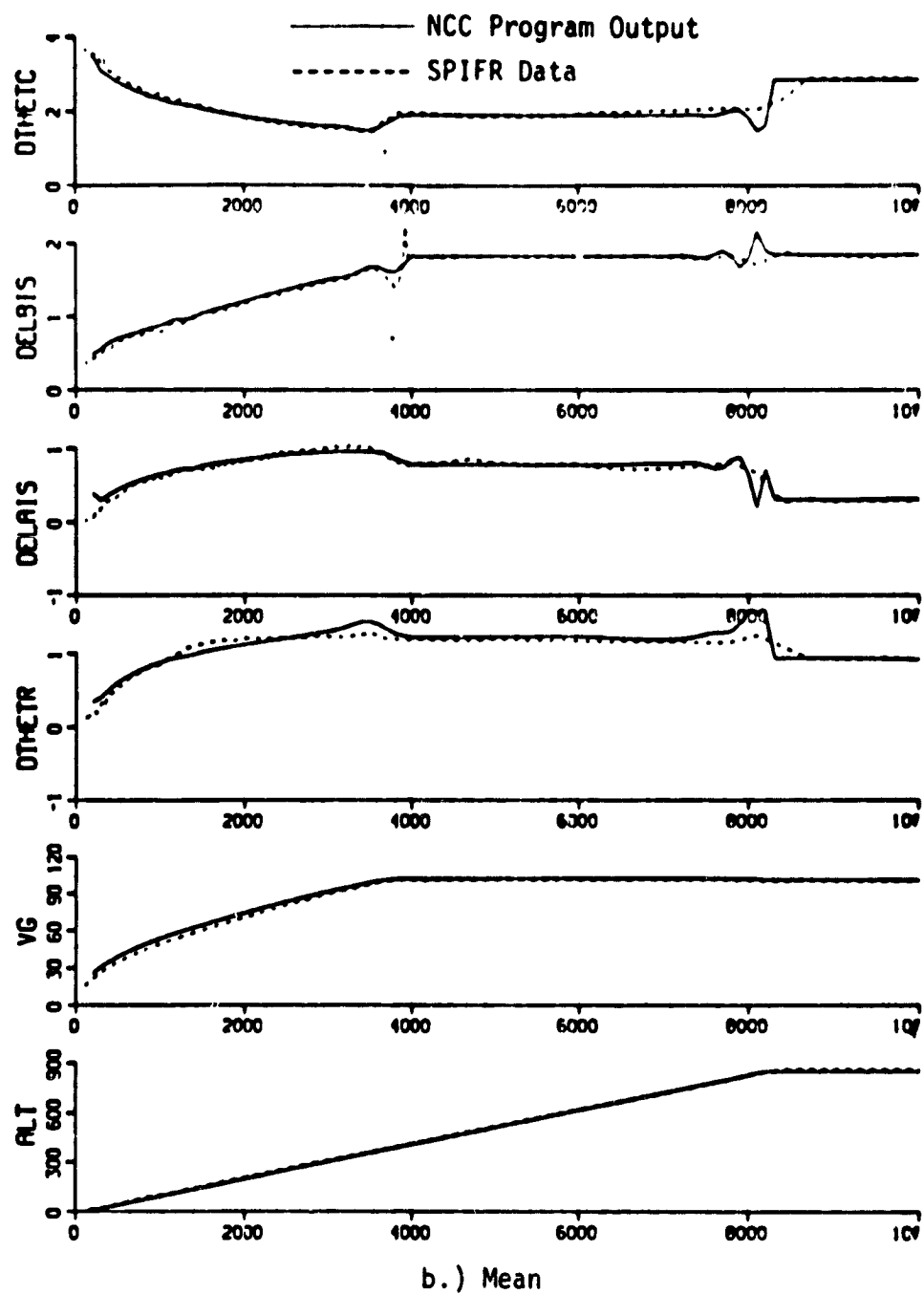
28

Figure 13.   NCC Program Simulation Results: CSS/AP/NO WIND/DH = 0 ft, 10 runs

d.) Standard Deviation

Figure 13. NCC Program Simulation Results: CSS/AP/NO WIND/DH = 0 ft, 10 runs

30

Figure 14. NCC Program Simulation Results: NCC/AP/WIND/DH = 0 ft, 10 runs
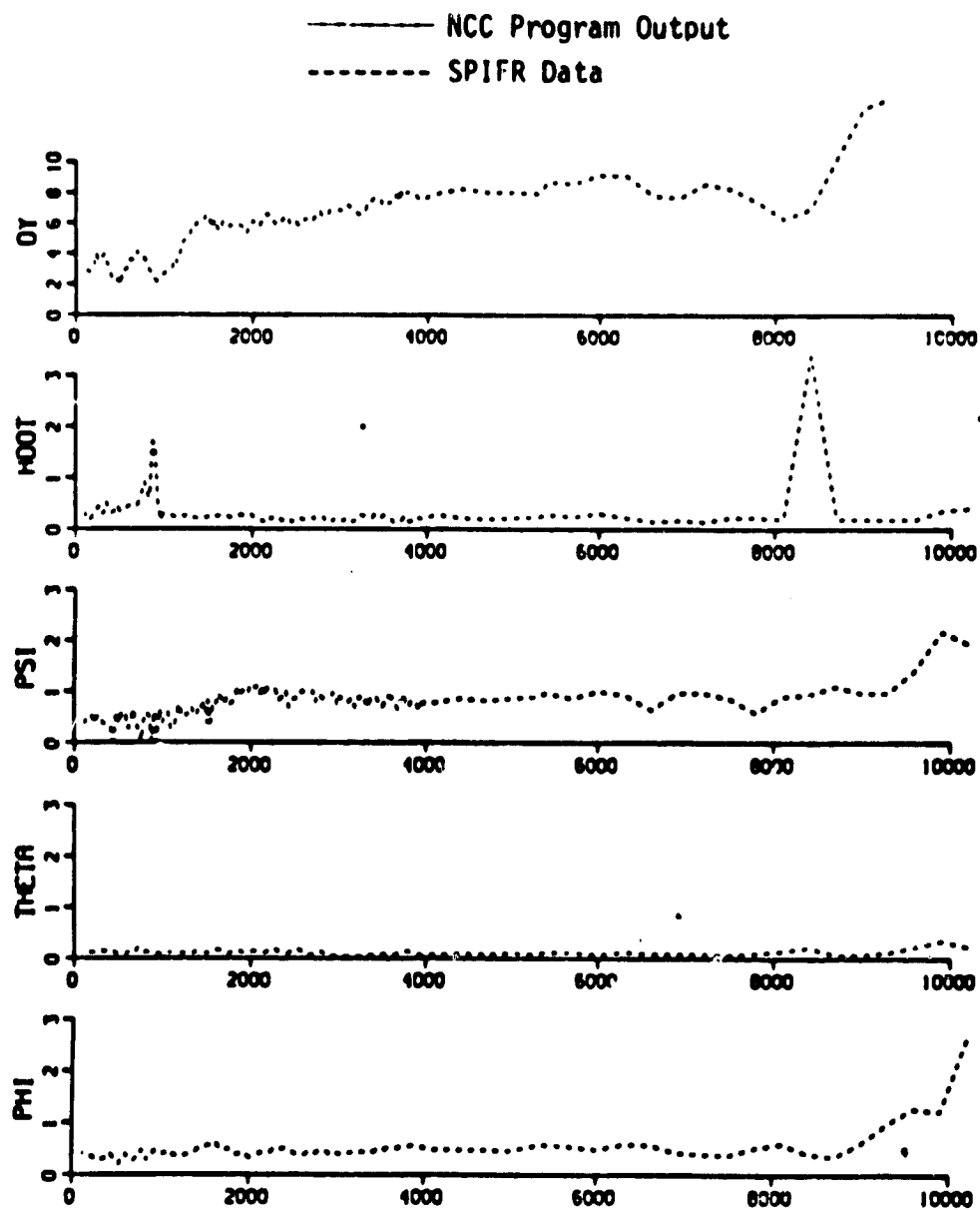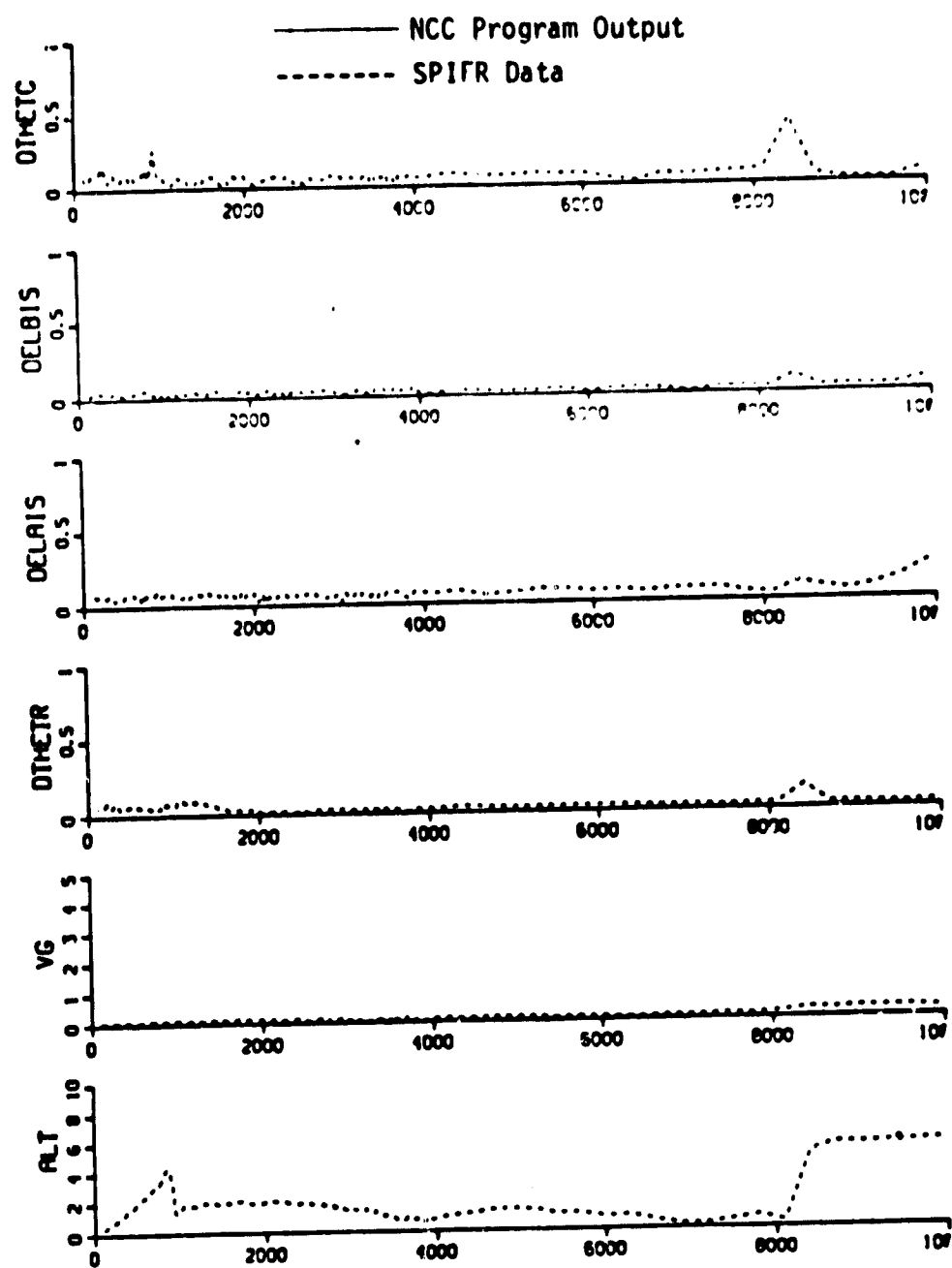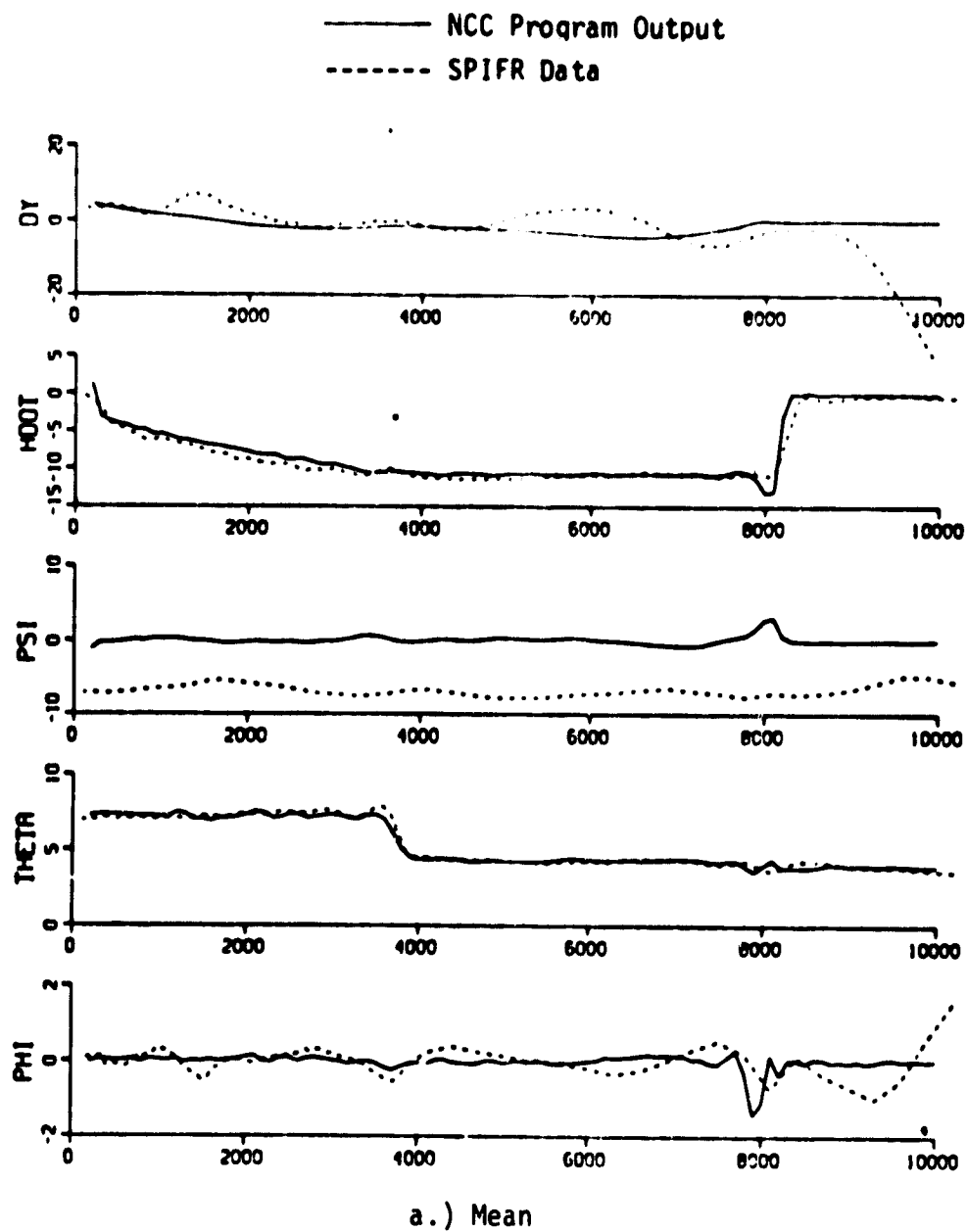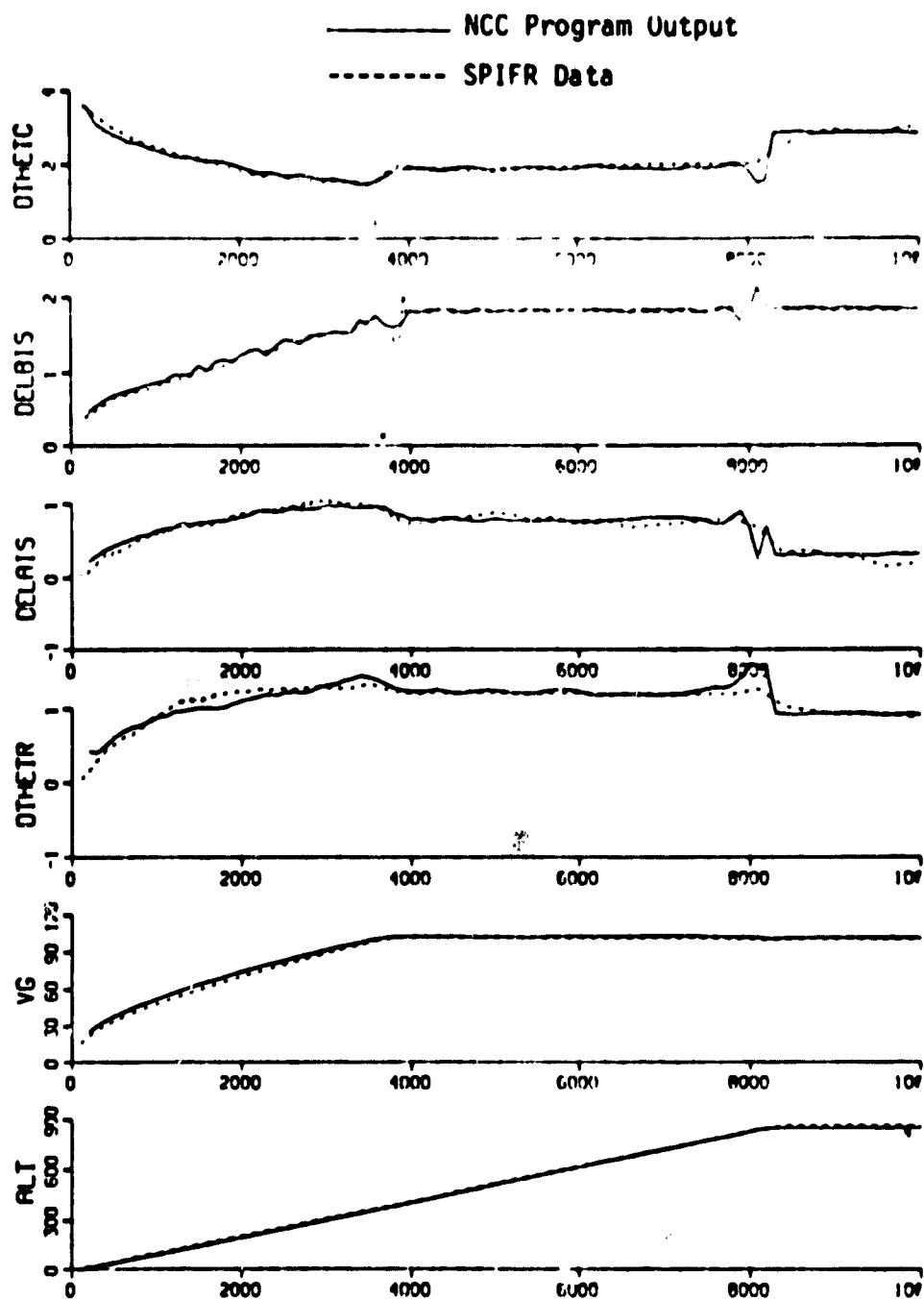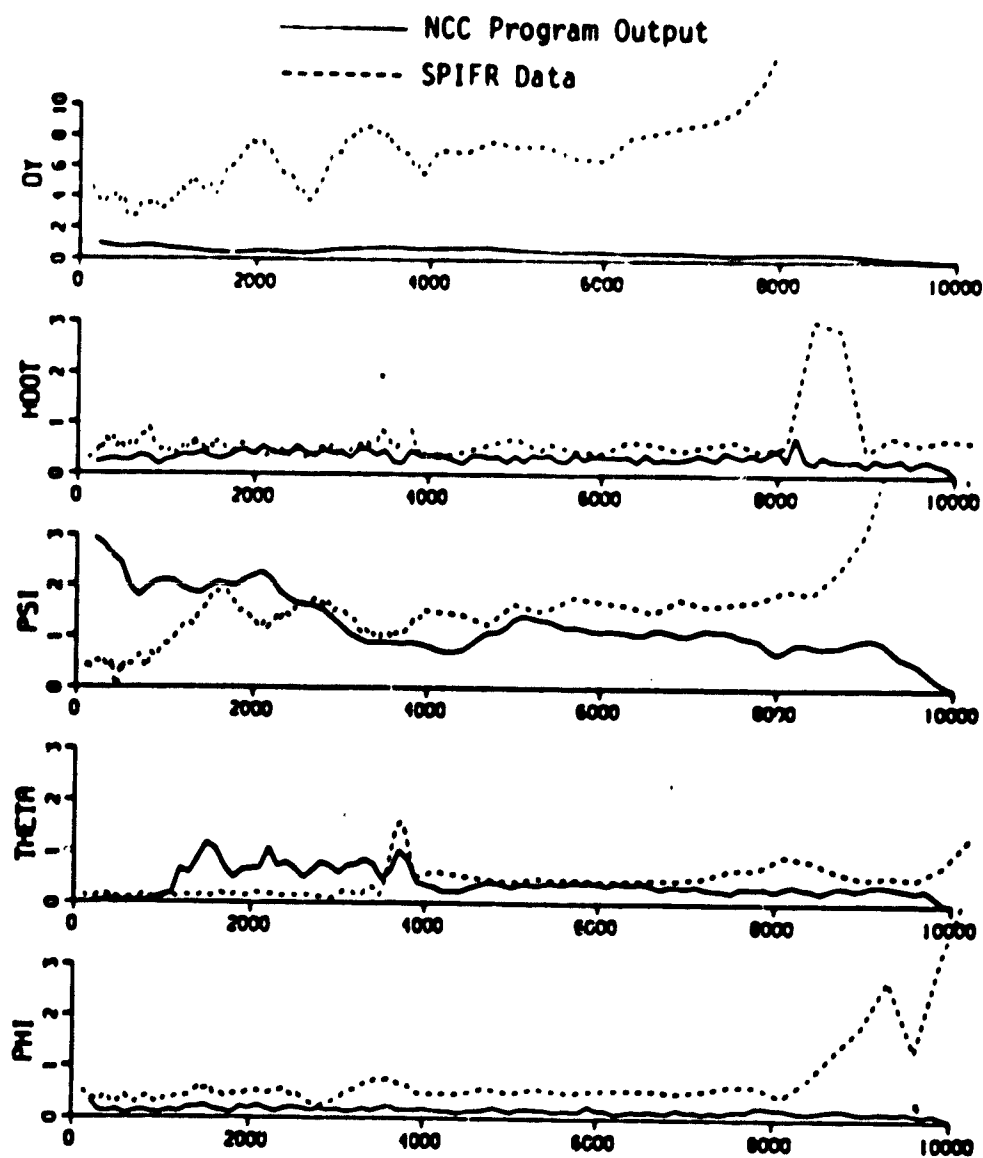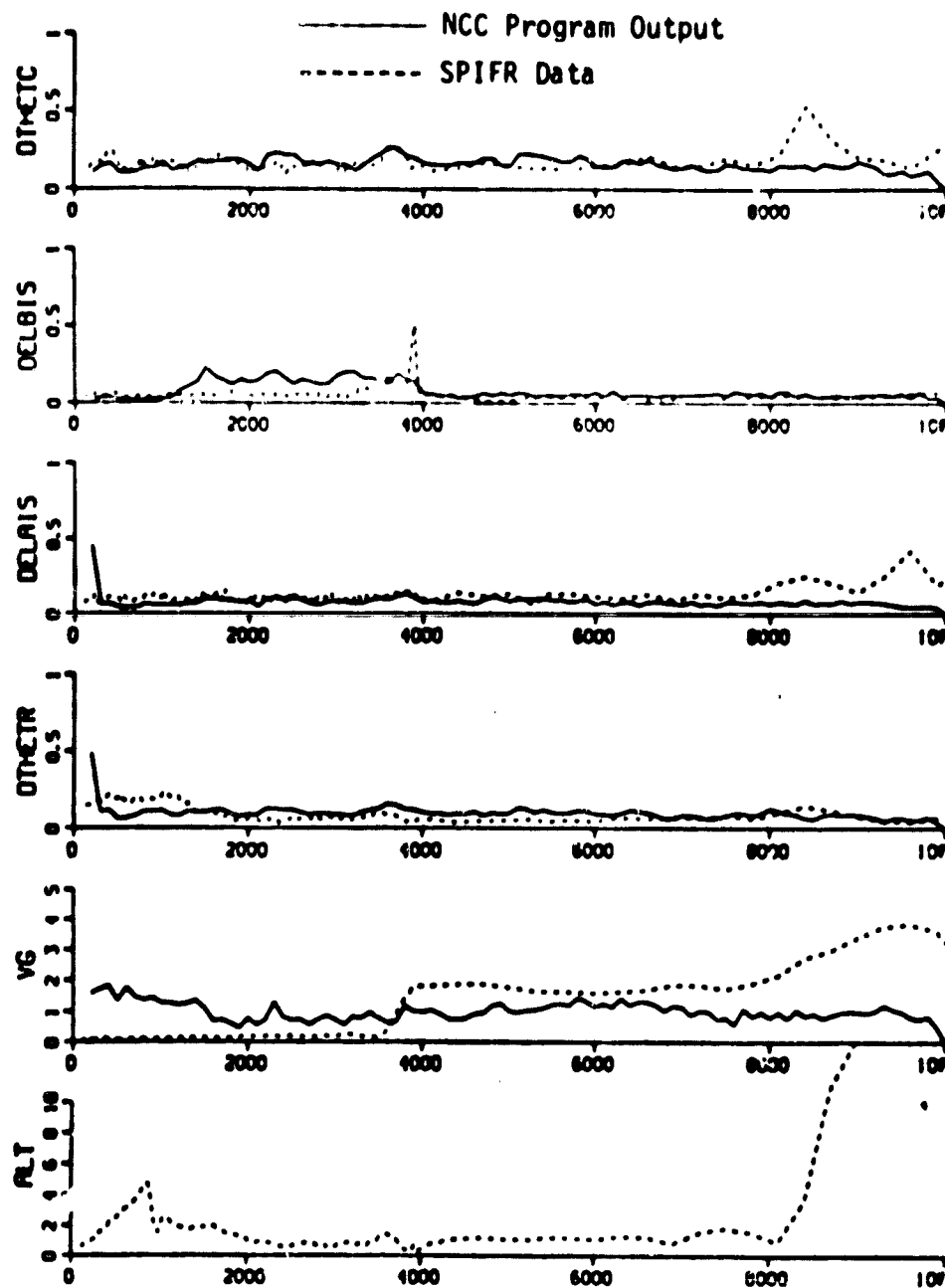
31

b.) Mean

Figure 14.   NCC Program Simulation Results: CSS/AP/WIND/DH = 0 ft, 10 runs

32

c.) Standard Deviation

Figure 14. NCC Program Simulation Results: CSS/AP/WIND/DH = 0 ft, 10 runs

33

d.) Standard Deviation

Figure 14. NCC Program Simulation Results: CSS/AP/WIND/DH = 0 ft, 10 runs

34

2. The reference heading angle ψ_{ref} for the SPIFR simulation experiments was -7.3 degrees (corresponding to Crow's landing runway); hence the apparent offset error in the PSI responses.

3. The NCC program does not include the blending logic for capture and flare used in the SPIFR experiments. This discrepancy is responsible for the differences between the two outputs at glide slope capture and initiation of deceleration. However, this omission has no significant impact on the overall time response history.

4. The automatic mode ensemble standard deviation data from SPIFR experiments is significant even in the absence of wind gust disturbances as evidenced in Figure 13 c,d. In contrast the NCC program output standard deviations are zero as would be expected. The non-zero standard deviations must be the result of the peculiar hybrid mechanization of the simulation in the SPIFR experiments. Run to run variability and hence the non-zero standard deviations may be due to (1) the lack of synchronization between the on-board 1819B Sperry computer and the EAI 8400 machine used for simulating the aircraft dynamics; and (2) the variability in the initial conditions at the start of each run. Other unlikely sources include the quantization and truncation errors in the on-board computer or a variable time delay in the A/D and D/A mechanizations.

5. Comparison of the automatic mode standard deviation results with and without wind (Figures 14 c,d and 13 c,d, respectively) shows that the relative contribution of wind disturbances is roughly equivalent to that caused by the specific V/STOLAND system digital computer implementation.

6. Standard deviations of the ground speed , VG, and pitch attitude, THETA show a sudden decrease after initiation of flare at approximately 4000 ft to go. This is consistent with the inplementation of the velocity guidance law where the velocity feedback used for comparison against commanded speed V_c switches from airspeed VRW to ground speed VG. Hence groundspeed VG shows a higher standard deviation before the onset of deceleration.

35

Results for three CSS/FD approaches are shown in Figures 15-17. The zero decision height response comparison is shown in Figure 15, where the experimental data is for pilot number 1, the only pilot who attempted the zero/zero approach to a hover. Comparisons for the decision height of 50 ft. are shown in Figure 16. The 2 cue flight director results corresponding to the automatic collective configuration are presented in Figure 17. SPIFR data for pilot number 2 is displayed in both Figures 16-17. The following characteristics may be noted:

1. The mean response comparisons in the flight director mode are satisfactory in all axes. The zero/zero case shown in Figure 15 shows the best match to the experimental data. The apparent error in the PSI response fit is due to the fact that the reference heading angle ψ_{ref} for the SPIFR simulation was -7.3 degrees (Crows Landing runway) while it is set to 0 degrees in the NCC program.

2. The pitch axis mean response comparisons show significant differences during the deceleration phase. The deceleration command is provided to the pilot through the pitch flight director bar PFDIN. At the initiation of flare (as indicated by a green FLR light on the ADI), the pilot must respond by attempting to track the pitch flight director signal while keeping the aircraft on the prescribed flight path. Any delay in responding to the pitch flight director command results in larger command attitude to compensate for the loss of distance remaining to decelerate to a hover. Pitch axis data in Figures 15-17 demonstrate this type of behavior on behalf of the human pilot, e.g., see THETA, THCOM, PFDIN and VG. A pure gain (no lead/lag or time delay) model for the pilot is assumed in all three control axes. Improvements in fit may be obtained using a more realistic pilot model.

3. Response differences in the lateral axis variables, in particular, the localizer error DY and bank angle PHI, are due to the high variability of the initial conditions evident in the SPIFR simulation data. In the SPIFR experiments, the automatic

36

Figure 15. NCC Program Simulation Results: CSS/FD/WIND/DH = 0 ft, 10 runs

37

Figure 15.   NCC Program Simulation Results: CSS/FD/WIND/DH = 0 ft, 10 runs

c.) Standard Deviation

Figure 15. NCC Program Simulation Results: CSS/FD/WIND/DH = 0 ft, 10 runs

Figure 15.   NCC Program Simulation Results: CSS/FD/WIND/DH = 0 ft, 10 runs

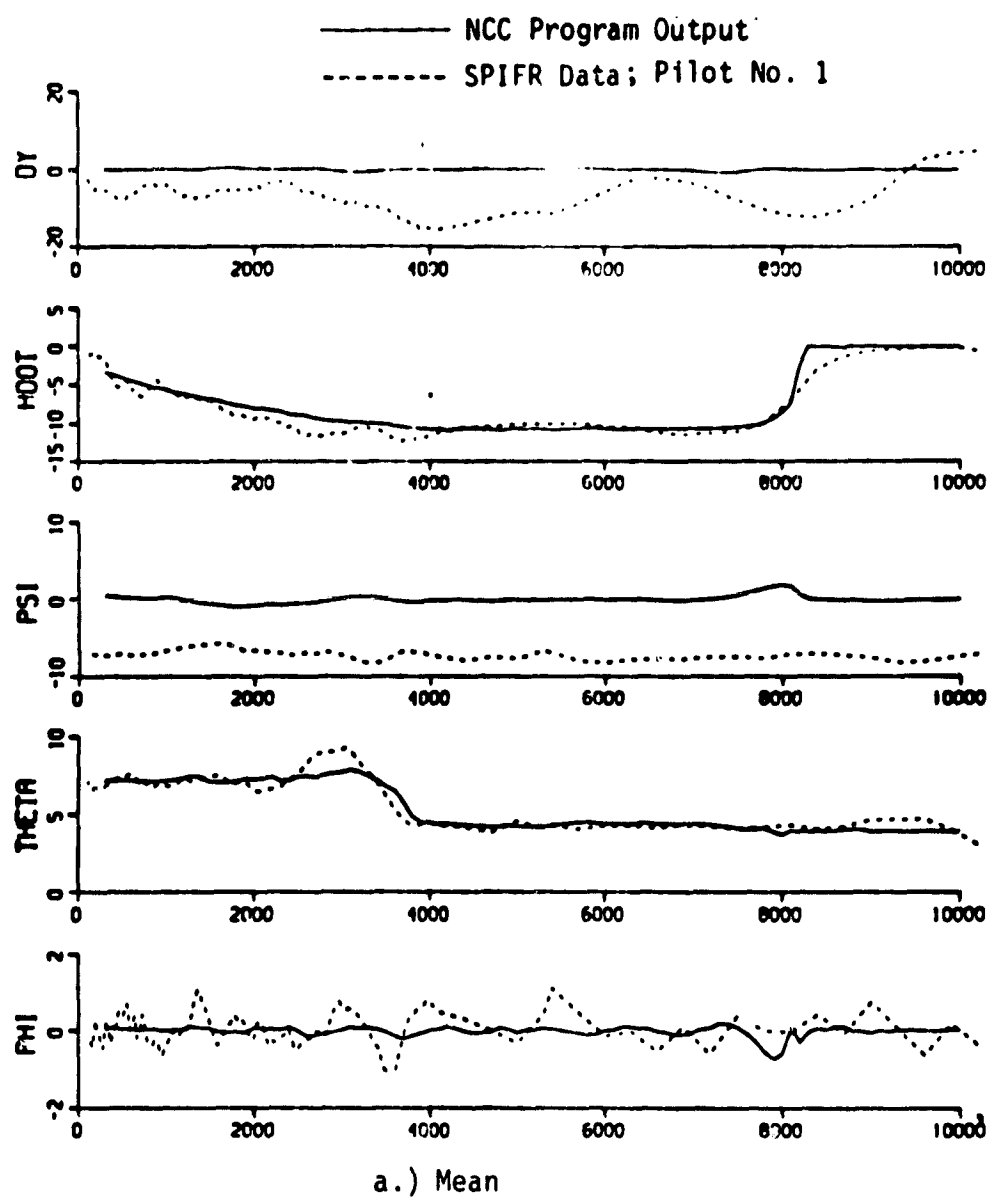Figure 16.   NCC Program Simulation Results: CSS/FD/WIND/DH = 50 ft, 12 runs

41

Figure 16. NCC Program Simulation Results: CSS/FD/WIND/DH = 50 ft, 12 runs

Figure 16.   NCC Program Simulation Results: CSS/FD/WIND/DH = 50 ft, 12 runs

43

d.) Standard Deviation

Figure 16. NCC Program Simulation Results: CSS/FD/WIND/DH = 50 ft, 12 runs

44

Figure 17. NCC Program Simulation Results: CSS/FD/AC/WIND/DH = 50 ft, 12 runs

45

b.) Mean

Figure 17. NCC Program Simulation Results: CSS/FD/AC/WIND/DH = 50 ft, 12 runs
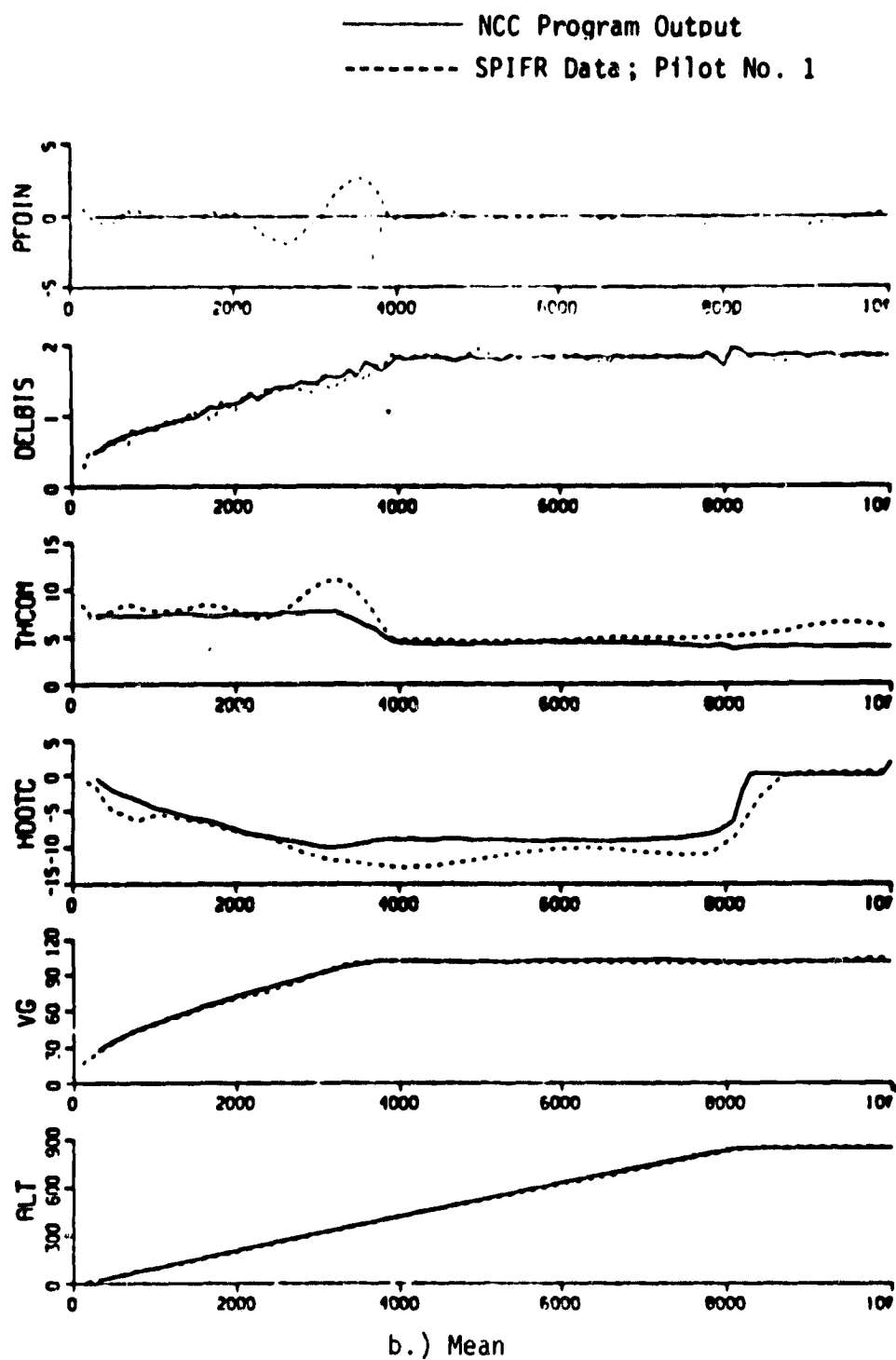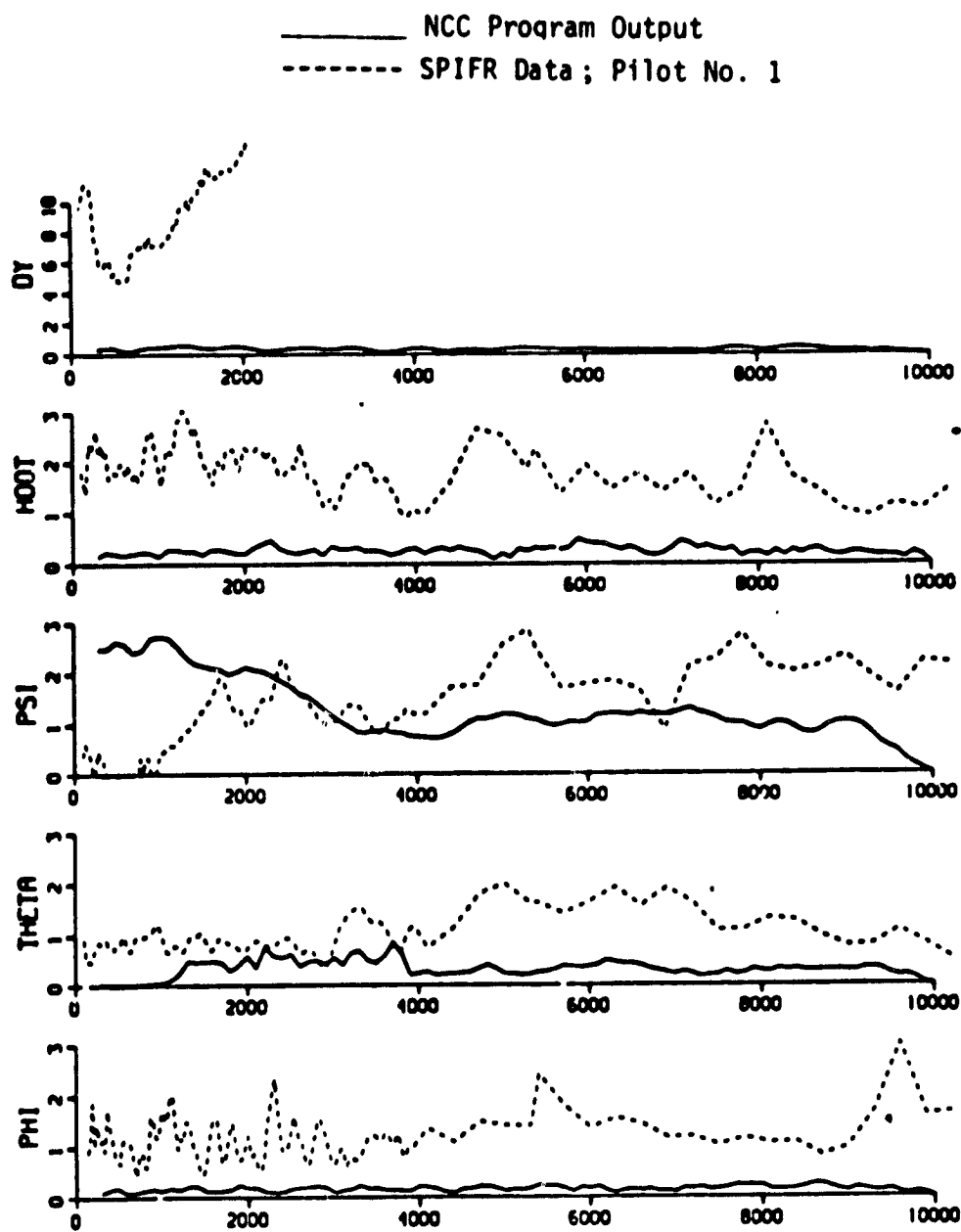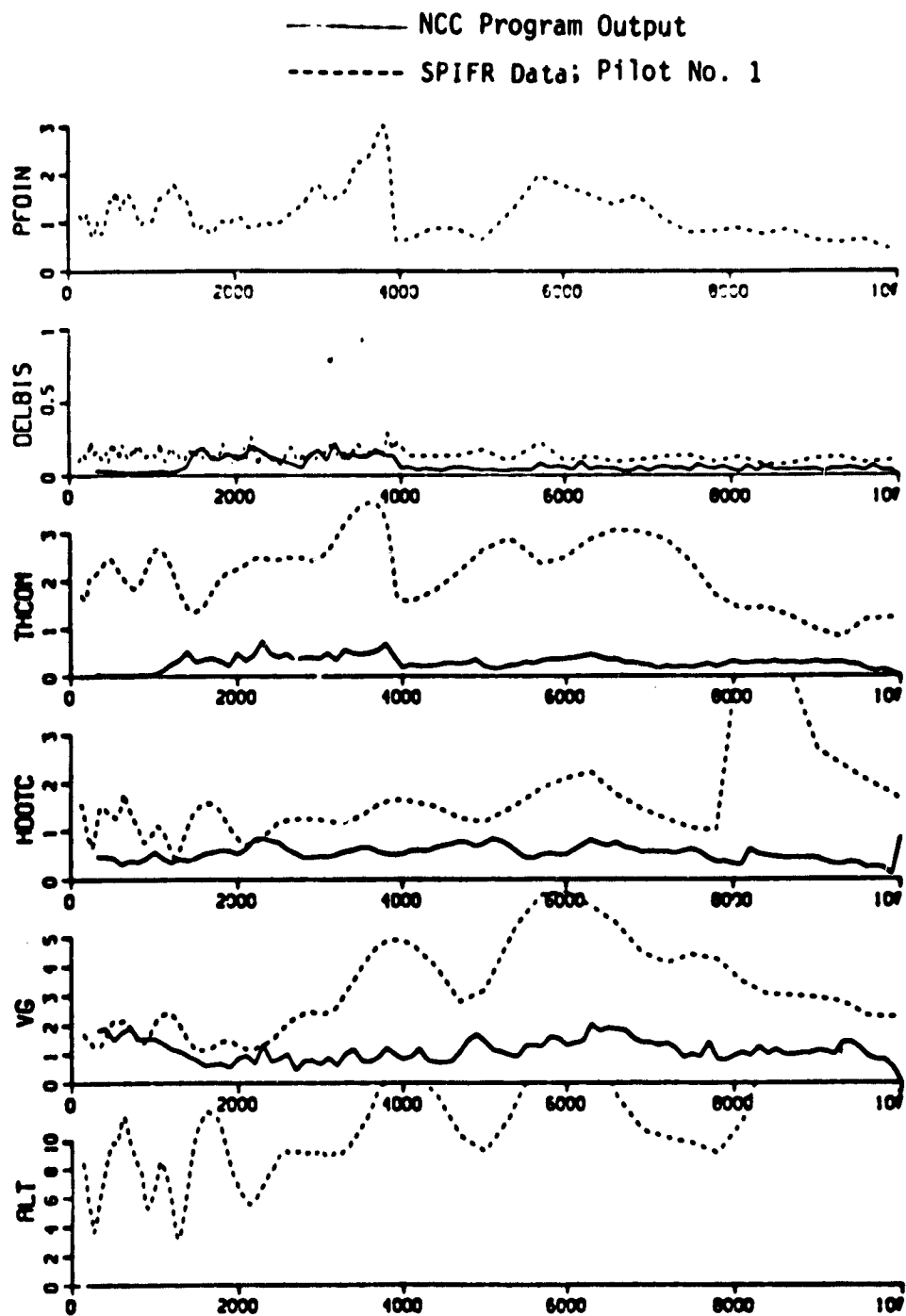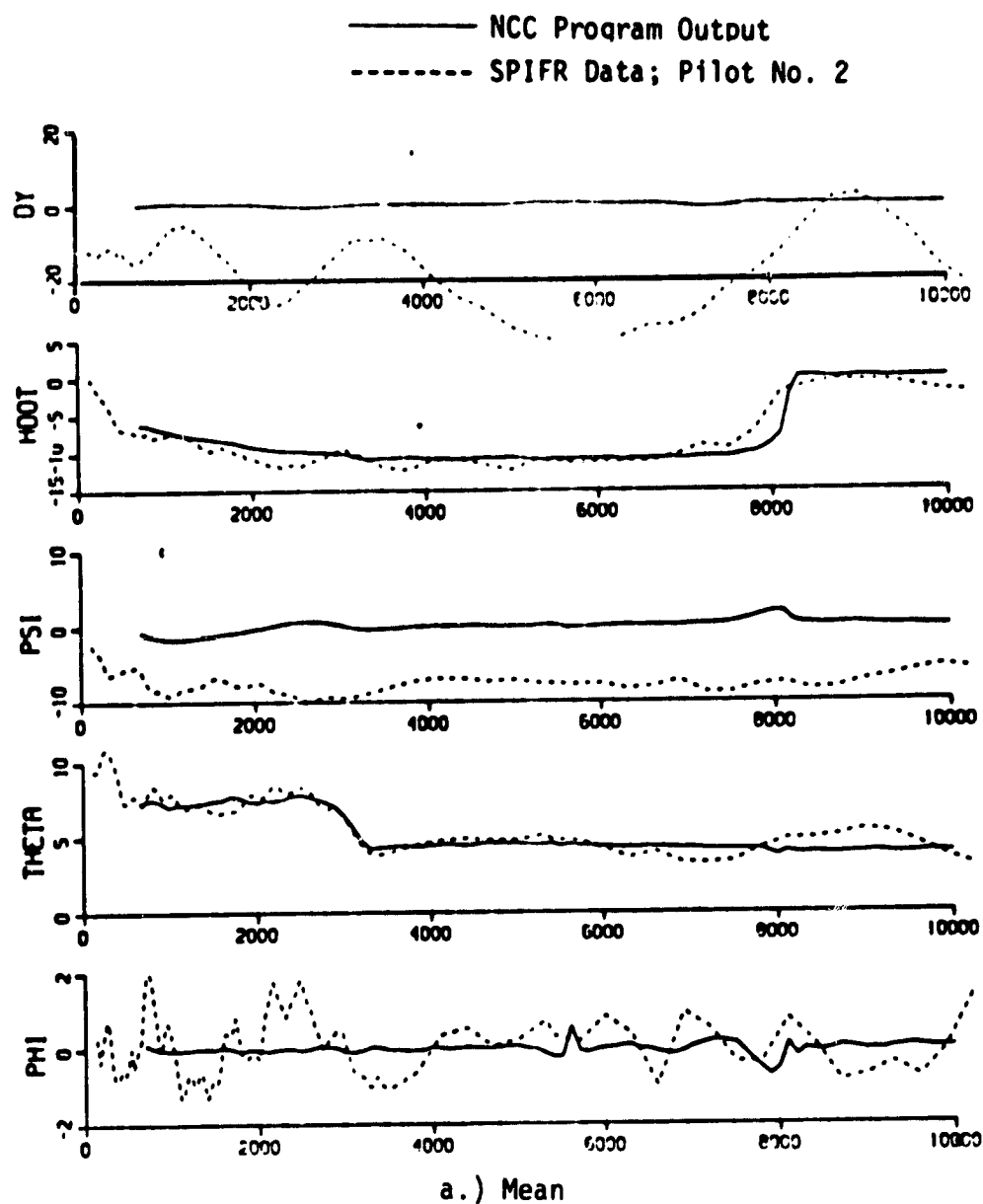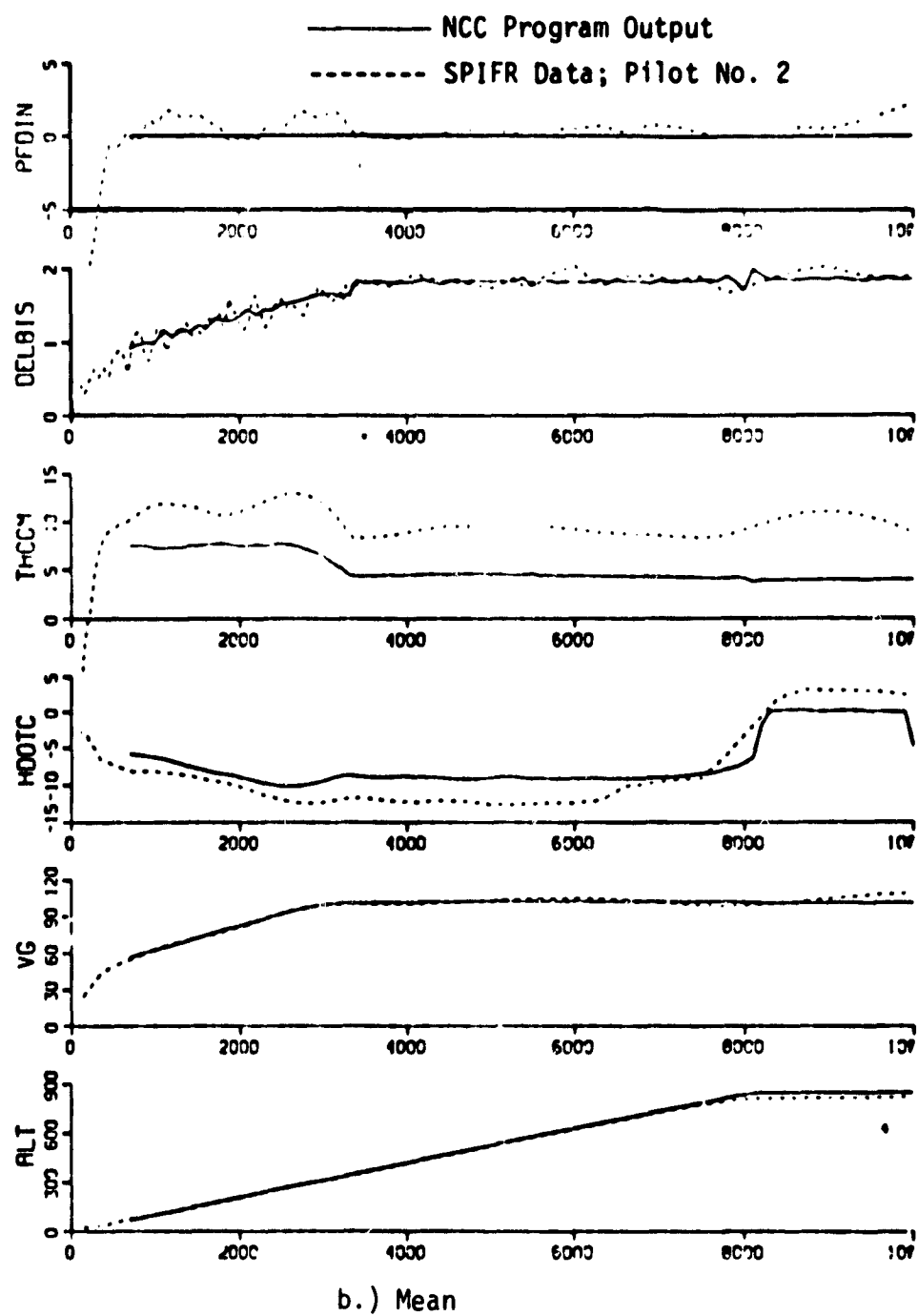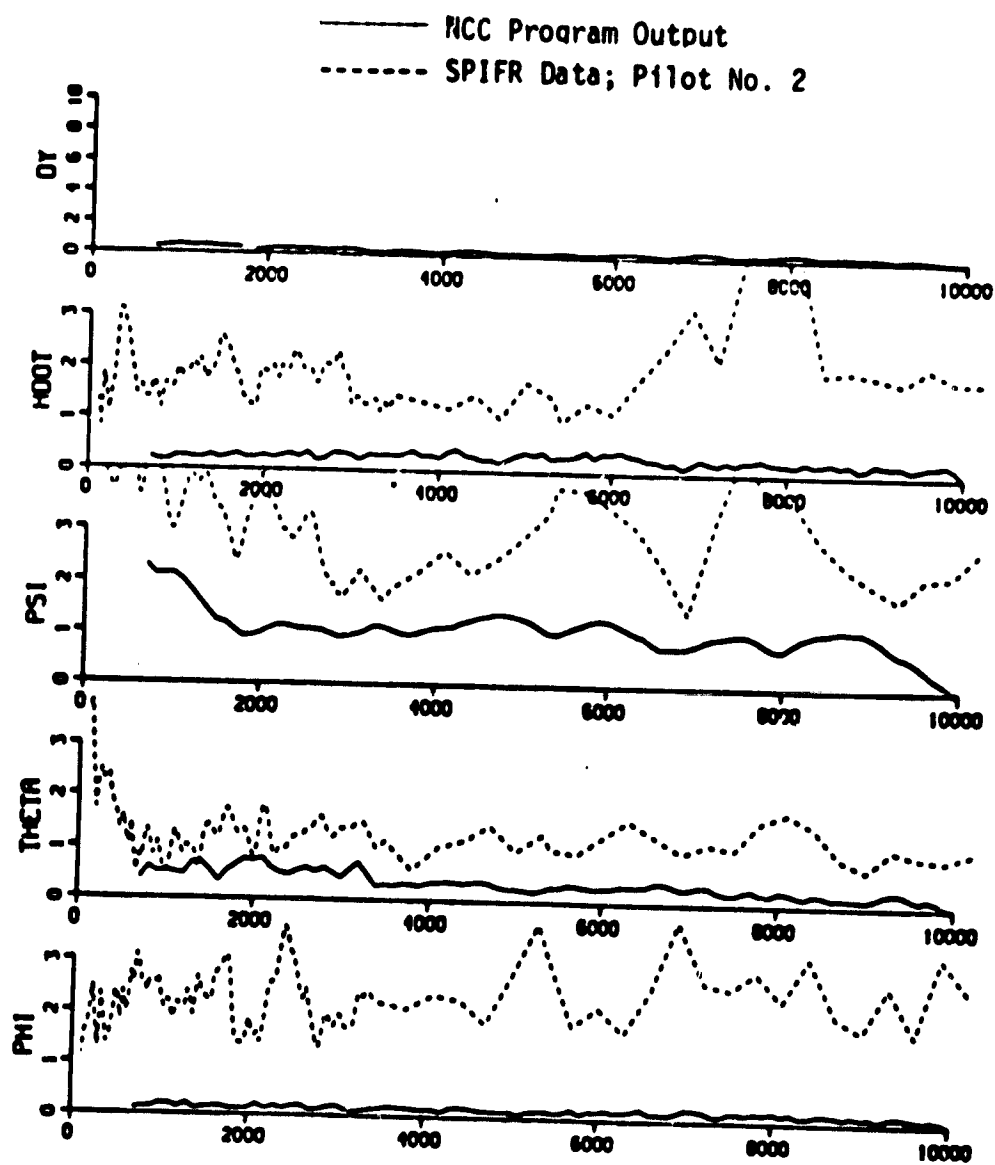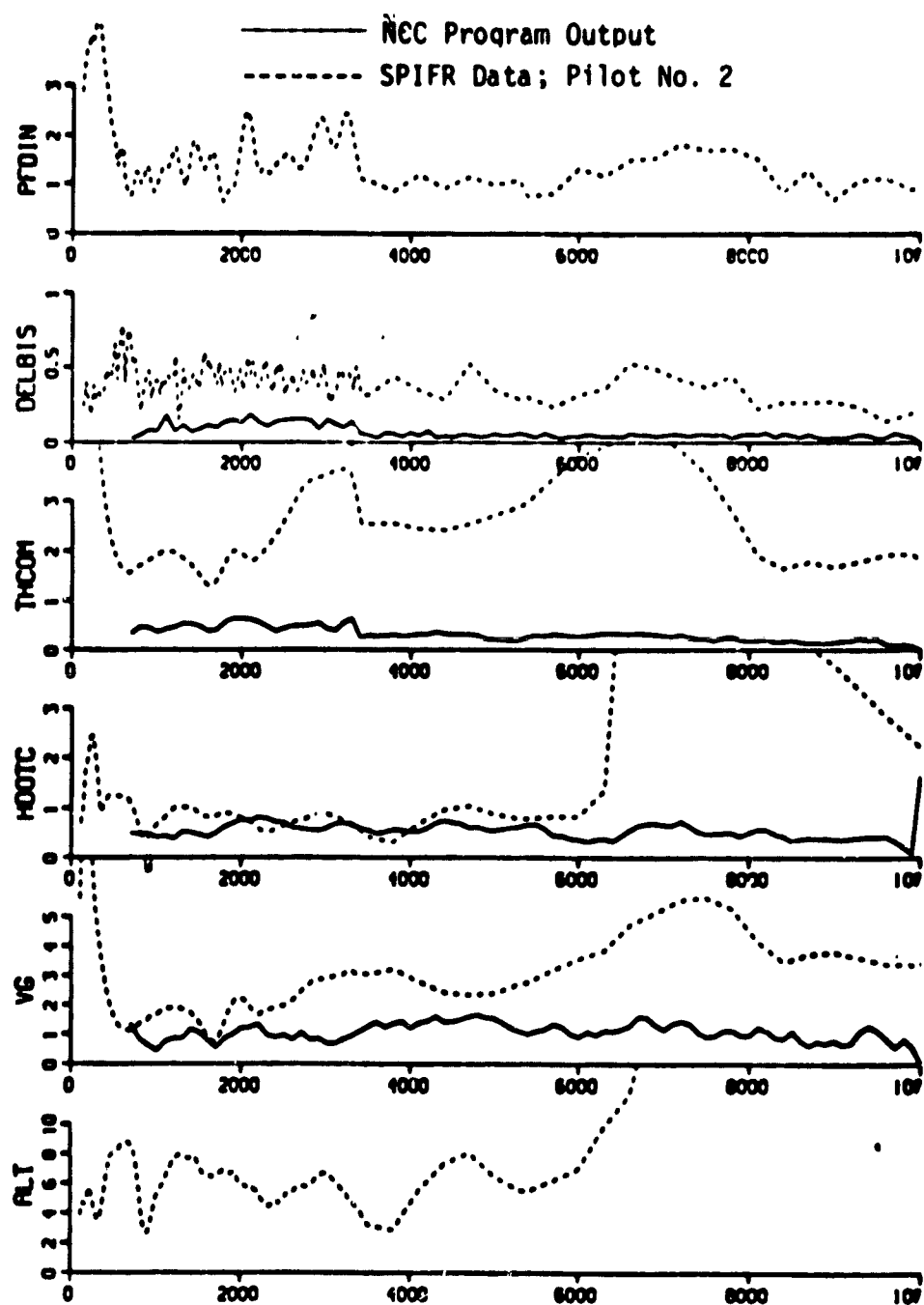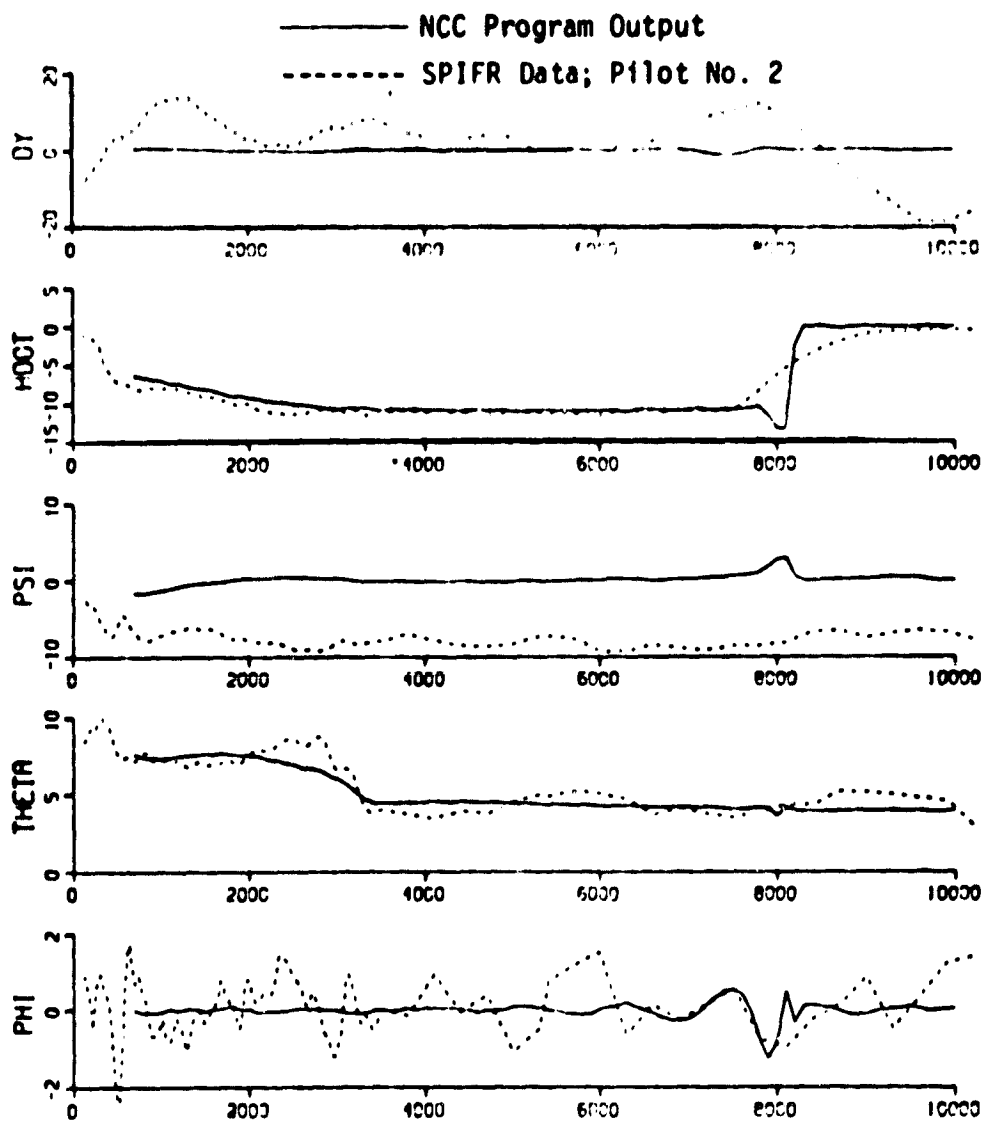
46

Figure 17. NCC Program Simulation Results: CSS/FD/AC/WIND/DH = 50 ft, 12 runs

47

d.) Standard Deviation

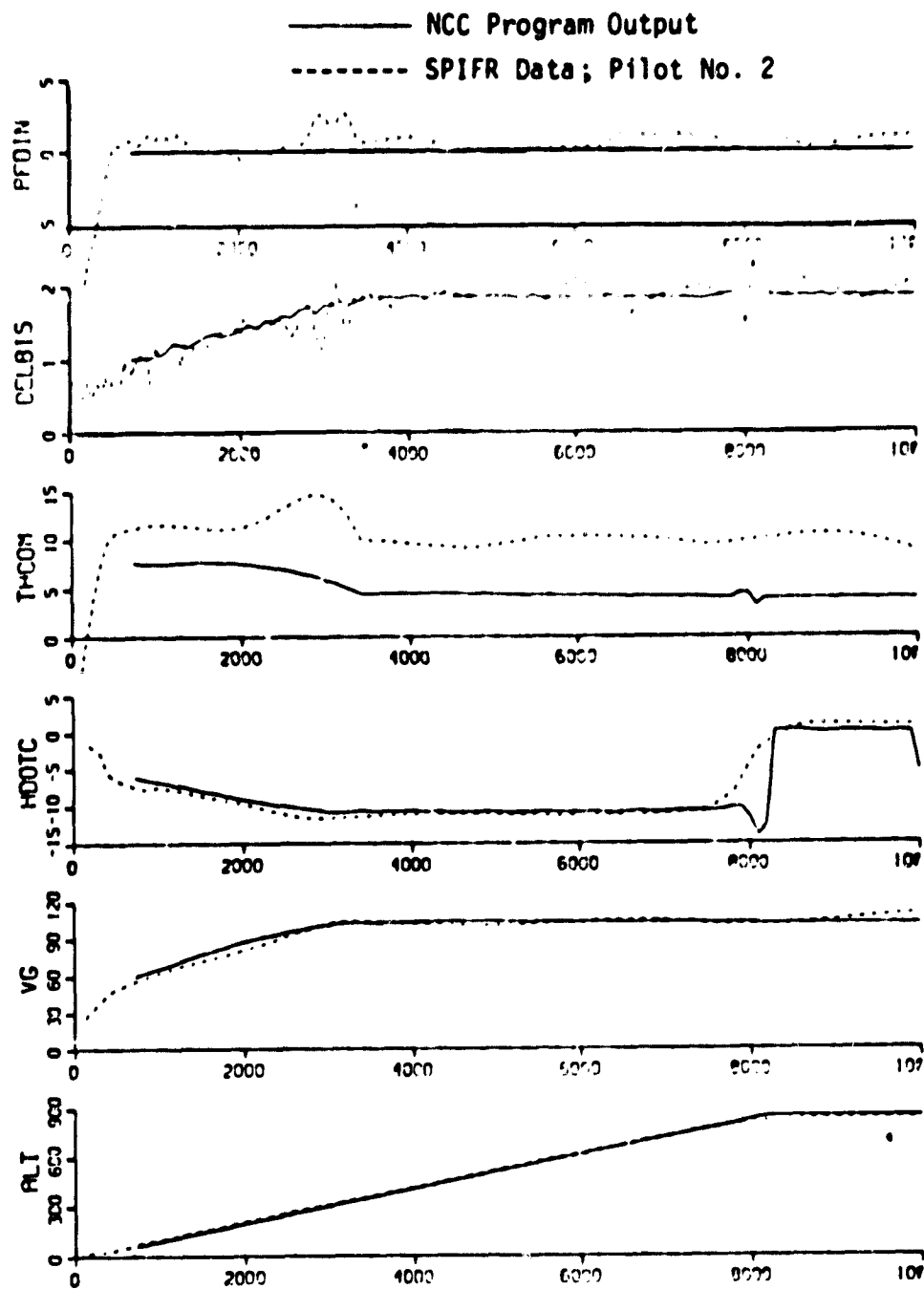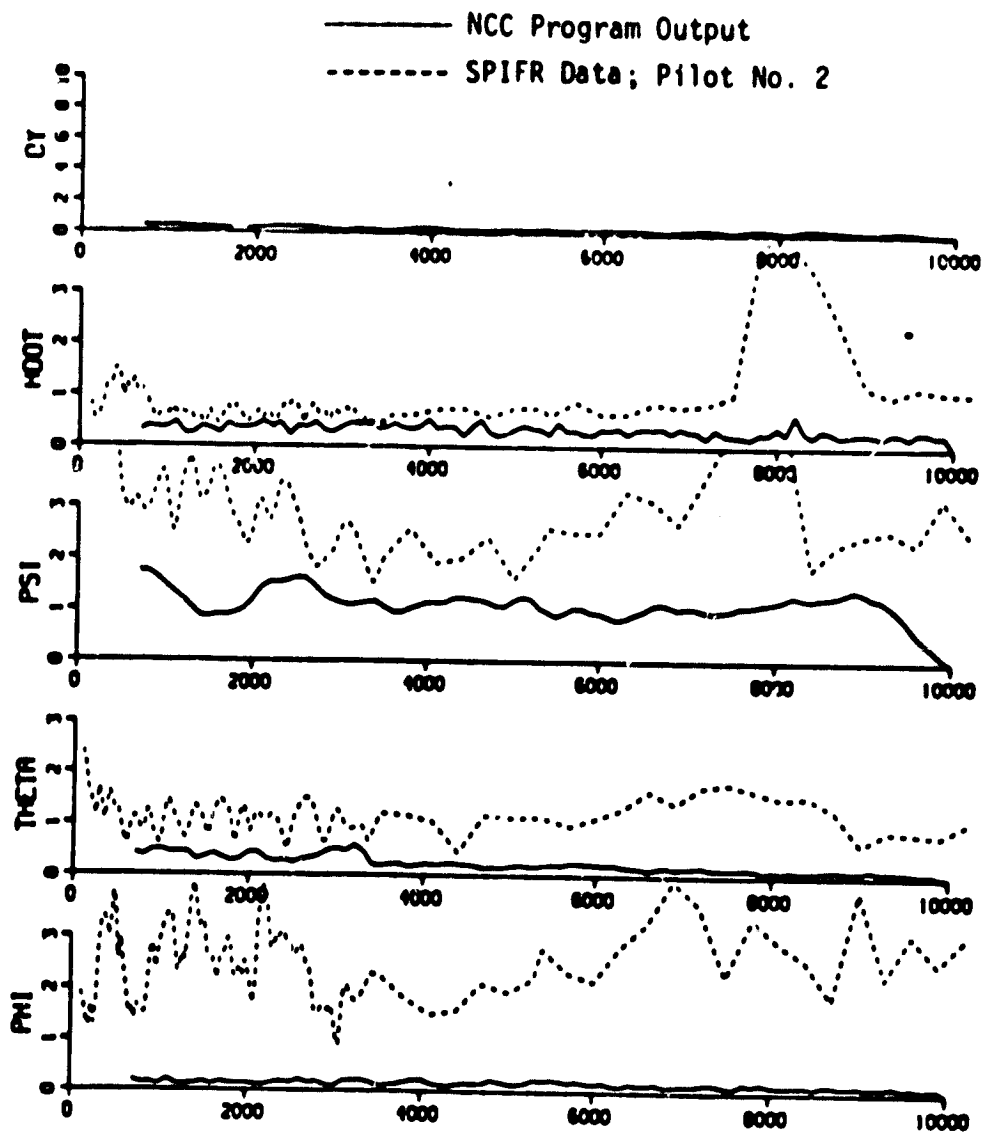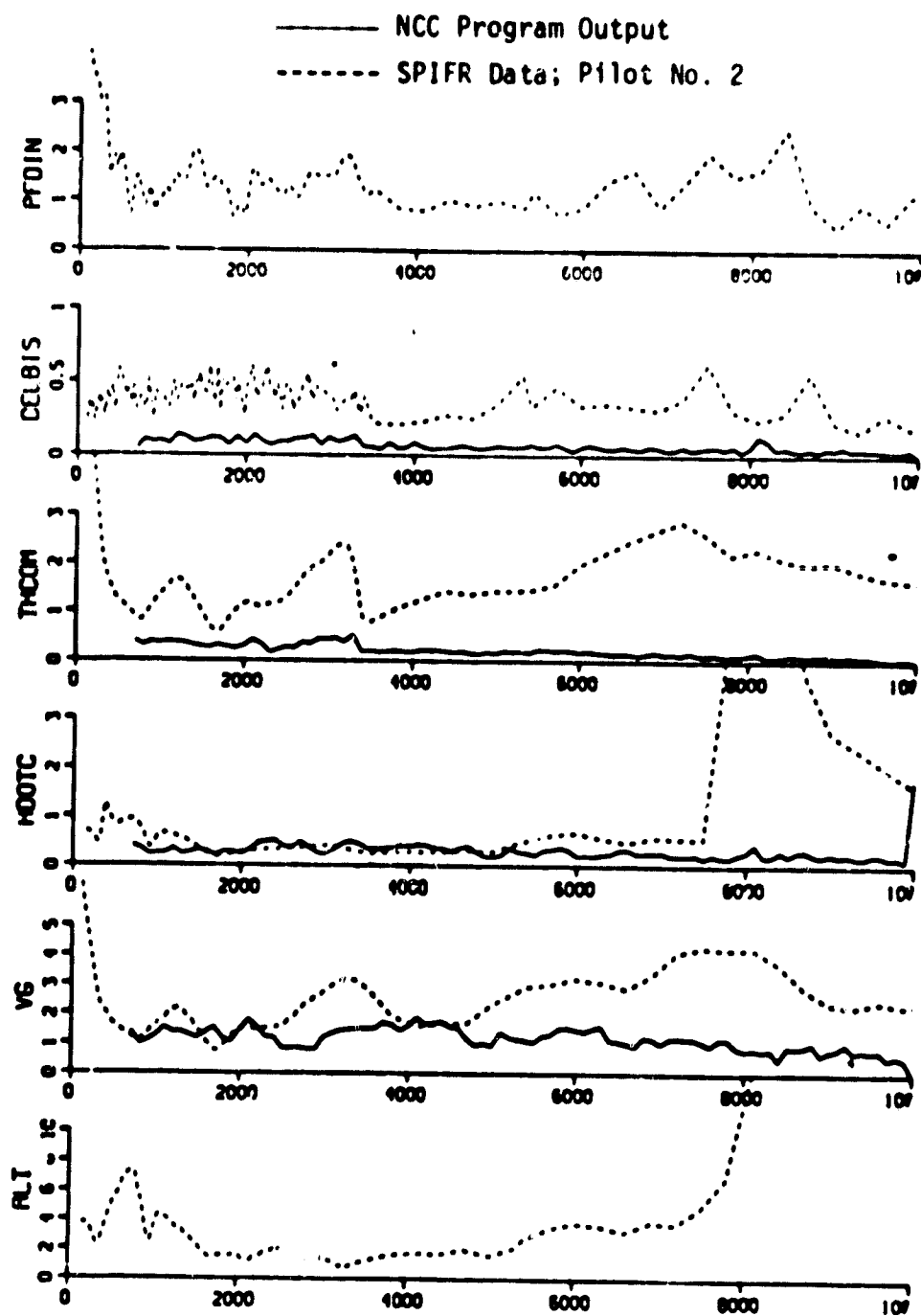Figure 17. NCC Program Simulation Results: CSS/FD/AC/WIND/DH = 50 ft, 12 runs

48

mode was used for the first few seconds in the run before the pilot took over manual control. Therefore the variability of the initial conditions is partially the result of the run-to-run variations in engaging the CSS/FD mode. In addition, data is recorded from a distance of 10,200 ft from the landing pad while the actual runs were initiated at a distance of 13,200 ft. As a result initial conditions on DY when data recording was initiated are typical large (non zero) and display a large standard deviation as witnessed by the data in Figures 15-17.

NCC program initial conditions for each run in the Monte Carlo process are set to zero or equivalent trim conditions. A fair comparison demands, wherever feasible, identical factors in the two simulations. If this were possible, errors between the two sets of data would be due to the discrepancies in the modeling of the pilot control strategy alone, and efforts could be directed towards developing a more realistic representation.

4. The standard deviation results display significant differences between the SPIFR data and the NCC program outputs, the latter being highly optimistic. As mentioned earlier in discussing the automatic mode results, some of the differences are due to the V/STOLAND digital implementation characteristics which are not modeled in the NCC program. However, a major source for discrepancy lies in the highly idealized representation of the human pilot as a pure gain servomechanism. Clearly, the human pilot does not behave as a robot or an autopilot. A more realistic model for the pilot would include an adequate representation of human information acquisition (scanning strategy), data processing and decision making capabilities. Such a model would show signifigant run-to-run variability and more closely match SPIFR experimental data.

Results presented here demonstrate the validity of the NCC program. Observed discrepancies have a rational explanation and can be alleviated by improving some of the individual modules in the overall program. Within

49

the scope of this effort, an improved representation of pilot response be-
havior is considered more important than developing more realistic models
for the V/STOLAND system implementation. Consequently, the NCC program
improvements are directed towards development of a realistic pilot model
for use in formulating an analytical methodology for determining helicopter
precision approach requirements.

Linear Time-Varying Covariance Propagation
(LTVCP) Program

An investigation of the existing LTVCP IBM/360 program was con-
ducted with the goal of determining its usefulness for application to the
SPIFR simulation data. The existing LTVCP program is suitable for solving
the standard covariance propagation equations as follows:

Given the linearized aircraft equations of motion

$$\dot{x} = Fx + Gu + \Gamma w \tag{8}$$

where x = perturbed state vector, u = input, $w = N(\mu,Q)$, the program solves
the equations for the mean $\bar{x} = E(x)$

$$\dot{\bar{x}} = F\bar{x} + Gu + \Gamma \mu \tag{9}$$

and covariance $X = E(x-\bar{x})(x-\bar{x})^T$

$$\dot{X} = FX + XF^T + \Gamma Q \Gamma^T \tag{10}$$

In general F, G, and Γ are matrices obtained by linearizing the aircraft
nonlinear equations of motion around some operating point (V_a, γ) where
V_a is airspeed and γ is the flight path angle. Thus,

$$F, G, \Gamma = f(V_a, \gamma) \tag{11}$$

The existing LTVCP program is not suitable for application to the SPIFR
experimental scenario because:

1) The program only solves for the frozen point or steady state
    solution for the state covariance using

50

$$\dot{X} = 0 = FX + XF^T + \Gamma Q \Gamma^T \tag{12}$$

where F and Γ are obtained by interpolation between the nominal flight conditions - namely trim values of airspeed V_a, flight path angle γ and longitudinal deceleration $\dot{V}_I$. Steady state or frozen point covariance computation is acceptable if changes in nominal operating flight conditions are slow compared to the system response time. For the SPIFR simulation, the changes in the commanded nominal flight conditions at glideslope capture ($\gamma = 0$ to $\gamma = -6°$) and initiation of the constant attitude deceleration maneuver ($\theta_{nom} = 3.94°$ to $\theta_{nom} = 7°$) occur too rapidly compared to the system response time to complete the transient maneuvers. For example, approximately 6 seconds are required to maneuver the pitch attitude of the aircraft from the trim value of approximately 3.94° during the glide slope trajectory phase to the commanded value of 7° following the onset of the CADP phase. Therefore, frozen point solutions are not applicable to the analysis of the precision approach and landing task.

2. The program allows for interpolation of the system matrices in only one independent variable - only V_a in this application. This is unacceptable for the SPIFR simulation reference flight trajectory where changes in flight path angle and airspeed may occur, independently or simultaneously.

3. The program has a peculiar structure which requires a specific input-output format. This puts undue restrictions on the practical use of the program for application to the SPIFR simulation structure.

4. The program by definition requires the use of data where time is the independent variable. Time ensemble data must, therefore, be used for validation. However, ensemble averaging with time as an independent variable is not appropriate in situations where the guidance commands are computed as a function of distance to go. In the SPIFR simulation, velocity and attitude commands are based on distance to go from the hover point. This could lead to situations where successive runs may be identical

51

with respect to distance to go as the independent variable but could be advanced or delayed with respect to each other in time. Time ensemble statistics would clearly be inappropriate in such circumstances.

5. The program only provides the ensemble mean x_p and covariance x_p of the perturbed state vector x_p. The total system response x is the sum of the nominal x_n and perturbed state x_p. Thus,

$$x(t) = x_n(t) + x_p(t)$$

and

$$\overline{x}(t) = x_n(t) + \overline{x}_p(t) \tag{13}$$

$$X(t) = X_p(t)$$

Thus knowledge of $x_n(t)$, the nominal state vector is essential for computing the total system vector. However, $x_n(t)$ can only be obtained by solution of the complete nonlinear simulation of the system as in the NCC program. The principal justification of using linear time varying covariance propagation is undermined if a nonlinear simulation is required for computing the nominal response.

6. Finally, the program also gives highly optimistic results for the state covariance propagation. Actual state vector dispersions are caused by wind as well as other factors such as the quantization and truncation errors due to the particular on-board computer implementation. The available linearized models do not allow for error models for digital computer error sources.

In conclusion, computation of approach and landing performance using linear time varying covariance propagation methods is not recommended. The problems with the approach are fundamental and not program specific. Specific limitations (1) - (4) given above can be remedied by developing a new program which uses distance as the independent variable for covariance propagation. However, restrictions (5) and (6) above are more fundamental to the methodology itself and cannot be removed creating a new program.

52

Linear time varying covariance propagation programs apply as long as the perturbations in the system state variable stay reasonably close to the nominal trim values. Application to the decelerating approach to a hover task is complicated by the requirement of large sudden changes in the operating point or helicopter trim conditions during glide slope capture and initiation of flare. The resulting dynamic trim change cannot be described as a string of frozen point trim (static or dynamic) data, and must be obtained through a nonlinear system simulation. Therefore, an approach using a nonlinear simulation of the complete system as in the NCC program is desirable, especially for systems involving dynamic maneuvers such as reference trajectory capture and deceleration to a hover.

PILOT ACCEPTANCE ANALYTICAL METHODOLOGY

The overall approach to the formulation of an analytical methodolgy for determining pilot acceptance consists of the following four steps:

1. Develop and validate an off-line simulation of the helicopter approach to a hover task in the automatic and flight director modes,

2. Select a generic pilot model structure that is applicable to manual flight director or raw data modes of operation,

3. Formulate candidate pilot model based workload metrics and evaluate their adequacy through simulation of the performance-workload tradeoffs, and

4. Summarize the results of the study by formulating a plausible analytical procedure for determining the pilot acceptance ratings of competing helicopter guidance, control and display systems.

Based on the results of the last section, the NCC program has been sufficiently validated to serve as the benchmark simulation of the heli-copter precision approach to a hover task.

The steps (2)-(4) are based on the implicit assumption that pilot acceptance is related to the information, decision and control require-ments imposed upon the human pilot in satisfactorily accomplishing a given task. In other words, determination of pilot acceptance or opinion rating is assumed to depend upon two factors: 1) a measure of system performance as perceived by the human pilot, and 2) a metric for human information, decision and control requirements usually lumped into the undefined but ubiquitous word "workload". However, both system performance and pilot workload depend upon the open loop aircraft characteristics and the struc-ture of the information processing, decision making and control strategy adopted by the human pilot. Thus, the need for a generic dynamical model for the pilot is apparent. Assuming this is feasible, pilot opinion rating may be specified as a linear or nonlinear function of the system performance measures and pilot model parameters.

55

The pilot model-based approach has been proposed by a number of investigators using a variety of pilot model structures. For example, the so-called "Paper Pilot" [9] approach, is based upon the use of describing function pilot model and assumes that the pilot opinion rating R is related to performance J and workload W by a functional of the form

$$R = J + W + 1$$

where system performance J and workload W represent multiattribute utility functions which depend on the individual components of a performance vector s and pilot model parameter vector θ. Figure 18 shows an application of the paper pilot concept to a longitudinal precision hover task [10]. In this application, system performance J is decomposed as a function of the rms values of longitudinal deviation (σ_x) and pitch rate (σ_q), where as pilot workload W is defined to be a nonlinear function of the pilot's pitch attitude lead ($T_{L\theta}$) and longitudinal position error lead (T_{LX}) parameters.

Pilot workload metrics and pilot-rating functionals in terms of the optimal control pilot model have also been proposed [11,12]. For example, in one approach proposed by Levison [12] pilot workload is assumed to be proportional to the fraction of attention devoted to the flying task as a whole. A visual curve fit or regression analysis is used to find the particular form of the functional relating pilot opinion rating to the system performance and workload metrics.

Another method based on the optimal control pilot model [13] suggests a pilot opinion rating functional that is monotonically related to the quadratic index of performance used in the model formulation. Thus,

$$R = U(I) \tag{14}$$

$$\text{where} \quad I = E\left\{ \lim_{T \to \infty} \frac{1}{T} \int_0^T (y^T Q y + u^T R u) dt \right\} \tag{15}$$

where y(t) represents the pertinent linear combination of the aircraft states and u represents the pilot's control vector (aircraft control

56
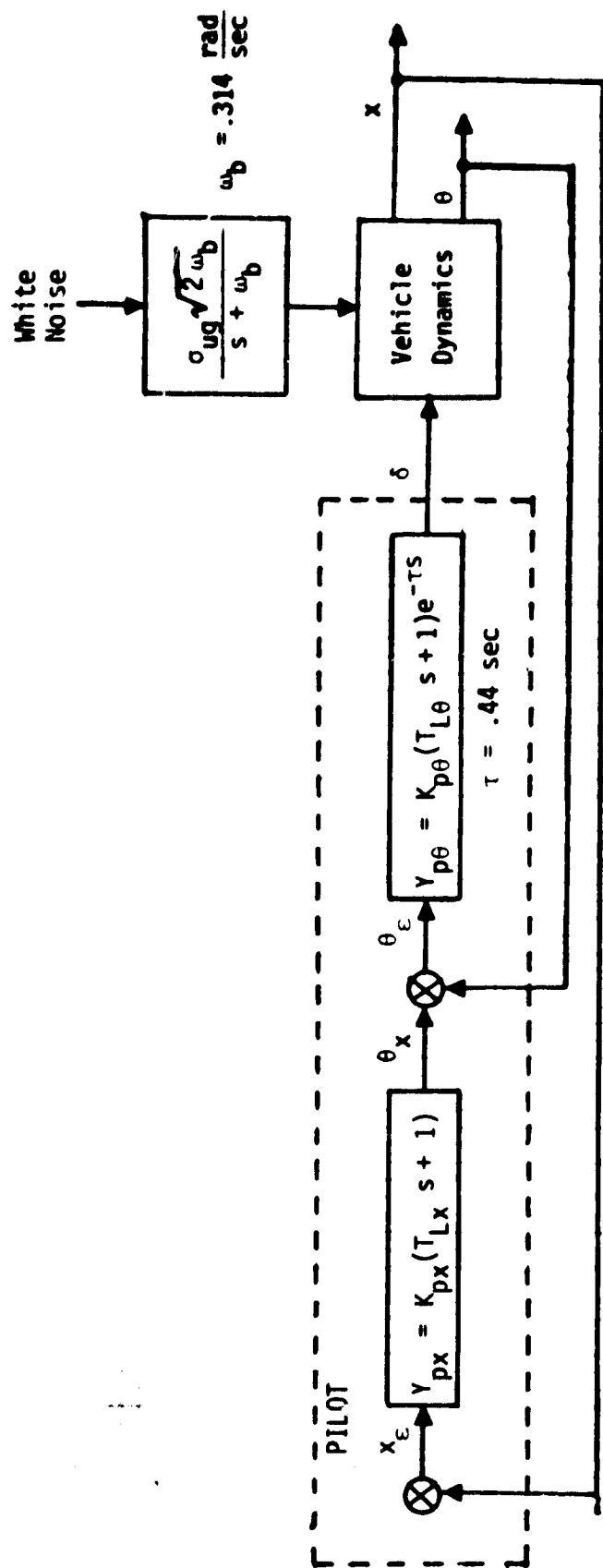
a. Pilot/Vehicle Model
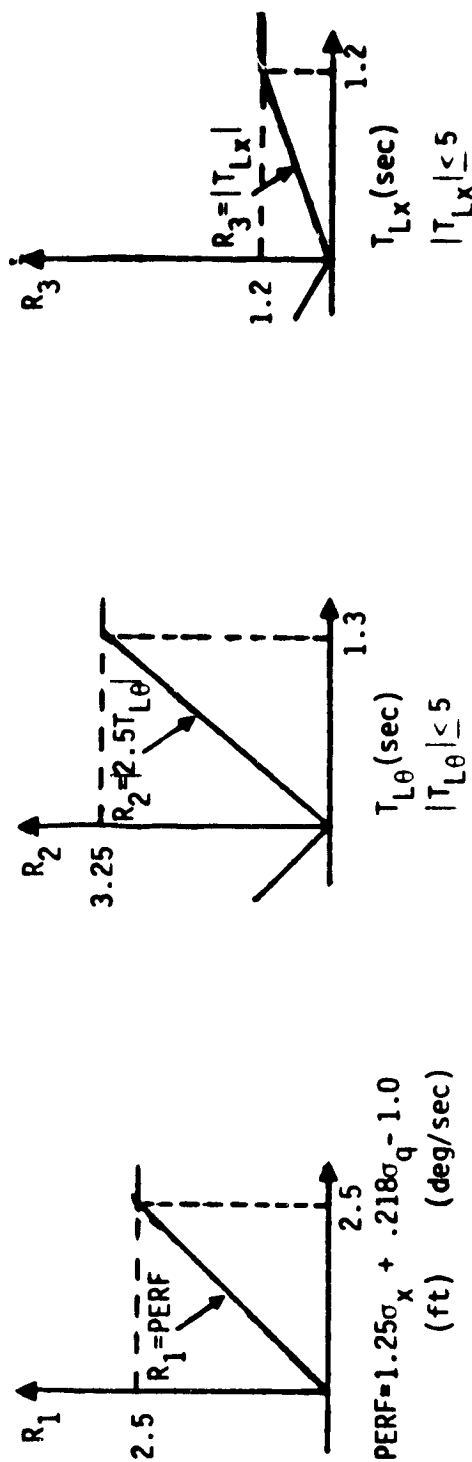
b. Pilot Rating Functional: $R = 1 + R_1 + R_2 + R_3$; Here $J = R_1$ and $W = R_2 + R_3$

Figure 18. Application of the "Paper Pilot" to a Hover Task [10]

57

inputs). Note, that implicit in the definition of the performance index
I is the partition into the two components of system performance J and
pilot workload W as

$$J = E\left\{\lim_{T\to\infty} \int_0^T (y^T Q y)dt\right\} \tag{16}$$

and

$$W = E\left\{\lim_{T\to\infty} \int_0^T (u^T R u)dt\right\} \tag{17}$$

These model based pilot rating functionals are usually derived for
stationary or frozen point conditions using a limited set of data. They
merely reflect the existence of a correlation between actual pilot opinion
ratings and model-based values, and should not be construed to have pre-
diction capability. The predictive capability of these model-based tech-
niques is intimately dependent upon the validity of the pilot model struc-
ture used, and the assumed values of the pertinent parameters.

The true value of the model based approach towards determining pilot
acceptance lies in the formulation of an acceptance methodology. The
weakest link is the process of selecting an appropriate pilot model for
the task under evaluation. Helicopter approach to a hover under IMC
is a very complex and demanding piloting task requiring deterministic
command maneuvers such as localizer and glideslope capture, and constant
attitude deceleration along a prescribed flight path.

Existing pilot models - namely the quasilinear describing function and
the standard optimal control models are not suitable for application to
the helicopter approach to hover task. These models have been developed
primarily for description of human input-output behavioral characteristics
in an aggregate or ensemble sense and are not suited for modeling response
to deterministic sample inputs on an individual run basis. Therefore, the
following structure for a generic dynamical model for the pilot that in-
corporates decision logic for attention allocation and control involvement
is formulated and incorporated as a module into the nonlinear covariance
computation (NCC) program. Description of the proposed model structure is
given next.

Pilot Model Formulation

The human pilot in a realistic flight control environment must con-
tinually perform the following three tasks: 1) Informating acquisition,
2) Information processing, and 3) aircraft control. Information acquisi-
tion involves the visual scanning of the cockpit displays to collect raw
data necessary for the particular flight segment. This raw data are then
processed by the human brain to generate an estimate of the significant
aircraft states. Finally, the estimated states may require further
aggregation in the form of a decision function, or decision rule, upon
which decisions regarding selection and implementation of a control
strategy are based. A pilot model incorporating these features can be
formulated as shown in the functional block diagram representation of
Figure 19. The selection of a specific form or structure for each of
the four block diagram components is assumed to be made at a higher
cognitive level (the brain) called the decision making center in Figure
19.

The pilot model formulation of Figure 19 is an attempt towards
homomorphic representation of human information acquisition, processing and
decision making behavior. This approach is significantly different from
currently used pilot models based on describing function methods and
optimal control theory. However, it is felt, that a functionally homo-
morphic model as formulated in Figure 19 is essential for analysis of
dynamic, nonlinear time varying tasks such as the helicopter decelerating
approach to a hover. Similar modeling concepts have been proposed
by investigators in Europe [14,15] and the United States [16]. The
function of the individual model components is described in the following.

Scanning Rule   The human pilot acquires primary information about the
state of the aircraft from the cockpit displays, through visual scanning
of the individual instruments. Several models for the human scanning
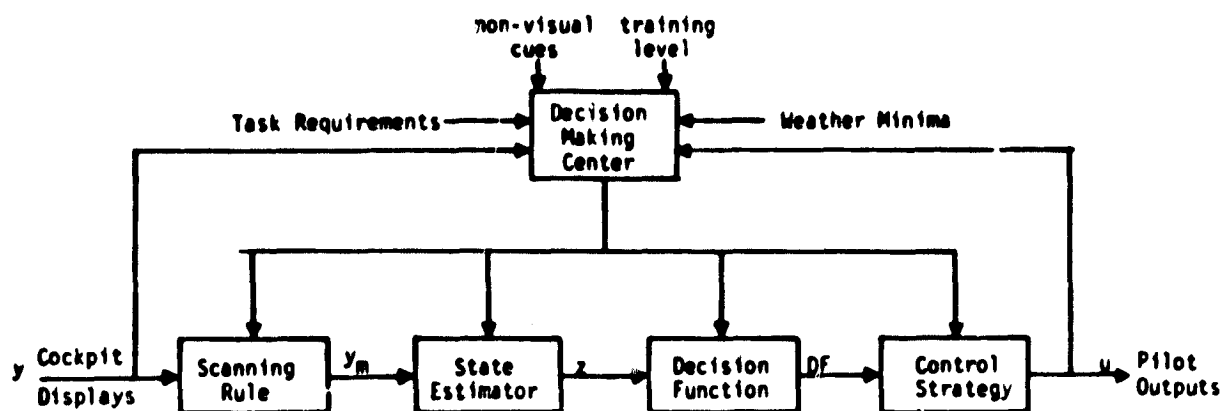strategy have been proposed in the literature [17-20]. The models are

Figure 19. Functional Model for the Human Pilot

based on information-theoretic concepts and represent various alternative hypotheses for human visual sampling behavior. However, formulation of a scanning rule is an intrinsic part of human pilot behavior, and, therefore, must be included in any realistic pilot model.

State Estimator   The raw data y_m obtained through scanning the aircraft instruments must be processed to estimate a state vector z which may consist of display variables as well as additional states such as the aircraft angular velocities not directly displayed on the cockpit panel.

Decision Function   The decision function DF consists of an aggregation of the estimated state variables in z, and is used in the selection of a control strategy for the given task. The human pilot has a choice of applying control in one or more axes, either simultaneously or sequentially. The

60

decision function reflects the degree of urgency or seriousness of each control axis in terms of its need for pilot corrective action or control inputs. Decision functions have otherwise been referred to as urgency functions by Onstott [16] or instantaneous seriousness functions by Cavalli [15].

Control Strategy Several control strategies are available tc the human pilot, ranging from simulataneous, continuous or intermittent, involvement in all control axes, to sequential and infrequent control based on the urgency for corrective action.

Decision Making Center The purpose of the decision center is to perform the high level supervisory task of coordinating the individual component functions in an efficient manner. The decision center has the authority to modify the scanning rule, the state estimator structure, the decision function formulation and the control strategy selection criteria depending upon the overall task requirements.

A framework for describing human pilot information processing, control and decision making response characteristics has been proposed. Utility of this approach to the determination of system performance, pilot workload and eventually pilot acceptance of a helicopter precision approach to a hover task is considered in the next section.

Application to the Helicopter
Approach and Landing Task

The purpose of this section is to demonstrate the applicability of the generic pilot model structure proposed above to a realistic flight control task as evidenced in a helicopter decelerated approach to a hover under IMC. The CSS/FD mode in the SPIFR simulation experiments is used to illustrate the key concepts.

61

The helicopter pilot uses information from the available cockpit displays to generate the appropriate control commands to the aircraft, so as to accomplish the desired flight control task objectives. In the CSS/FD mode, the pilot has three flight director inputs corresponding to the pitch, roll and collective axes. For the purpose of this study, the pilot model is restricted to single-input/single-output representations for each of the three control axes. The general structure of the single-axis pilot models is shown in Figure 20, where (x_i, u_i) $i = 1,2,3$ represent the three equivalent flight director inputs and corresponding pilot command outputs for the pitch, roll and collective axes, respectively.

In the raw data mode, the three equivalent inputs x_i must be treated as some linear or non-linear combination of the appropriate raw data signals. For example the roll and vertical axes equivalent inputs x_2 and x_3 in the raw data mode could easily be justified as the raw localizer and glide slope errors or filtered through some form of a dynamic compensator (e.g., lead network). The pitch axis equivalent input x_1 is more difficult to hypothesize. However, it may be reasonable to assume that the human pilot has developed some internal model for the desired velocity profile as a function of the radio altitude. This may be justified because the pilot does not have ground speed (or range rate) or range from hover pad available in the SPIFR simulation and must therefore rely on some form of heuristic relationship between airspeed V_A and radio altitude h (above hover pad). Errors must be expected in the presence of wind and due to non-zero glide slope tracking errors. An equivalent fourth directional flight director signal must be synthesized for the basic helicopter mode.

The model allows for two independent periodic samplers S_d and S_c - one on the display variables called the display sampler (S_d) and another on the pilots control output (S_c). The human pilot does not necessarily apply corrective control inputs to the aircraft at the same rate at which information from the display variables is being obtained. Thus, control sampling rates reflecting degree of pilot involvement in the control task need not be identical, and may in fact be lower than display sampling rates. For mathematical convenience, the two samplers S_c and S_d are assumed to operate at sampling intervals T_c and T_d, respectively, such that $T_c = (\text{integer})T_d$. The subsequent analyses are based on the assumption that pilot workload is related to the degree of pilot involvement in the information acquisition,
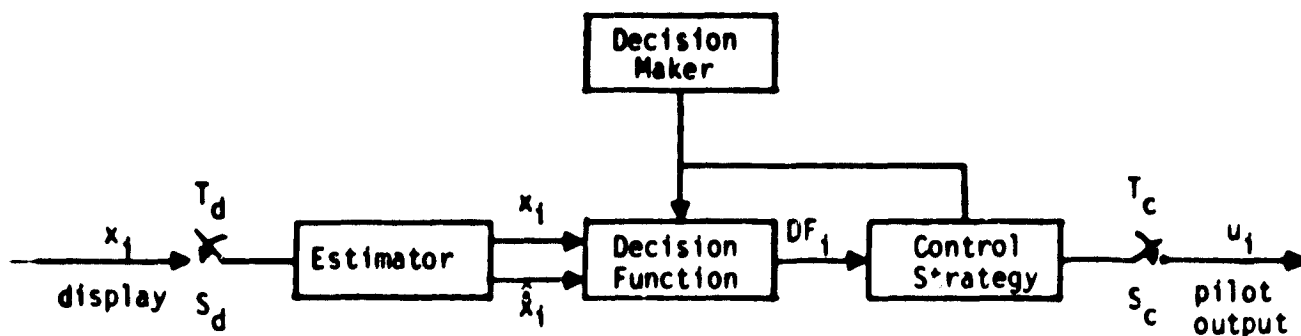
62

Figure 20.   Single Axis Pilot Model Structure

processing and control tasks.

Dynamic compensators in the form of the classical describing function model (gain, lead/lag and time delay) are allowed between the pilot's command outputs u_i and aircraft control inputs.

Several options are available to the supervisory decision maker in selecting the appropriate control strategy as described below.

Strategy Option 0:   (ISTRAT = 0) Independently adjustable and periodic control sampling rates

This option permits simultaneous control of all three axes with different levels of control involvement. Thus, if DTP $\triangleq$ integration step size, then the level of control involvement as defined by the control sampling period T_c (i.e., sampling intervals at which display variable is used for control purposes) in the pitch roll and vertical axes may be selected to be (INPTCH*DTP), (INROLL*DTP) and INCOLL*DTP) seconds, respectively, where the three multipliers INPTCH, INROLL and INCOLL are constrained to be positive integers. In this option, the estimator and decision function element are absent.

The maximum control sampling rate, $f_c = \frac{1}{T_c}$, for each axis is (1/DPT) Hz. Typically, the pilot aircraft system tends to become less stable with decreasing sampling frequency. Some adjustment, usually a reduction in the corresponding pilot gain K is required to increase the stability boundaries.

63

Strategy Option 1: (ISTRAT = 1) Single channel hypothesis with
state dependent control sampling rates

This strategy is based upon the assumption that the human pilot can
only operate one control at any given time with the others in hold or
slowly decaying towards trim condition. A higher level decision logic
is assumed for switching between the 3 axes and a possible fourth mode
corresponding to an auxiliary task or any other activity. The decision
logic assumed decision functions DF_i (i = 0,1,2,3) for each axis as
follows (from Onstott - reference 16):

$$DF_i = |\alpha_{x_i}|\hat{x}_i| + \beta_{x_i} sgn(\hat{x}_i)\hat{\hat{x}}_i| \quad , \quad i = 1,2,3 \tag{18}$$

$$= UMAX \quad , \quad i = 0 \tag{19}$$

The allocation rule is to choose axis i for active control if

$$DF_i = \underset{j = 0,1,2,3}{Max} |DF_j| \tag{20}$$

with the remaining control outputs in hold or exponentially decaying to
trim with some time constant. Only the collective controls is put in
hold; the pitch and roll cyclic control are set to decay towards their
trim values. The decision function DF_0 = UMAX may be used as a measure
for the reserve attention capacity of the pilot. If UMAX = 0, attention
is shared, one axis at a time, between the pitch, roll and vectical con-
trol axes, depending upon which of the 3 decision functions DF_i is largest.
A very large value for UMAX would result in essentially open loop control
of the aircraft and would lead to instability. The largest value of UMAX
allowable within allowable performance constraints on all 3 axis serves
as a measure of reserve attention capacity and hence pilot workload.

The decision function computation and comparison may be carried out
every sample (DTP seconds) or every (INUMB2*DTP) seconds where INUMB2 can
be set to any positive integer value.

64

An option is provided whereby the continuous control involvement in any one axis is limited to a prescribed time or consecutive number of samples INUMB3 after which the control must be switched to one of the remaining alternatives according to the same decision function rule.

In addition control sampling rates reflecting degree of pilot involvement in the axis under active control may also be adjusted by manipulating the appropriate multipliers INPTCH, INROLL and INCOLL.

Strategy Option 2: (ISTRAT = 2) Simultaneous control of all axis
                   with state dependent control sampling rates

This control strategy is akin to control strategy 1 with the exception that all three control axes may operate independently. The decision functions DF_i are defined as in option 1. The attention allocation rule operates on each axis independently of the others. Decision to control axis i is made if

$$DF_i \geq ULIM_i \qquad\qquad i = 1,2,3 \qquad\qquad (21)$$

Thus, at any given time none, one, two or all three axes may be under active control. The limits $ULIM_i$ represent threshold values for deciding between active control of axis i or open loop control.

As in option 1, the periodic interval at which the decision functions are calculated and compared to their respective thresholds is adjustable by varying the positive integer INUMB2.

Candidate Pilot Workload Metrics

Pilot workload may be assumed to depend upon the minimum required level of pilot involvement in the information acquisition and control actuation tasks for a given acceptable level of system performance. Three different hypotheses or options have been presented as candidates for describing human pilot input-output characteristics. Consequently, three different workload metric vectors may be defined corresponding to the three options as follows.

65

Option 0: Here the model parameters INPTCH, INROLL and INCOLL specify the control sampling intervals in the pitch, roll and vertical axis. Pilot workload in the pitch axis may be assumed to be inversely related to the maximum allowable sampling interval INPTCH for a given level of longitudinal system performance. Similar relationships apply to the roll and vertical axis. Thus workload metrics for each o. the three control axes may be defined as

$$WLPTCH = h_1 (INPTCH)$$
$$WLROLL = h_2 (INROLL)$$
$$WLCOLL = h_3 (INCOLL)$$
(22)

where h_1, h_2 and h_3 are inverse monotonic functions of their respective arguments. Total pilot workload WL may be defined as some linear or nonlinear function of the individual workload metrics; thus

$$WL = h(h_1, h_2, h_3)$$
(23)

Option 1: This option is characterized by decision functions DF_i, $i = 1,2,3$ and the reserve attention capacity measure $DF_0 = UMAX$. Thus, UMAX may be used as a workload index for the overall task. Relative workload of the three control axes may be defined as in Option 0 in terms of the relative fractions of the total time spent on each axis. These numbers must be obtained through Monte Carlo simulation of the NCC program.

Option 2: This option allows for simultaneous control of one or more axes depending upon the values chosen for the three decision function limits $ULIM_i$, $i = 1,2,3$. Pilot workload may again be defined in terms of the relative attention requirements of each axis for a given level of system performance. These fractions of total time spent on each axis must be obtained through Monte Carlo computer simulation of the NCC program.

Model Simulation Results

The generic dynamical model for the pilot as described above was in-
corporated as a module into the nonlinear covariance computation (NCC) pro-
gram. A program description in the form of a flowchart is given in the
Appendix. A flowchart and listing of subroutine F2T incorporating the
pilot decision/control logic subroutine DECSN is also included. The three
different decision and control strategy options corresponding to ISTRAT
of 0, 1 and 2 were simulated in the CSS/flight director configuration to
study the sensitivity of the system performance to key control strategy
parameters. The different cases investigated for each mode are described
below:

1.   Strategy Option ISTRAT = 0

     The following sets of parameters were simulated.

Set No.	INPTCH	INROLL	INCOLL
1	1	1	1
2	5	5	5
3	10	10	10
4	1	5	10
5	1	10	10
6	5	10	10

Figures 21-26 show the ensemble mean and standard deviation responses for
11 key system variables.

The results demonstrate the sensitivity of the system variables to
the attention allocation parameters INPTCH, INROLL and INCOLL for the pitch,
roll and vertical axes, respectively. The ensemble plots are terminated
around the time that the system goes unstable. The parameters INPTCH,
INROLL and INCOLL provide a measure of the degree of control involvement
in the pitch, roll and vertical axes, respectively. Pilot workload may
be assumed to be related to the degree of control involvement required
to achieve a prescribed level of performance. Decreasing the control

ISTRAT = 0, ICARLO = 10,

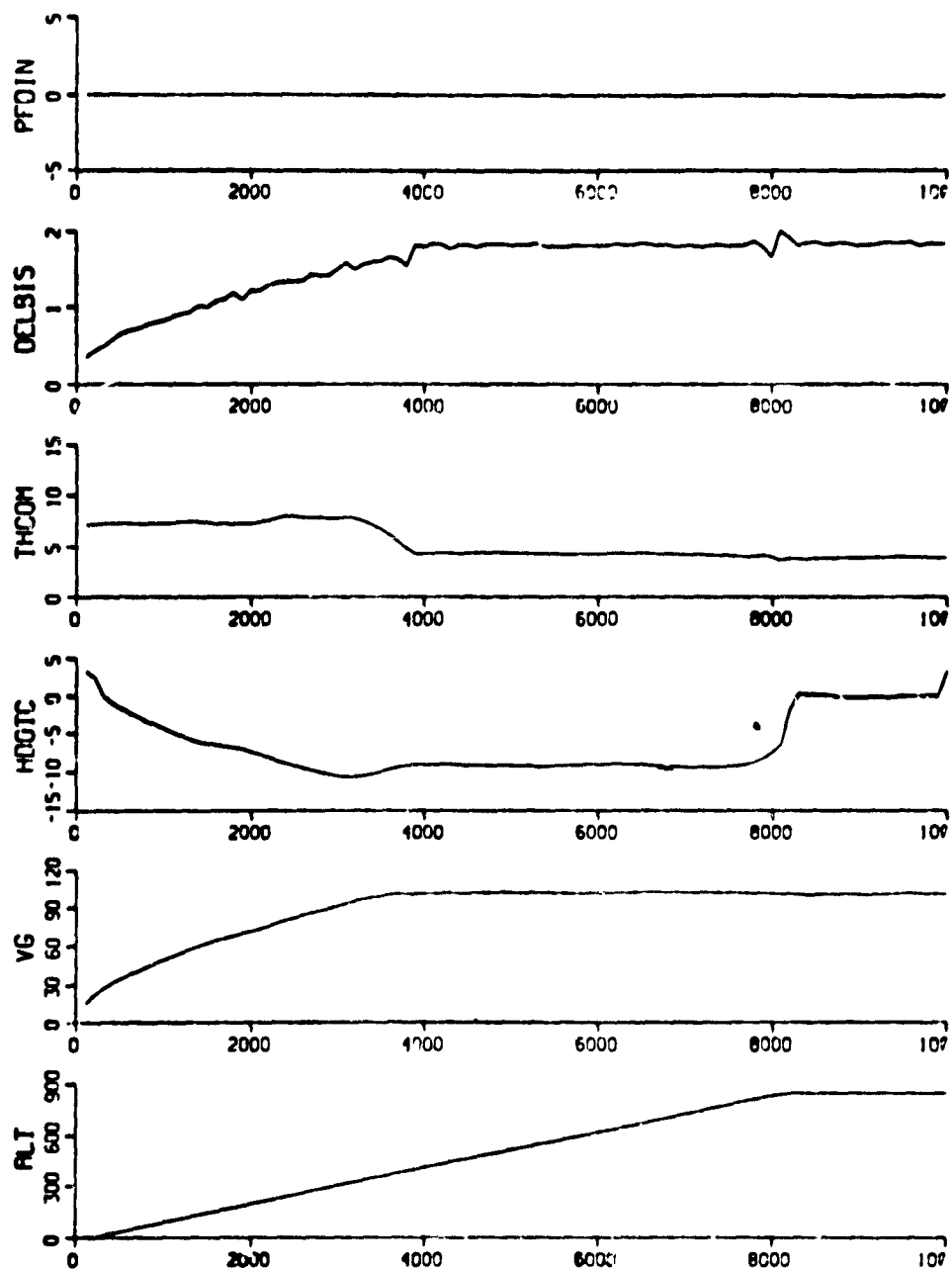INPTCH = INROLL = INCOLL = 1
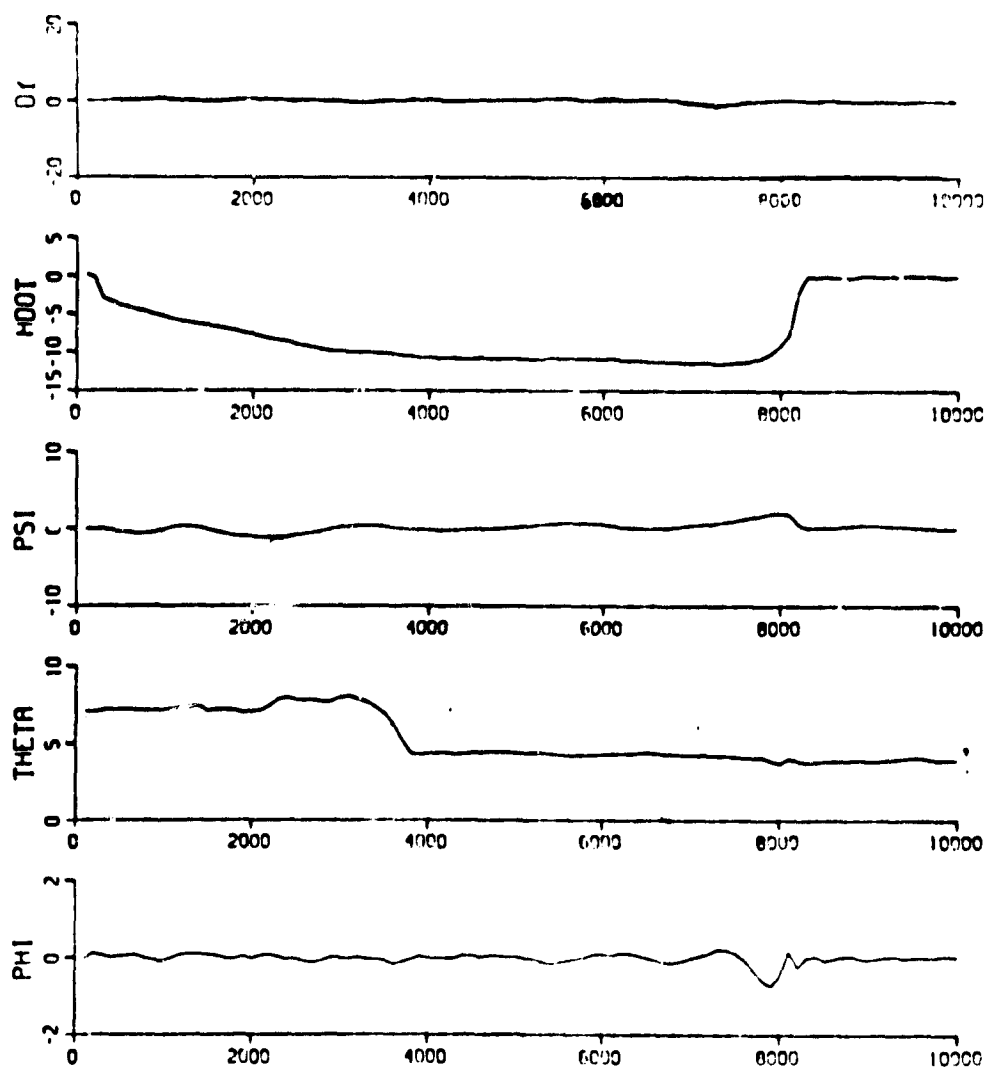
a.) Mean

Figure 21. NCC Program Simulation Results: CSS/FD/WIND/DH = 0 ft
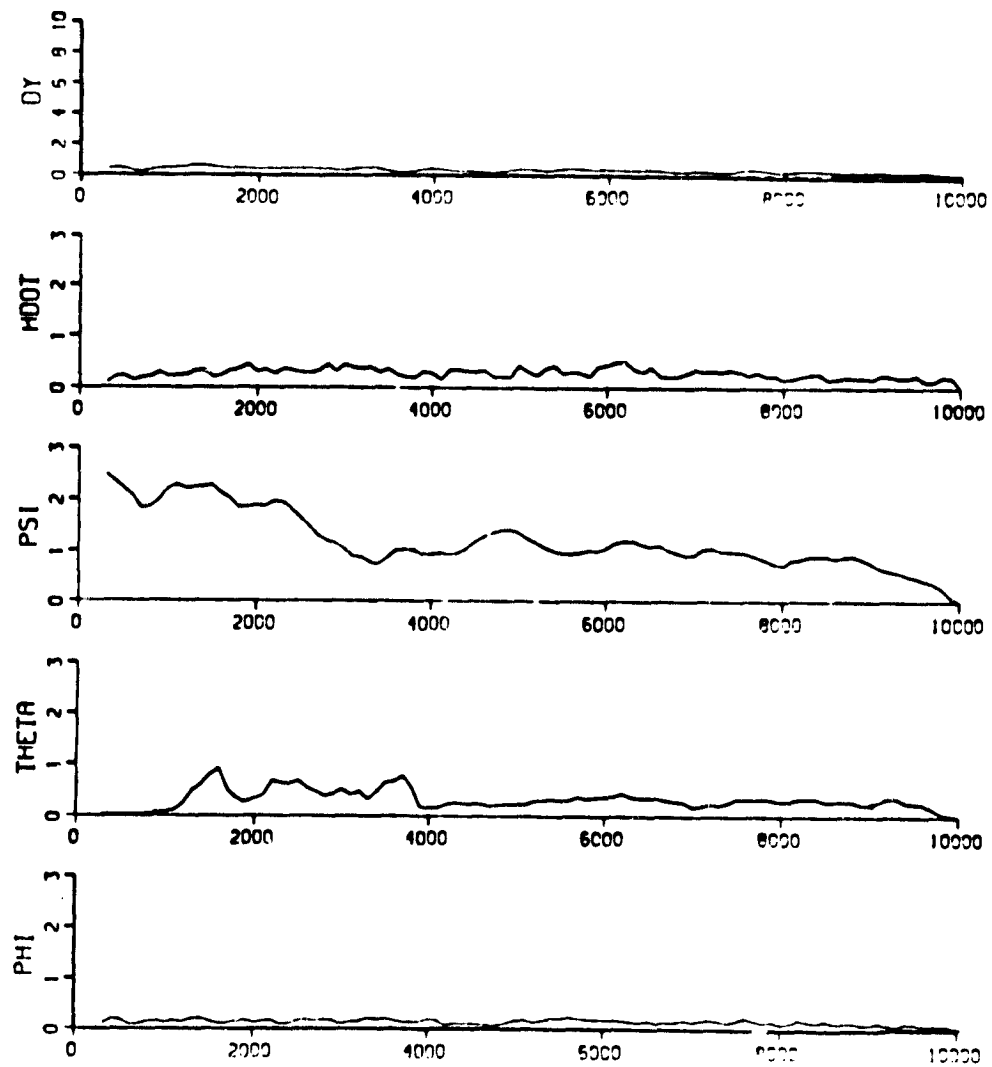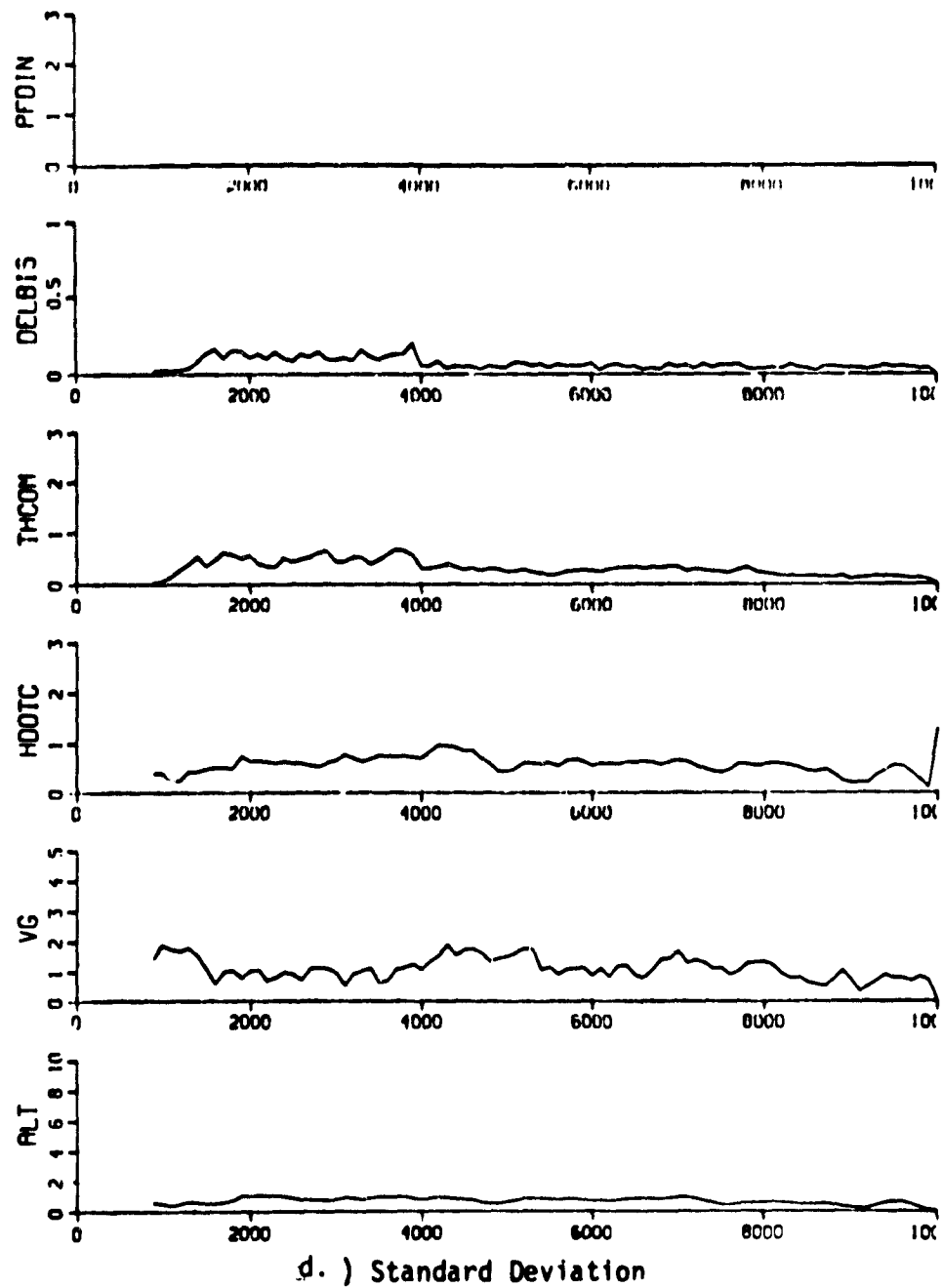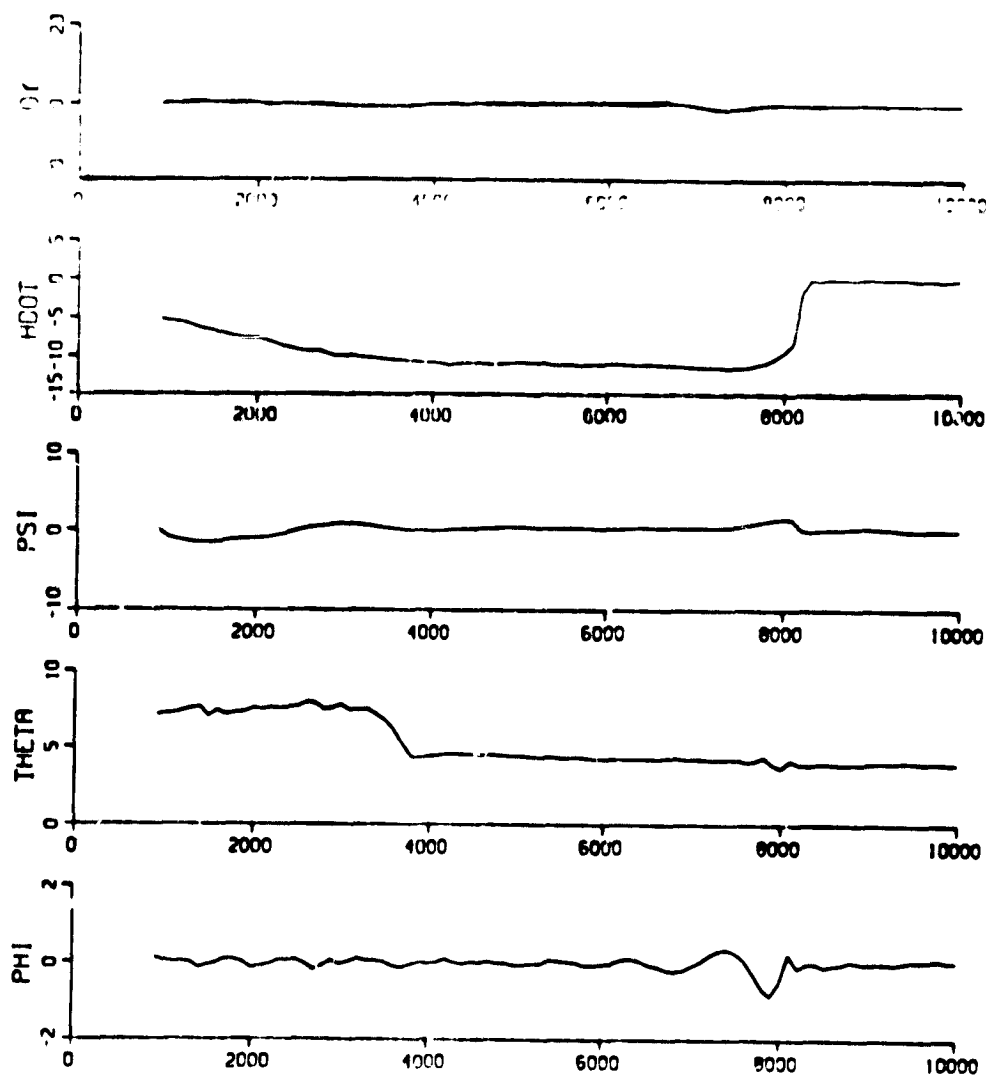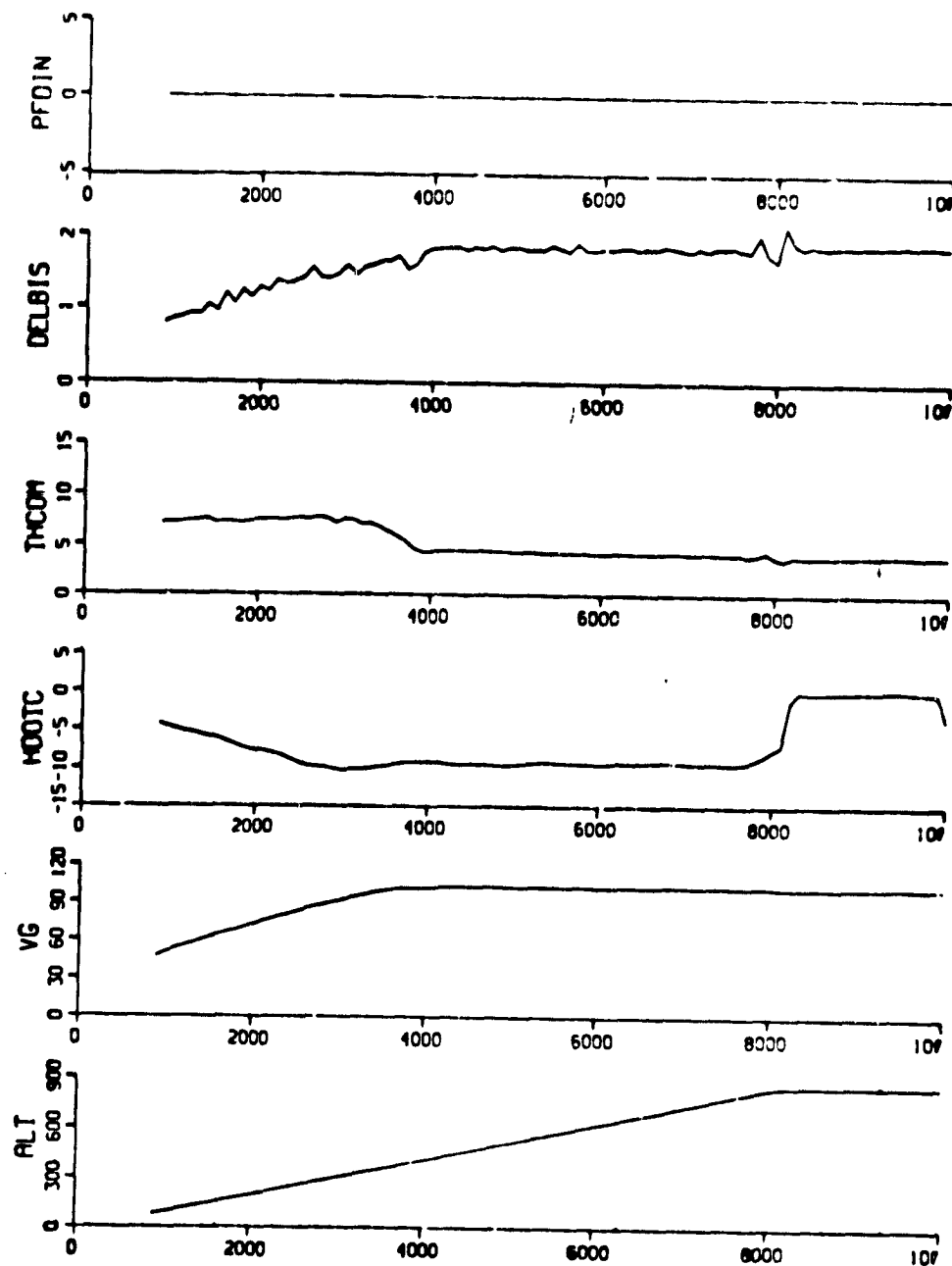
ISTRAT = 0, ICARLO = 10,

INPTCH = INROLL = INCOLL = 1

b.) Mean

Figure 21. NCC Program Simulation Results: CSS/FD/WIND/DH = 0 ft

ISTRAT = 0, ICARLO = 10,

INPTCH = INROLL = INCOLL = 1

c.) Standard Deviation

Figure 21. NCC Program Simulation Results: CSS/FD/WIND/DH = 0 ft

ISTRAT = 0, ICARLO = 10,

INPTCH = INROLL = INCOLL = 1

d.) Standard Deviation

Figure 21.   NCC Program Simulation Results: CSS/FD/WIND/DH = 0 ft

71

ISTRAT = 0. ICARLO = 10,

INPTCH = INROLL = INCOLL = 5

a). Mean

Figure 22. NCC Program Simulation Results: CSS/FD/WIND/DH = 0 ft

72

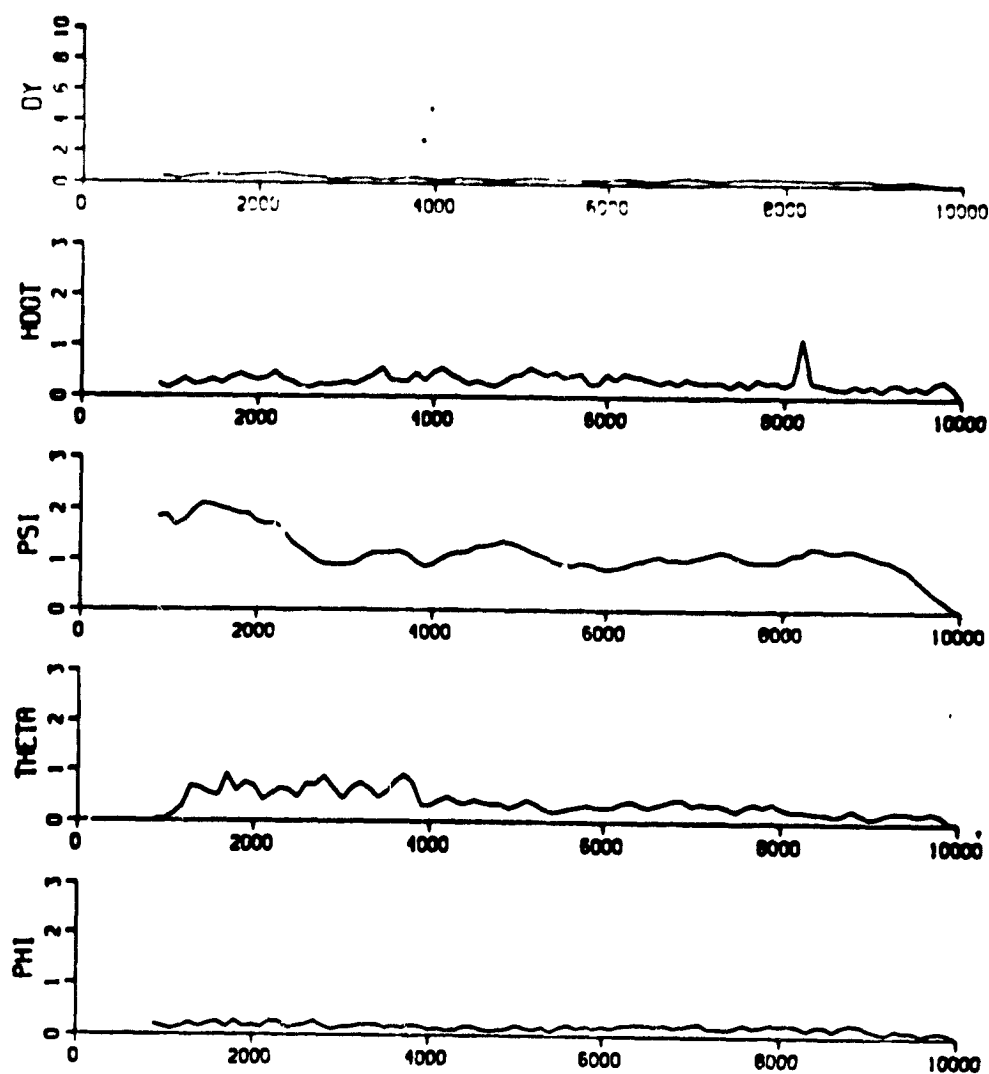ISTRAT = 0, ICARLO = 10,

INPTCH = INROLL = INCOLL = 5

b.) Mean

Figure 22.   NCC Program Simulation Results: CSS/FD/WIND/DH = 0 ft

73

INSTRAT = 0, ICARLO = 10,
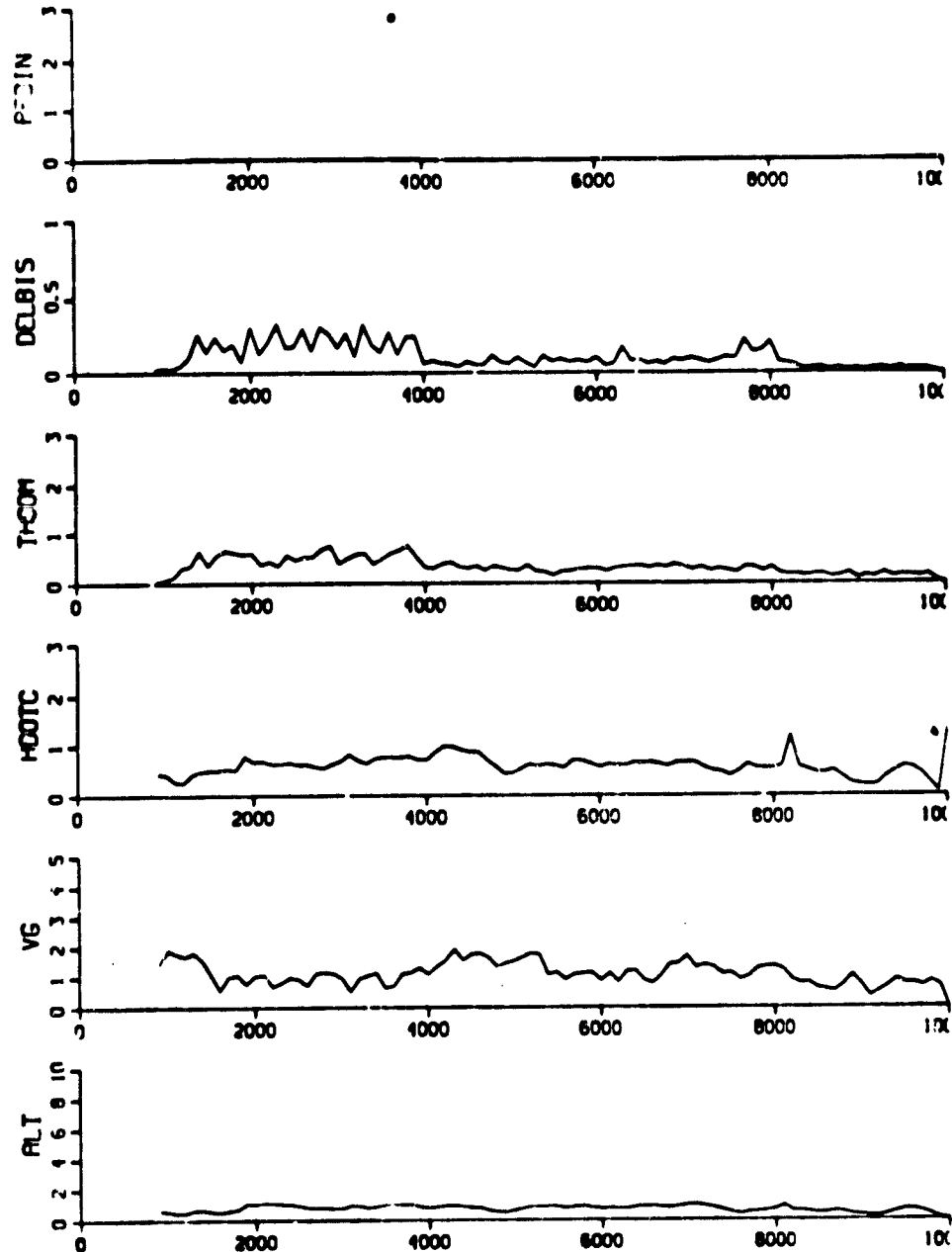
INPTCH = INROLL = INCOLL = 5

c.) Standard Deviation

Figure 22. NCC Program Simulation Results: CSS/FD/WIND/DH = 0 ft

74

ISTRAT = 0, ICARLO = 10,
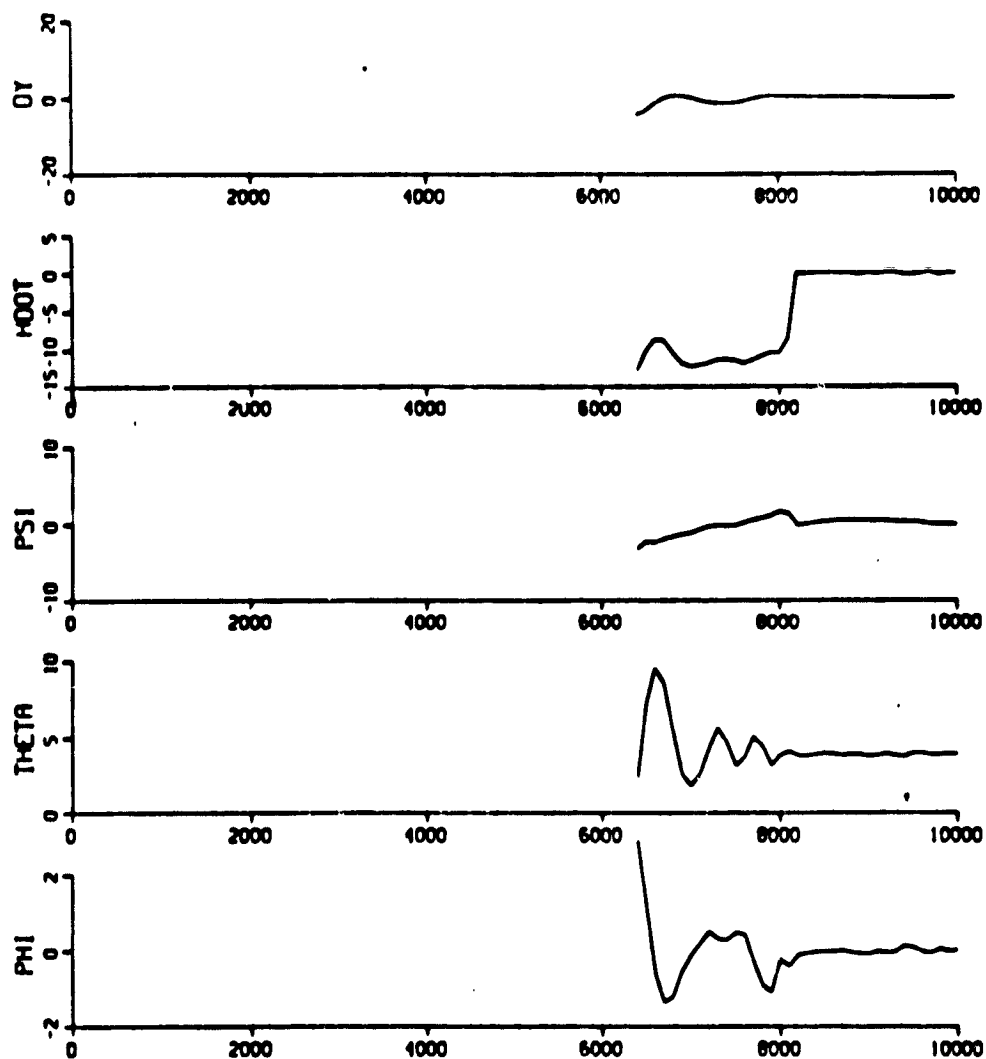
INPTCH = INROLL = INCOLL = 5

d.) Standard Deviation

Figure 22. NCC Program Simulation Results: CSS/FD/WIND/DH = 0 ft

ISTRAT = 0, ICARLO = 10,
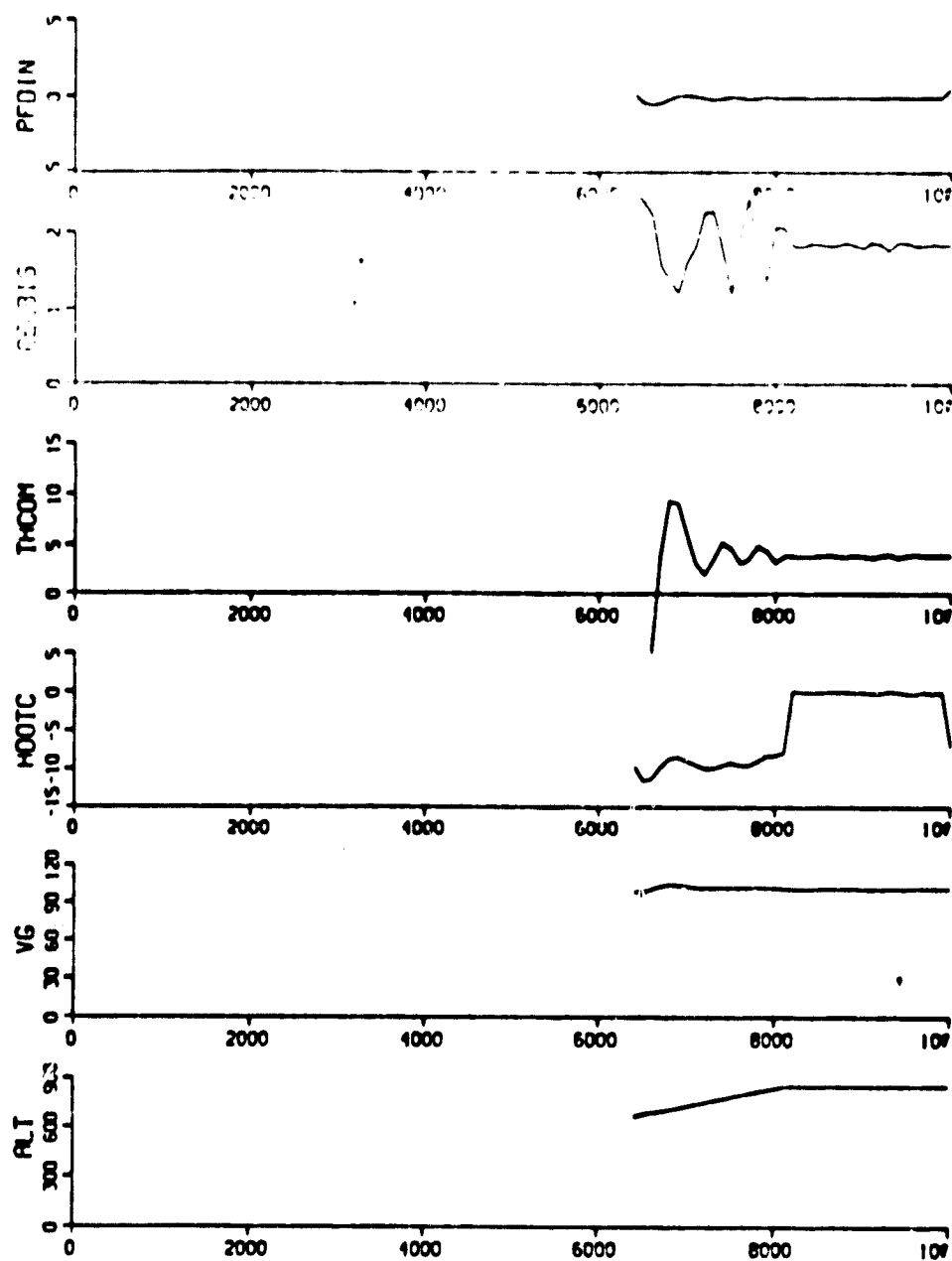
INPTCH = INROLL = INCOLL = 10

a.) Mean

Figure 23. NCC Program Simulation Results: CSS/FD/WIND/DH = 0 ft

ISTRAT = 0, ICARLO = 10,
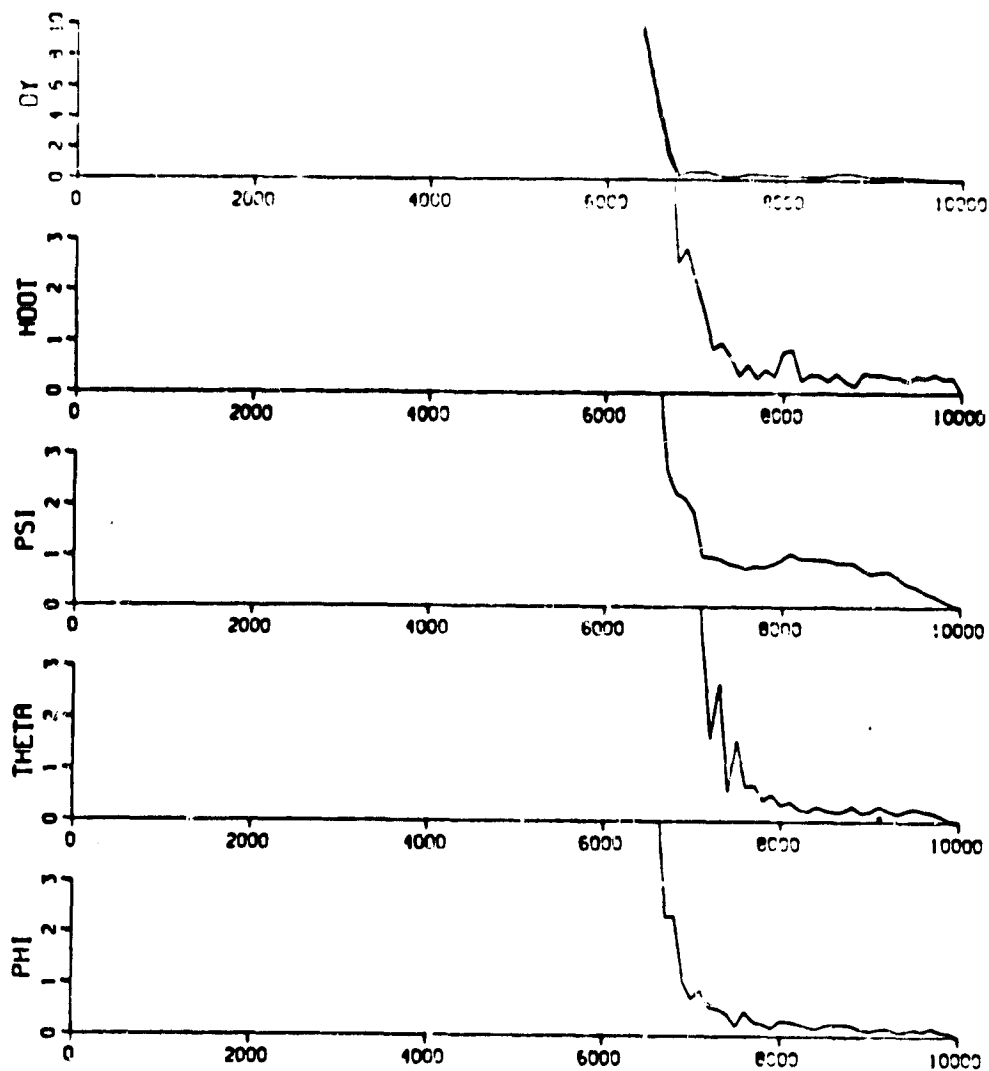
INPTCH = INROLL = INCOLL = 10

b.) Mean

Figure 23.   NCC Program Simulation Results: CSS/FD/WIND/DH = 0 ft

77

ISTRAT = 0, ICARLO = 10
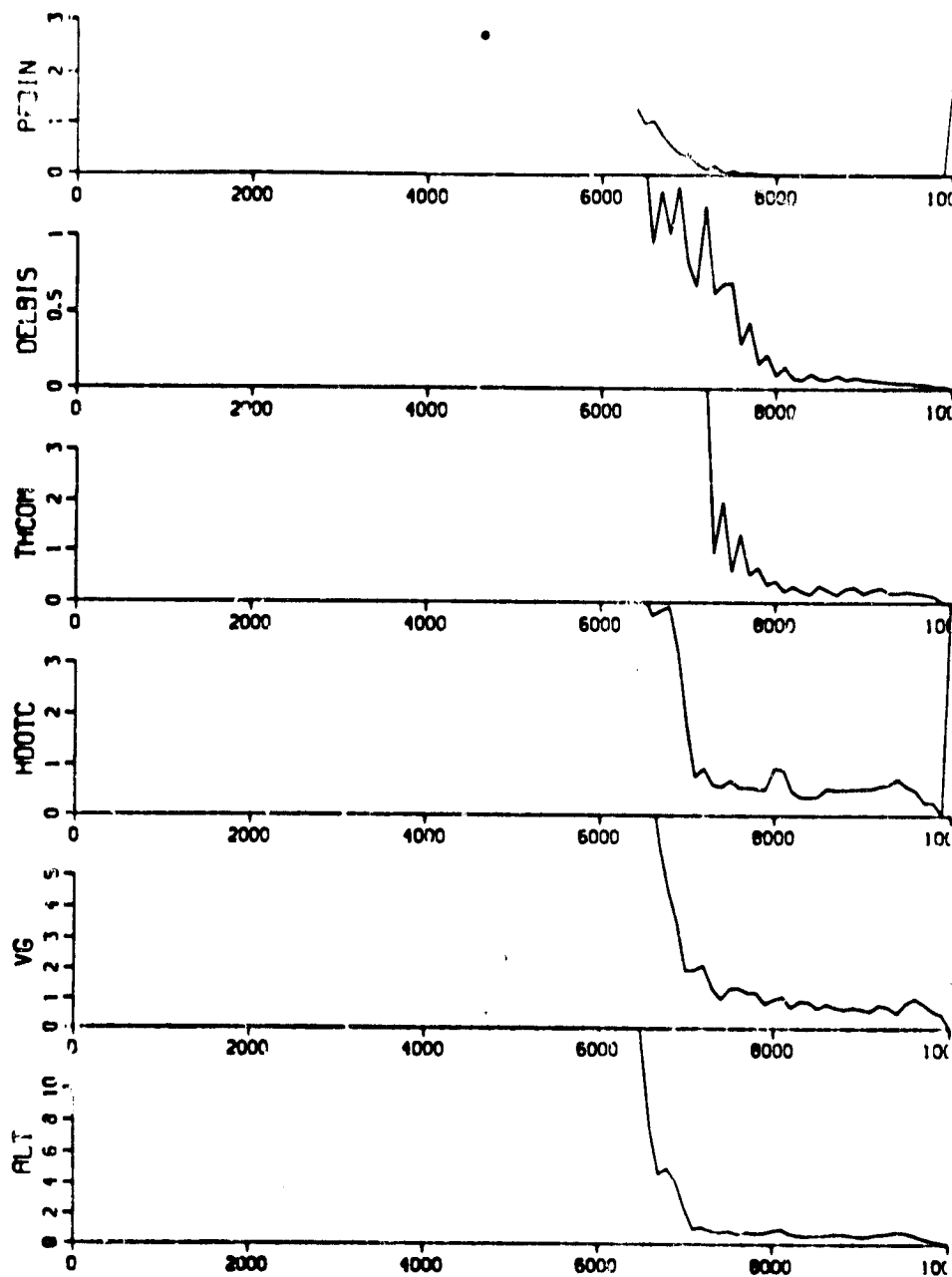
INPTCH = INROLL = INCOLL = 10

c.) Standard Deviation

Figure 23. NCC Program Simulation Results: CSS/FD/WIND/DH = 0 ft

IS⁻RAT = 0, ICARLO = 10

INPTCH = INROLL = INCOLL = 10

d.) Standard Deviation

Figure 23. NCC Program Simulation Results: CSS/FD/WIND/DH = 0 ft

79

INSTRAT = C, ICARLO = 10,

INPTCH = 1, INROLL = 5, INCOLL = 10

a.) Mean

Figure 24. NCC Program Simulation Results: CSS/FD/WIND/DH = 0 ft

80

ISTRAT = 0, ICARLO = 10,

INPTCH = 1, INROLL = 5, INCOLL = 10

b.) Mean

Figure 24.   NCC Program Simulation Results: CSS/FD/WIND/DH = 0 ft

81

ISTRAT = 0, ICARLO = 10,

INPTCH = 1, INROLL = 5, INCOLL = 10

c.) Standard Deviation

Figure 24. NCC Program Simulation Results: CSS/FD/WIND/DH = 0 ft

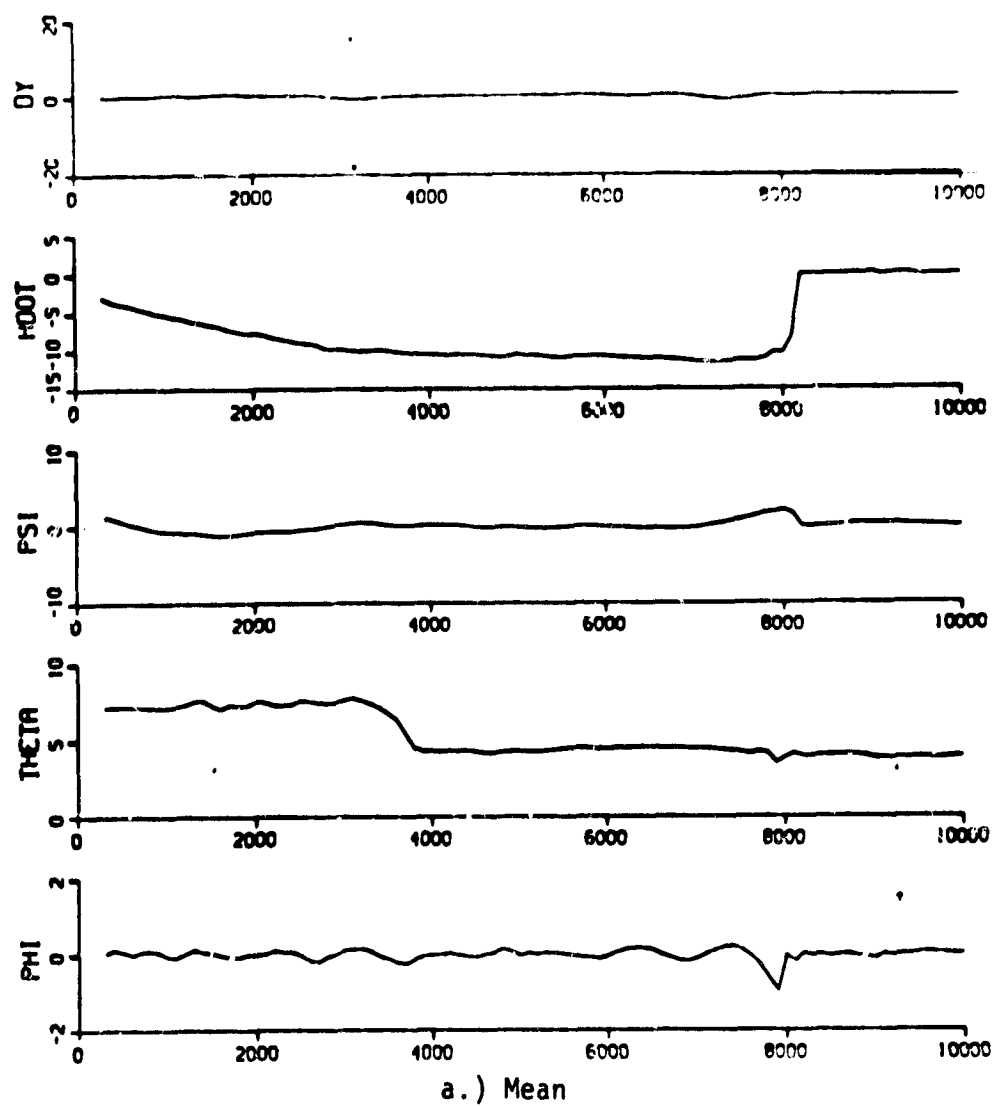ISTRAT = 0, ICARLO = 10,

INPTCH = 1, INROLL = 5, INROLL = 10

d.) Standard Deviation

Figure 24. NCD Program Simulation Results: CSS/FD/WIND/DH = 0 ft

83

ISTRAT = 0, ICARLO = 10,

INPTCH = 1, INROLL = 10, INCOLL = 10

a.) Mean

Figure 25. NCC Program Simulation Results: CSS/FD/WIND/DH = 0 ft

84

ISTRAT = 0, ICARLO = 10,
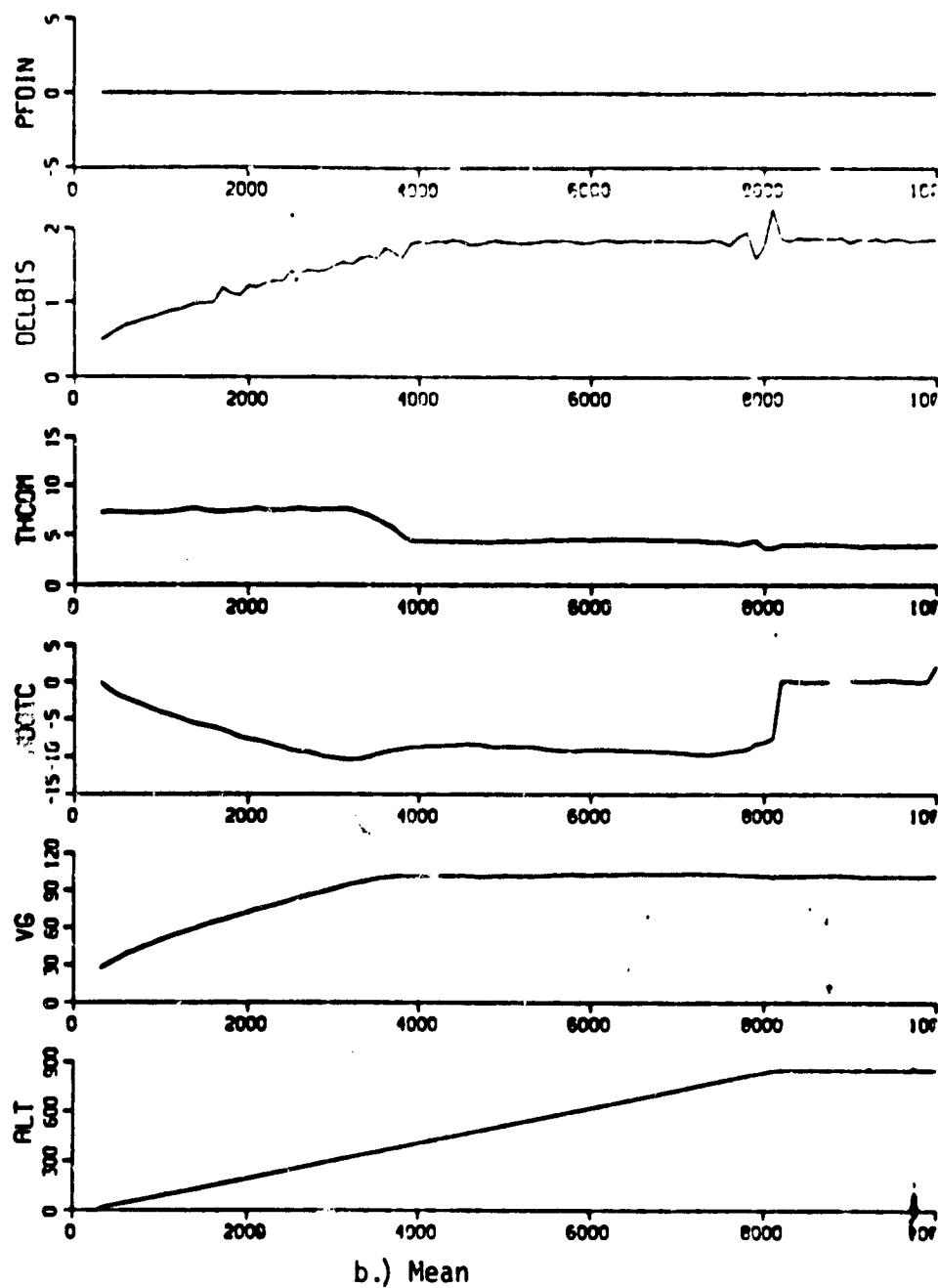
INPTCH = 1, INROLL = 10, INCOLL = 10
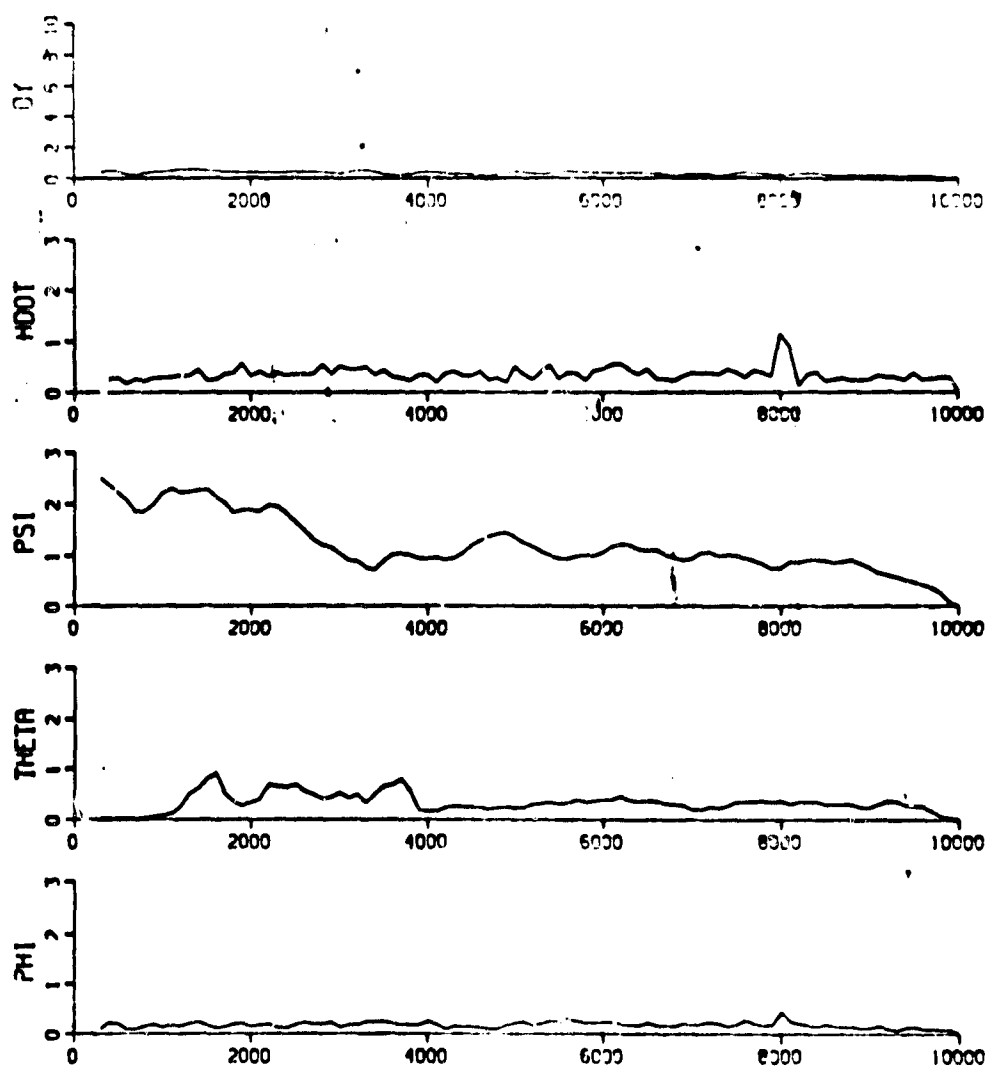

b.) Mean

Figure 25. NCC Program Simulation Results: CSS/FD/WIND/DH = 0 ft

85

ISTRAT = 0, ICARLO = 10,

INPTCH = 1, INROLL = 10, INCOLL = 10

c.) Standard Deviation

Figure 25. NCC Program Simulation Results: CSS/FD/WIND/DH = 0 ft

86

INSTRAT = 0, ICARLO = 10,

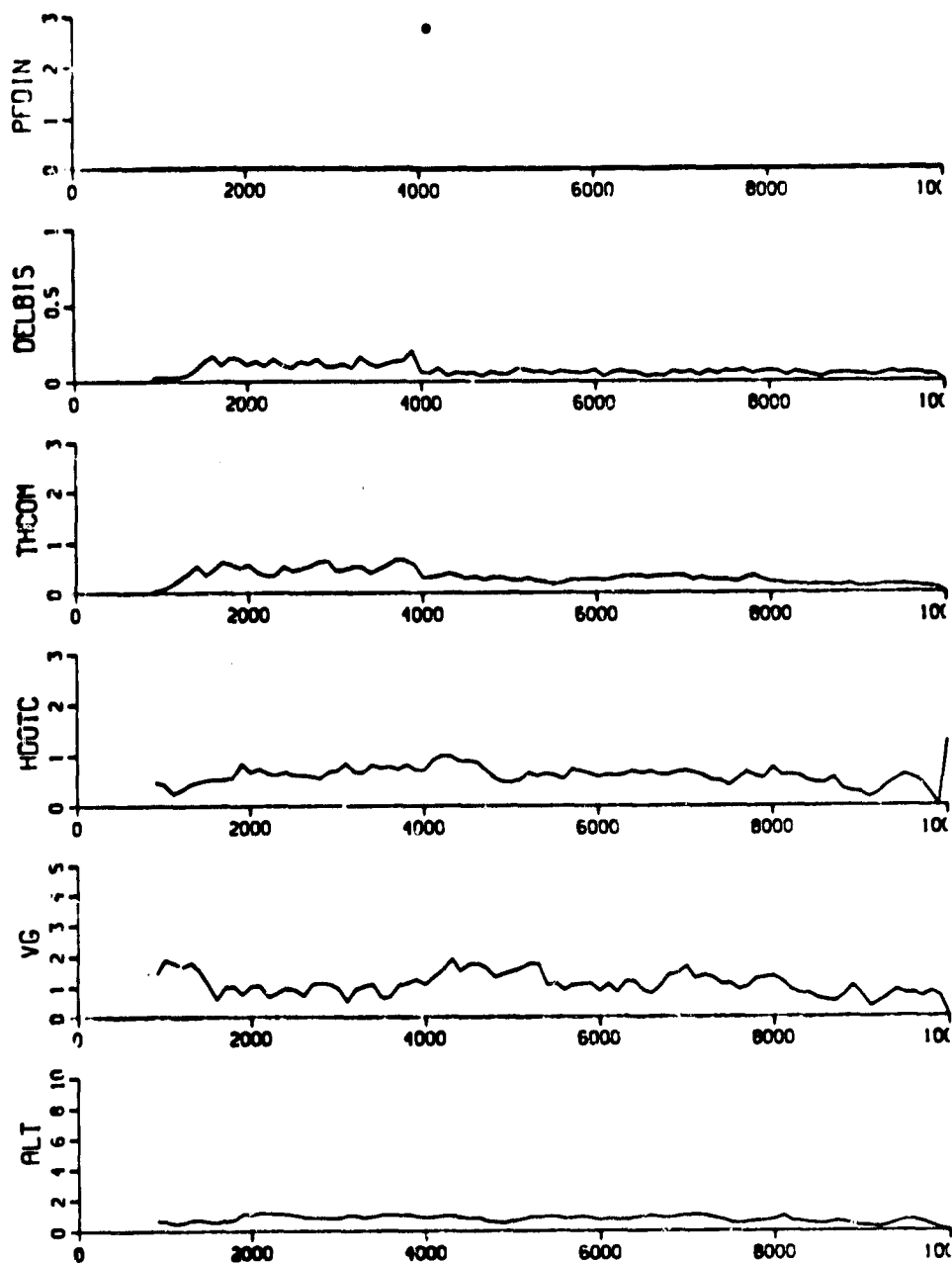INPTCH = 1, INROLL = 10, INCOLL = 10

d.) Standard Deviation

Figure 25. NCC Program Simulation Results: CSS/FD/WIND/DH = 0 ft

ISTRAT = 0, ICARLO = 10,

INPTCH = 5, INROLL = 10, INCOLL = 10

a.) Mean

Figure 26. NCC Program Simulation Results: CSS/FD/WIND/DH = 0 ft

88

ISTRAT = 0, ICARLO = 10,

INPTCH = 5, INROLL = 10, INCOLL = 10

b.) Mean

Figure 26.   NCC Program Simulation Results: CSS/FD/WIND/DH = 0 ft

ISTRAT = 0, ICARLO = 10,

INPTCH = 5, INROLL = 10, INCOLL = 10

c.) Standard Deviation

Figure 26. NCC Program Simulation Results: CSS/FS/WIND/DH = 0 ft

90

ISTRAT = 0, ICARLO = 10,
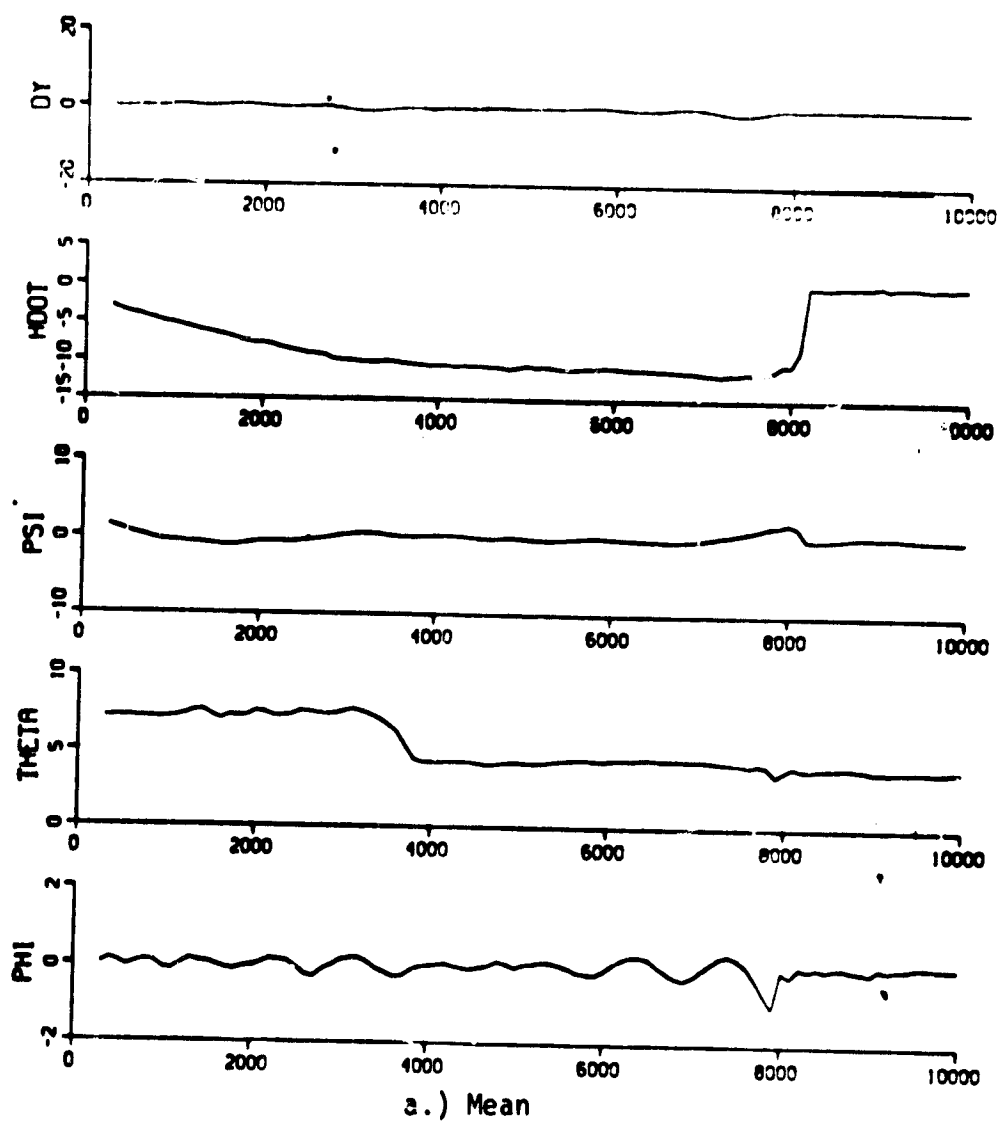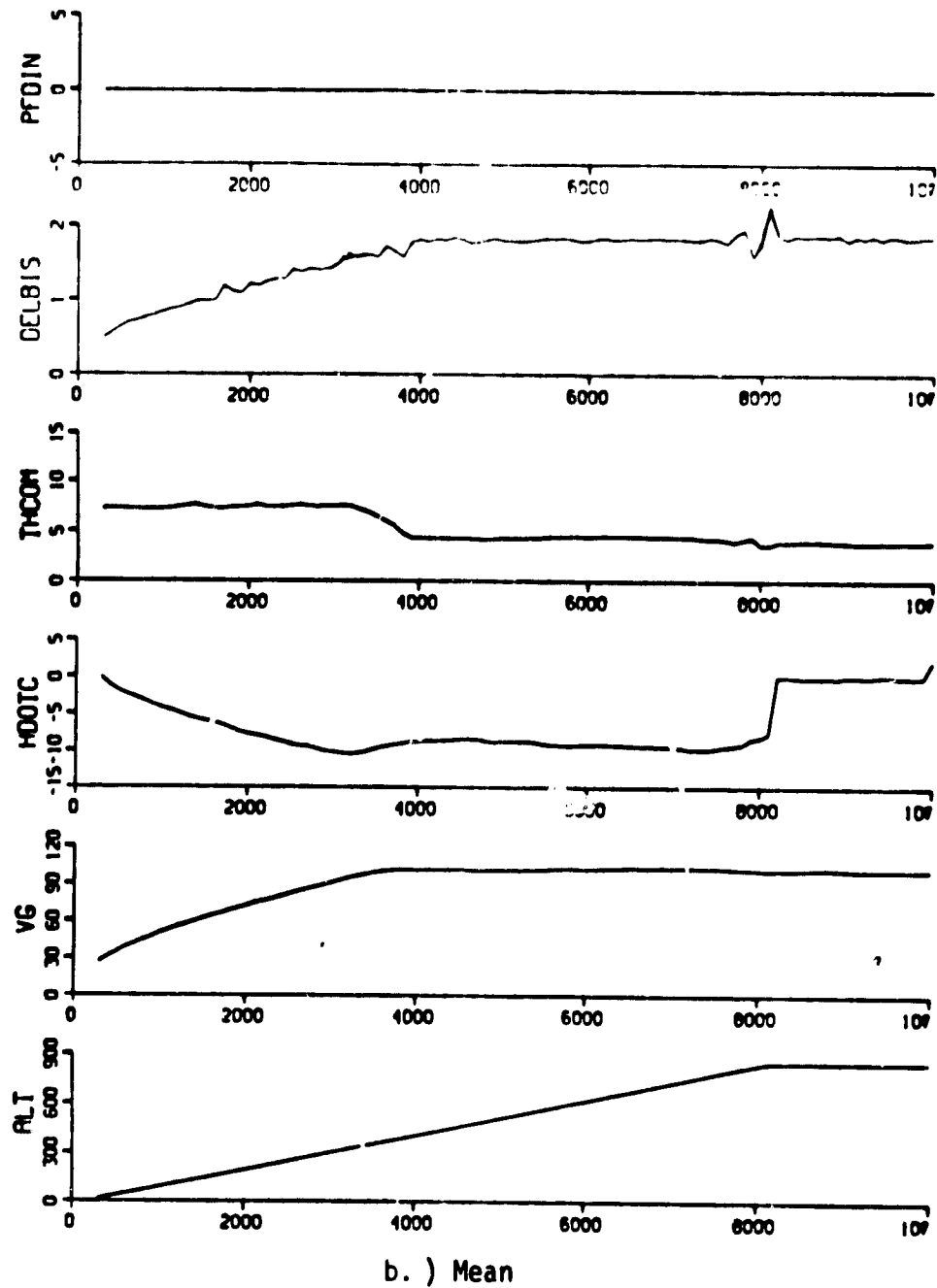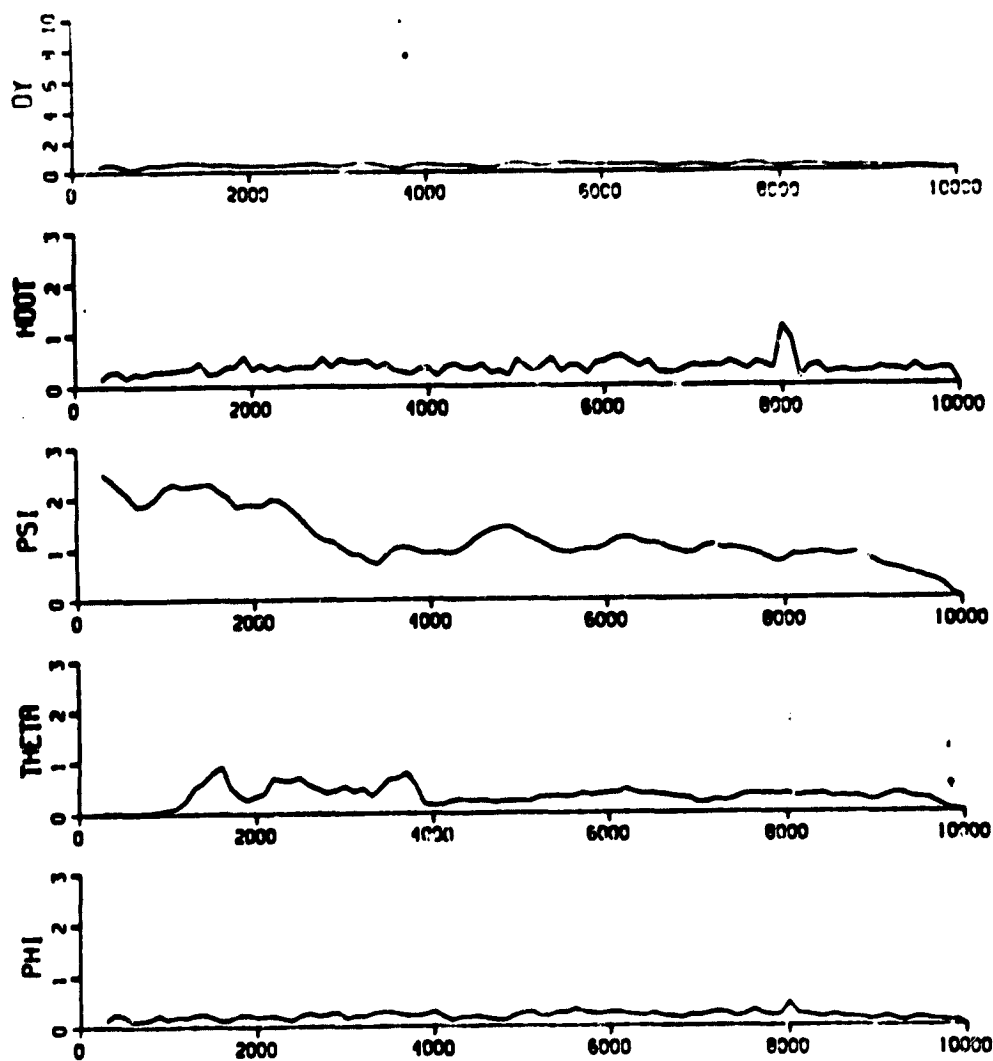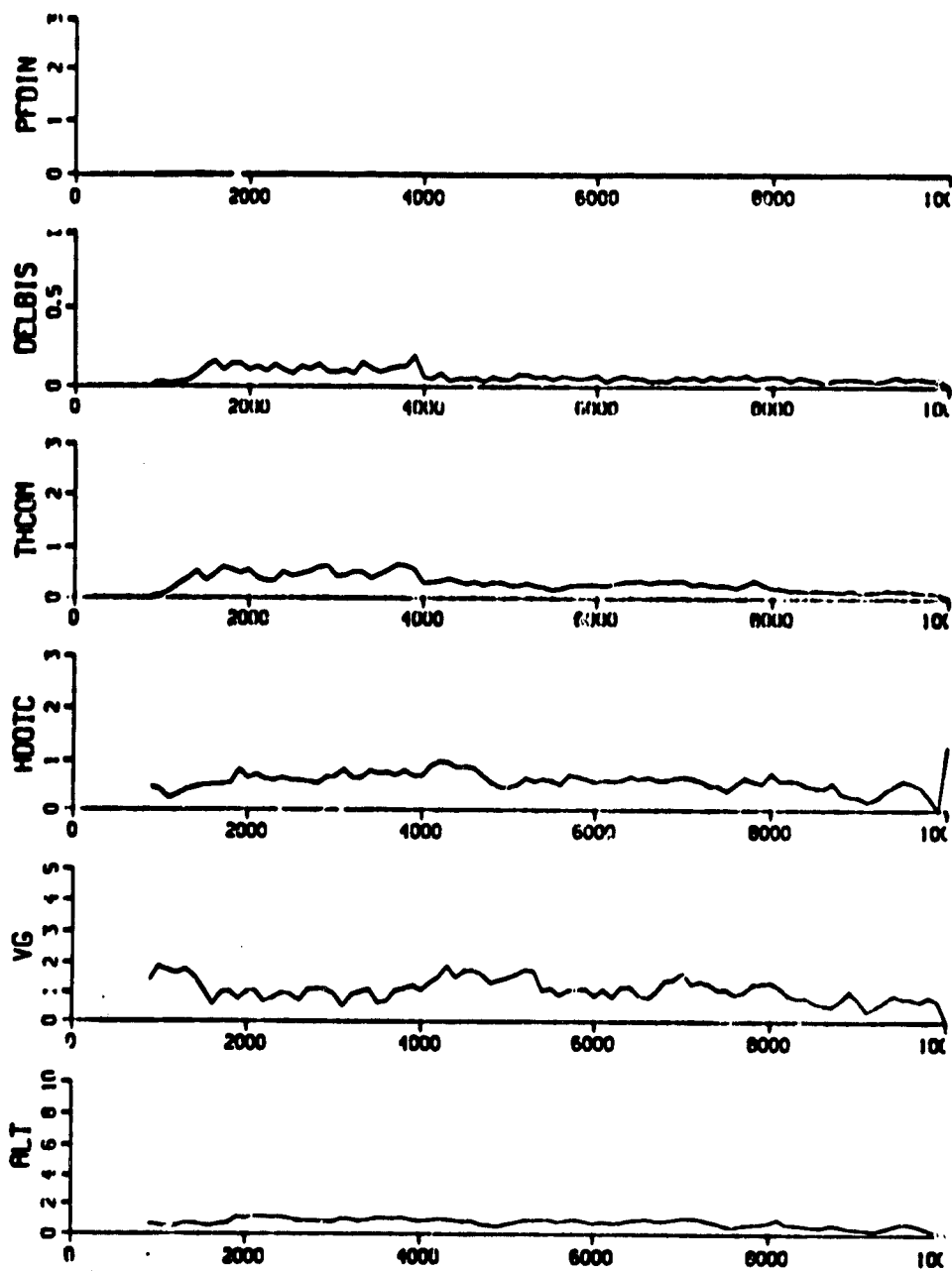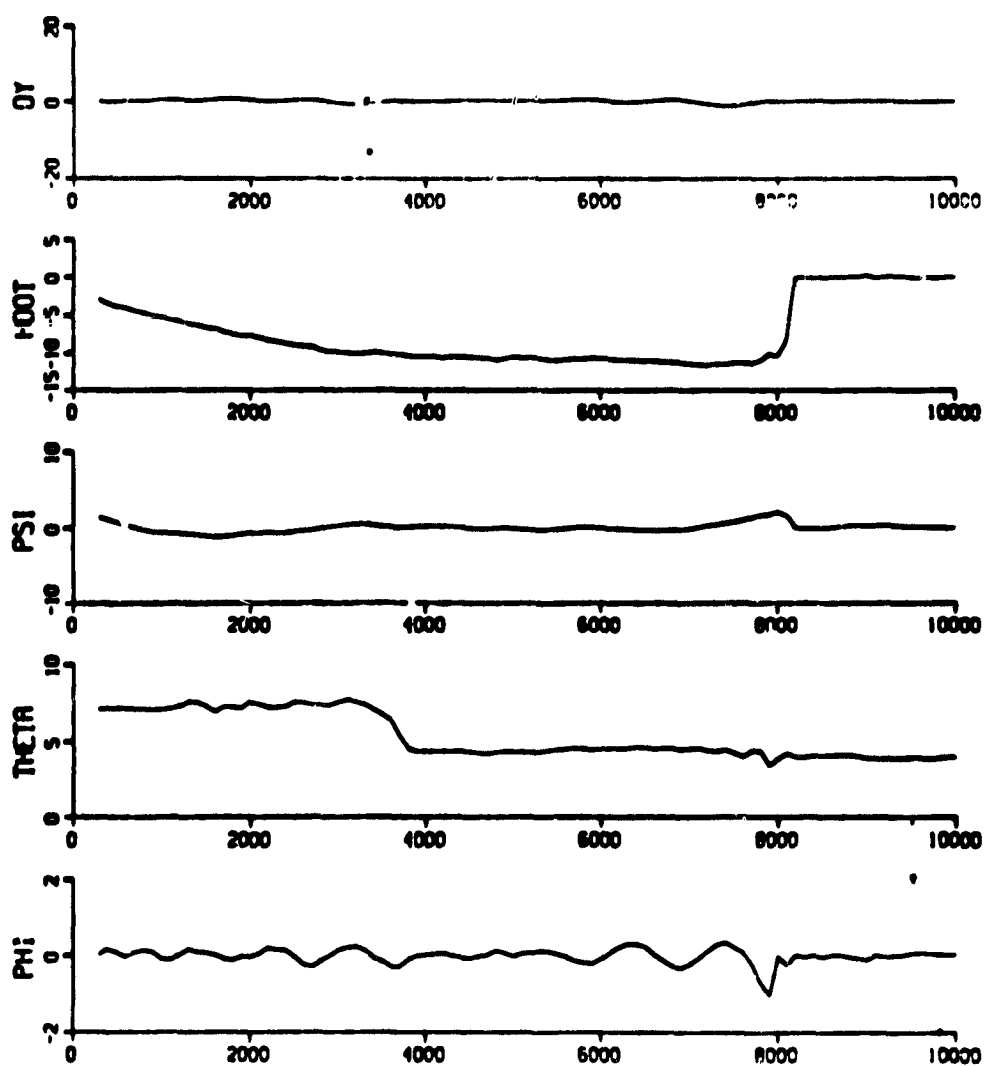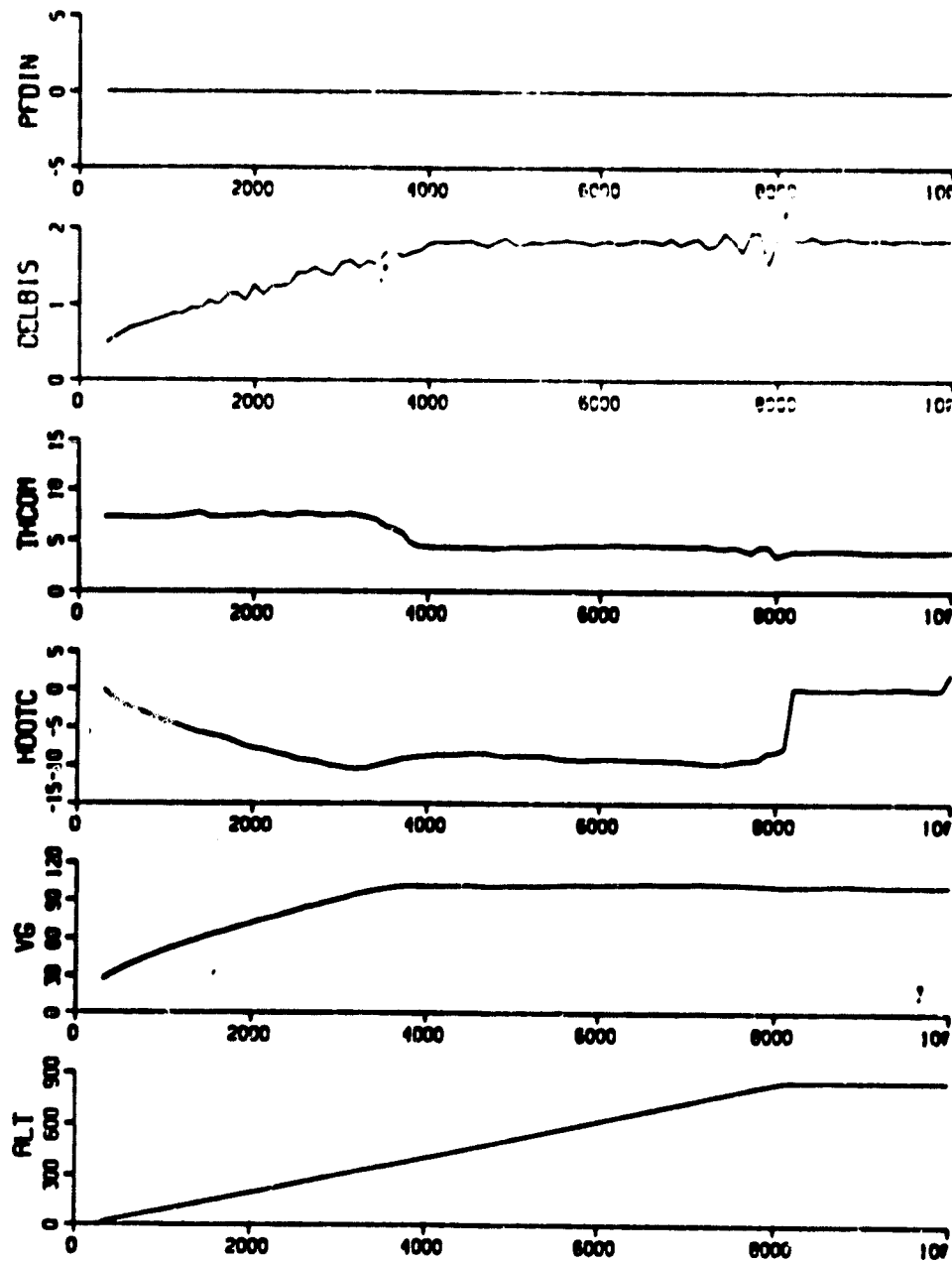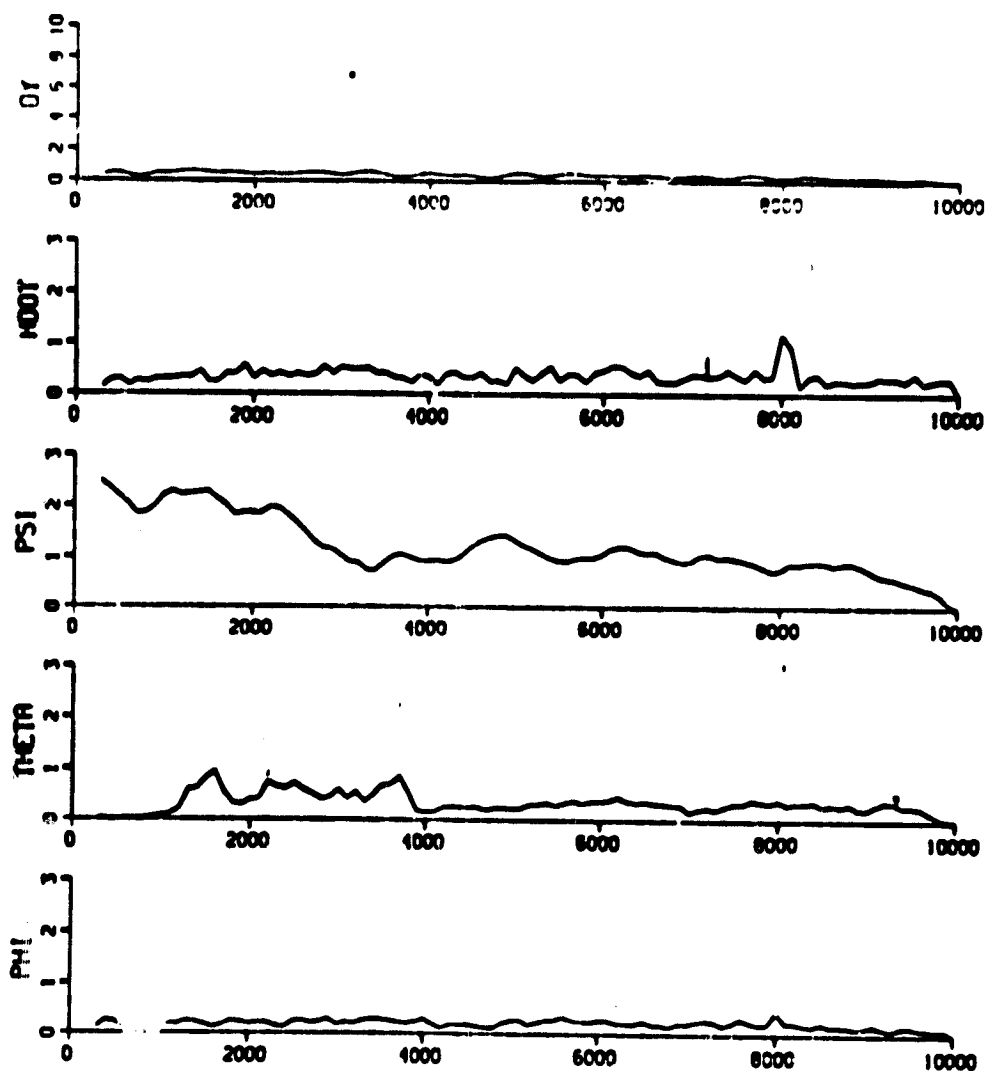
INPTCH = 5, INROLL = 10, INCOLL = 10
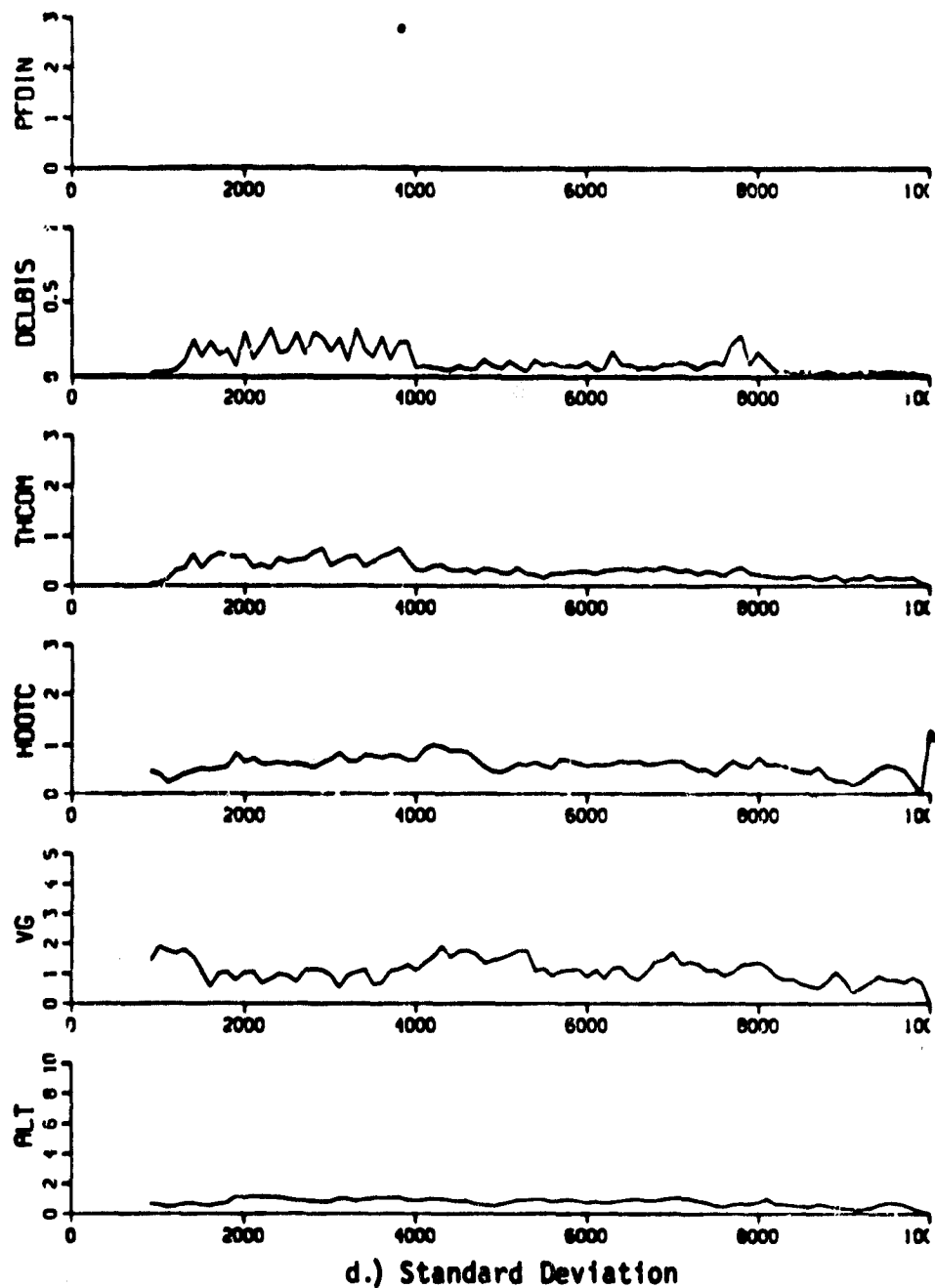

d.) Standard Deviation

Figure 26. NCC Program Simulation Results: CSS/FD/WIND/DH = 0 ft

91

involvement equally in each axis by simultaneously increasing INPTCH, INROLL and INCOLL from 1 through 10 results in early instability as seen in Figures 21-24. The relative difficulty of the individual control axes may be measured by comparison of the maximum allowable values of INPTCH, INROLL and INCOLL compatible with acceptable overall system performance. Results show that the pitch axis is the most sensitive to the degree of attention allocation and control involvement as evidenced by the rapid degradation of system performance with increasing values of INPTCH.

Additional single run (ICARLO = 1) simulations for varying values of the three parameters show that the limiting values of INPTCH, INROLL and INCOLL are 7, 15 and 20 respectively.

Eventually the values of INPTCH, INROLL and INCOLL in addition to being independent of each other may be allowed to vary with the nature of the control task or as a function of the distance to go from the hover pad. Thus, the 3 parameters could vary from relatively large values during the cruise phase towards smaller values (approaching 1) as the flight progresses through glideslope capture, deceleration and flare to hover over the prescribed landing pad. This would be compatible with the increasing difficulty or workload level of the piloting task with decreasing range from the hover pad. Eventually, the 3 parameters may be programmed to be adaptive to system performance according to some adaptive control law mimicking human adaptive response capabilities.

2.   Strategy Option ISTRAT = 2

In this option, the degree of control involvement in each axis is assumed to be directly related to the magnitude of the instantaneous errors in following the pitch, roll and vertical flight director commands (i.e., $\alpha_1 = \alpha_2 = \alpha_3 = 1$, $\beta_1 = \beta_2 = \beta_3 = 0$ in Eq. 18). The following parameter sets were simulated to illustrate the effects of varying the performance threshold levels ULIM(I), $I = 1,2,3$.

C-2

Set No.	ULIM(1) (1"=15°)	ULIM(2) (1"=66°)	ULIM(3) (1=20ft/s)
1	0.0 in	0.0 in	0.0 in
2	0.034 in	0.03 in	0.05 in
3	0.067 in	"	"
4	0.134 in	"	"

Figures 27-29 show the simulation results for set numbers 2-4 above. Set 1 results are identical to those in Figure 1 for ISTRAT = 0, INPTCH = INROLL = INCOLL = 1 as should be expected. Larger threshold values result in increasingly oscillatory behavior in the corresponding control axes. This is evidenced in Figures 27-29 which demonstrate increasing oscillatory behavior in the pitch axis as the corresponding pitch flight director threshold parameter ULIM(1) is increased from 0.0 in (equivalent to continuous control) to 0.134 in (or a deadzone of $\pm$ 2° in responding to the pitch flight director signal). Similar behavior could be elicited in the roll and vertical axes by increasing ULIM(2) and ULIM(3) threshold values.

Finally, parameters ULIM(I) could be scheduled to vary with range to go from the helipad or be made adaptive to system performance levels (e.g., instantaneous groundspeed, localizer and glideslope errors) to reflect plausible human pilot decision and control strategies.

3.   Strategy Option ISTRAT = 1

This option allows for closed loop piloted control of only one axis at a time. At any given instant the pilot must decide to control either of the pitch, roll or vertical axes or none of the three based upon some internal criterion for evaluating the individual axis urgency for attention and control. Here the pilot is assumed to compare three decision functions $\alpha(1)$ * pitch flight director signal, $\alpha(2)$ * roll flight director signal and (3) * collective flight director signal and choose the axis with the largest decision function magnitude. Simulations with various reasonable values for $\alpha(I)$, I = 1,2,3 (e.g., such that 1" pitch = 1", roll = 1" collective flight director signals which is the same as saying

93

ISTRAT = 2, ICARLO = 10,

ULIM(1) = 0.034 in (= 0.5 deg)
ULIM(2) = 0.03 in (= 2 deg)
ULIM (3) = 0.05 in (= 1 ft/s)
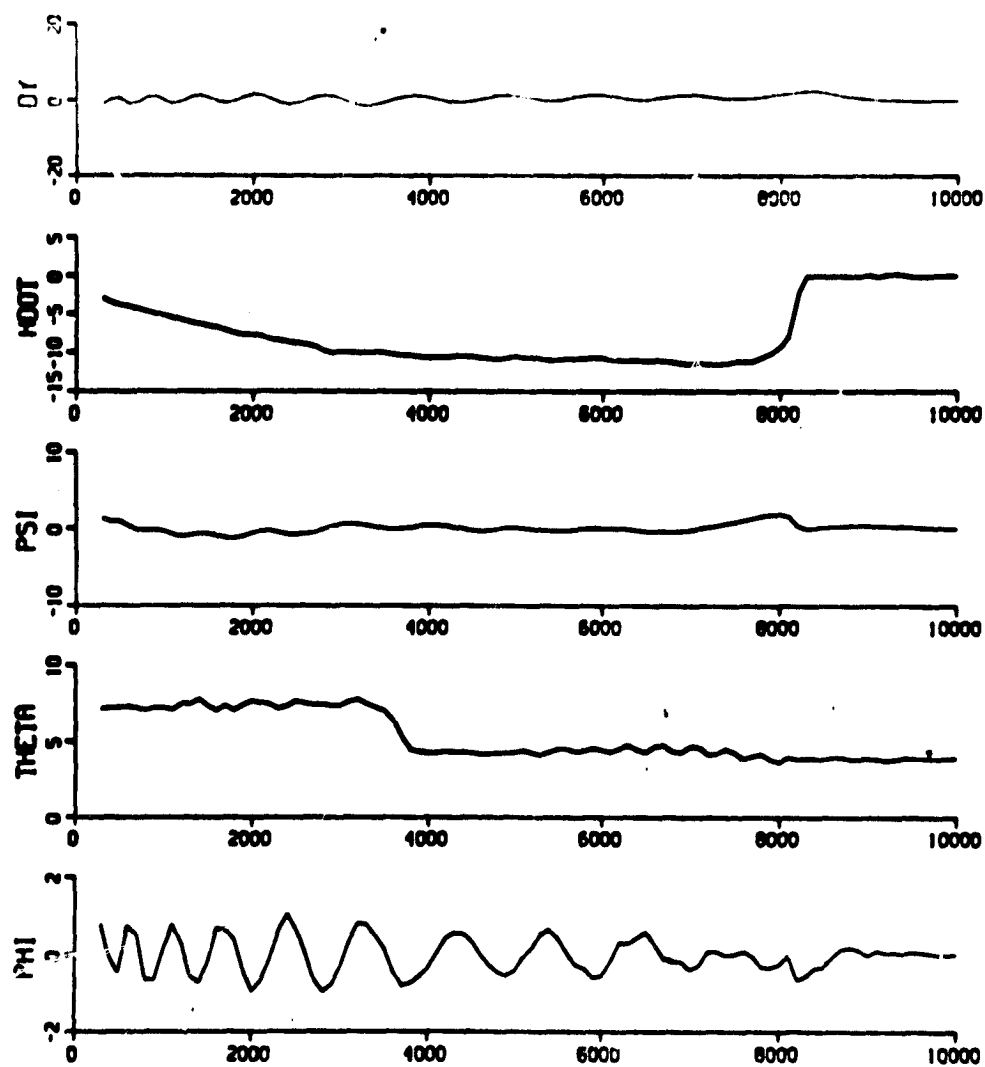
a.) Mean

Figure 27. NCC Program Simulation Results: CSS/FD/WIND/DH ≅ 0 ft

94

ISTRAT = 2, ICARLO = 10

ULIM(1) = 0.034 in (= 0.5 deg)
ULIM(2) = 0.03 in (= 2 deg)
ULIM(3) = 0.05 in (= 1 ft/s)

b.) Mean

Figure 27. NCC Program Simulation Results: CSS/FD/WIND/DH = 0 ft

95

ISTRAT = 2, ICARLO = 10

ULIM(1) = 0.034 in (= 0.5 deg)
ULIM(2) = 0.03 in (= 2 deg)
ULIM(3) = 0.05 in (= 1 ft/s)

c.) Standard Deviation

Figure 27. NCC Program Simulation Results: CSS/FD/WIND/BH = 0 ft

96

ISTRAT = 2, ICARLO = 10

ULIM(1) = 0.034 in (= 0.5 deg)
ULIM(2) = 0.03 in (= 2 deg)
ULIM(3) = 0.05 in (= 1 ft/s)

d.) Standard Deviation

Figure 27.   NCC Program Simulation Results: CSS/FD/WIND/DH = 0 ft

ISTRAT = 2, ICARLO = 10

ULIM(1) = 0.067 in (= 1 deg)
ULIM(2) = 0.03 in (= 2 deg)
ULIM(3) = 0.05 in (= 1 ft/s)

a.) Mean

Figure 28. NCC Program Simulation Results: CSS/FD/WIND/DH = 0 ft

98

Figure 28.   NCC Program Simulation Results: CSS/FD/WIND/DH = 0 ft

99

ISTRAT = 2 , ICARLO = 10

ULIM(1) = 0.067 in (= 1 deg)
ULIM(2) = 0.03 in (= 2 deg)
ULIM(3) = 0.05 in (= 1 ft/s)

c.) Standard Deviation

Figure 28. NCC Program Simulation Results: CSS/FD/WIND/DH = 0 ft

100

ISTRAT = 2, ICARLO = 10

ULIM(1) = 0.067 in (= 1 deg)
ULIM(2) = 0.03 in (= 2 deg)
ULIM(3) = 0.05 in (= 1 ft/s)

d.) Standard Deviation

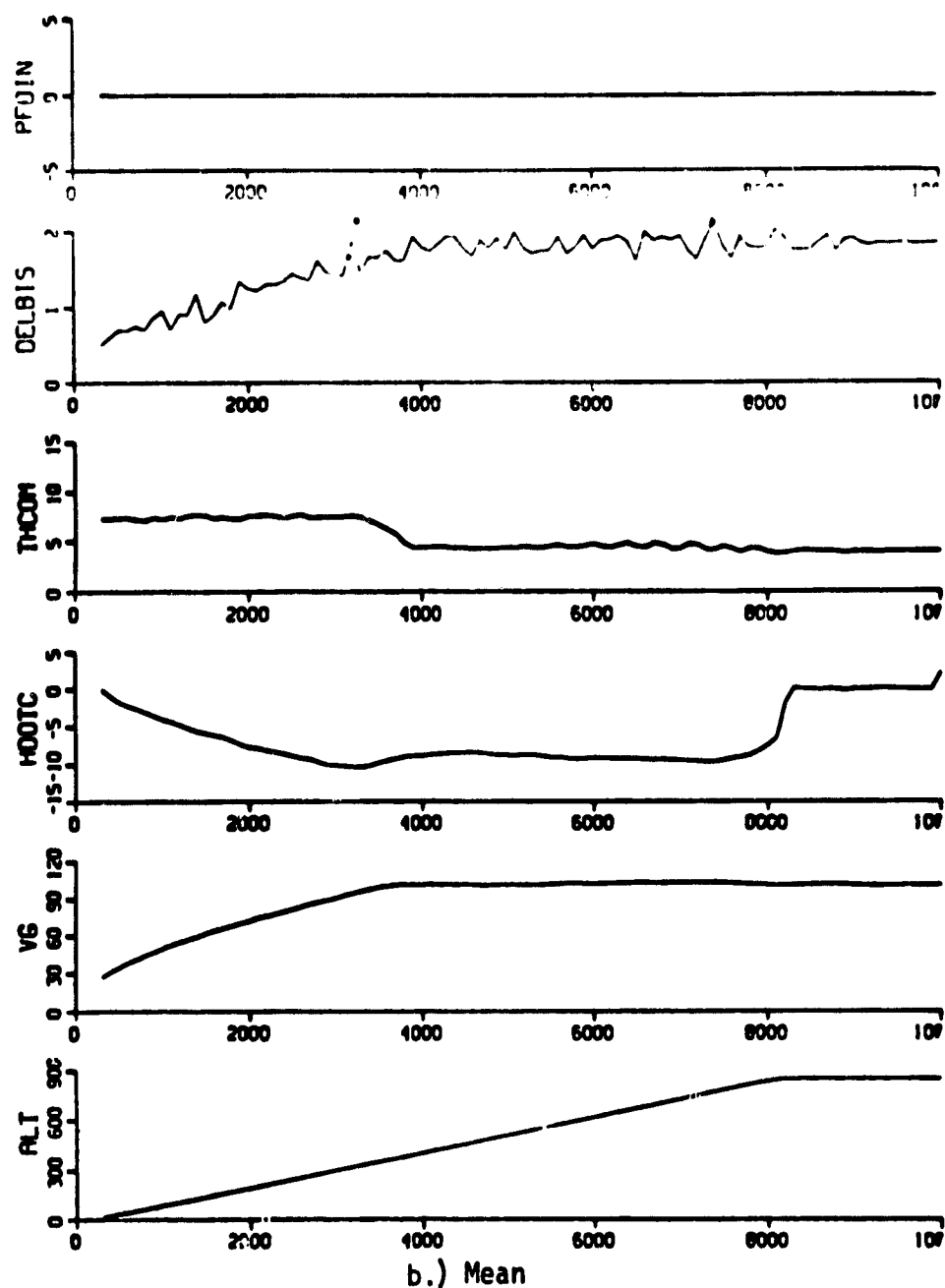Figure 28.   NCC Program Simulation Results: CSS/FD/WIND/DH = 0 ft

ISTRAT = 2, ICARLO = 10,

ULIM(1) = 0.134 in (= 2 deg)
ULIM(2) = 0.03 in (= 2 deg)
ULIM(3) = 0.05 in (= 1 ft/s)

a.) Mean

Figure 29. NCC Program Simulation Results: CSS/FD/WIND/DH = 0 ft

102

ISTRAT = 2, ICARLO = 10

ULIM(1) = 0.134 in (= 2 deg)
ULIM(2) = 0.03 in (= 2 deg)
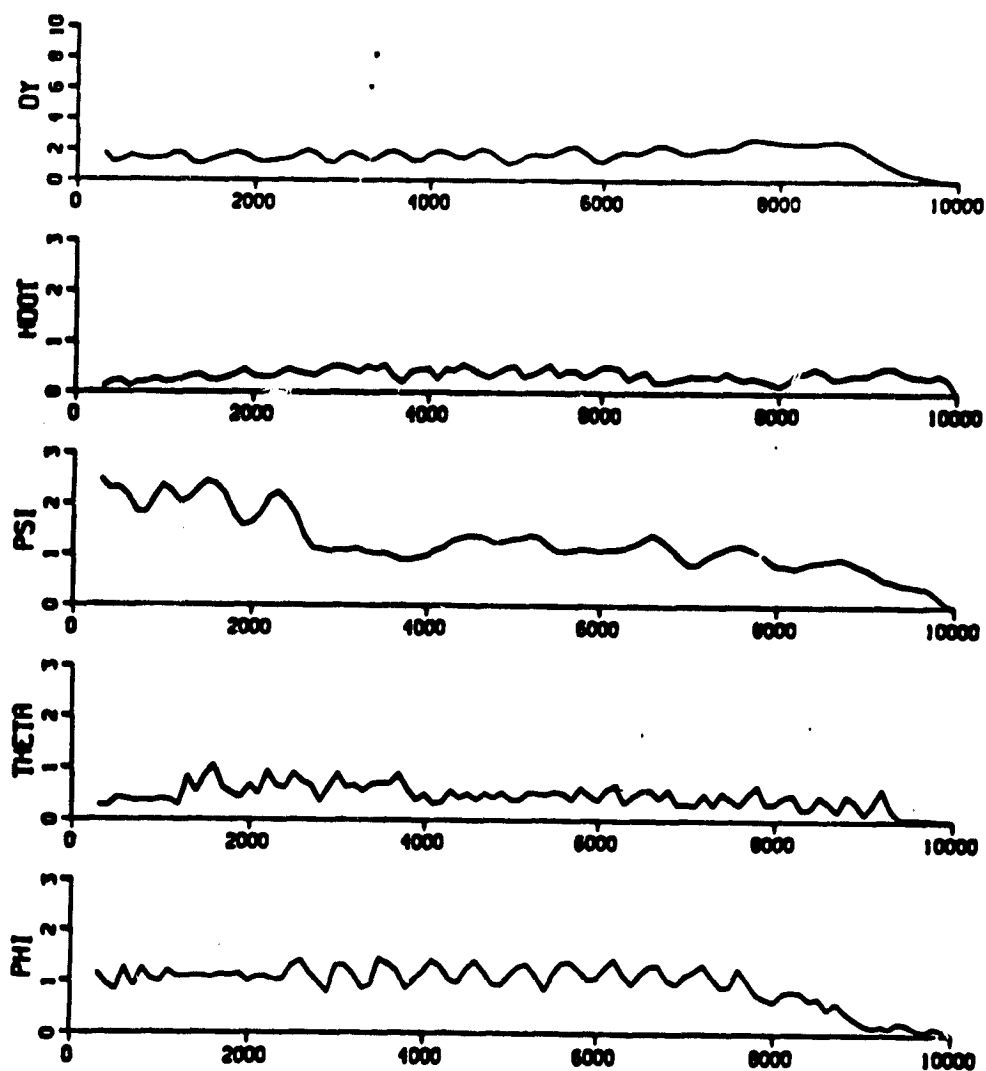ULIM(3) = 0.05 in (= 1 ft/s)

b.) Mean

Figure 29.   NCC Program Simulation Results: CSS/FD/WIND/DH = 0 ft

103

ISTRAT = 2, ICARLO = 10

ULIM(1) = 0.134 in (= 2 deg)
ULIM(2) = 0.03 in (= 2 deg)
ULIM(3) = 0.05 in (= 1 ft/s)

c.) Standard Deviation

Figure 29. NCC Program Simulation Results: CSS/FD/WIND/DH = 0 ft

104

ISTRAT = 2, ICARLO = 10,

ULIM(1) = 0.134 in (= 2 deg)
ULIM(2) = 0.03 in (= 2 deg)
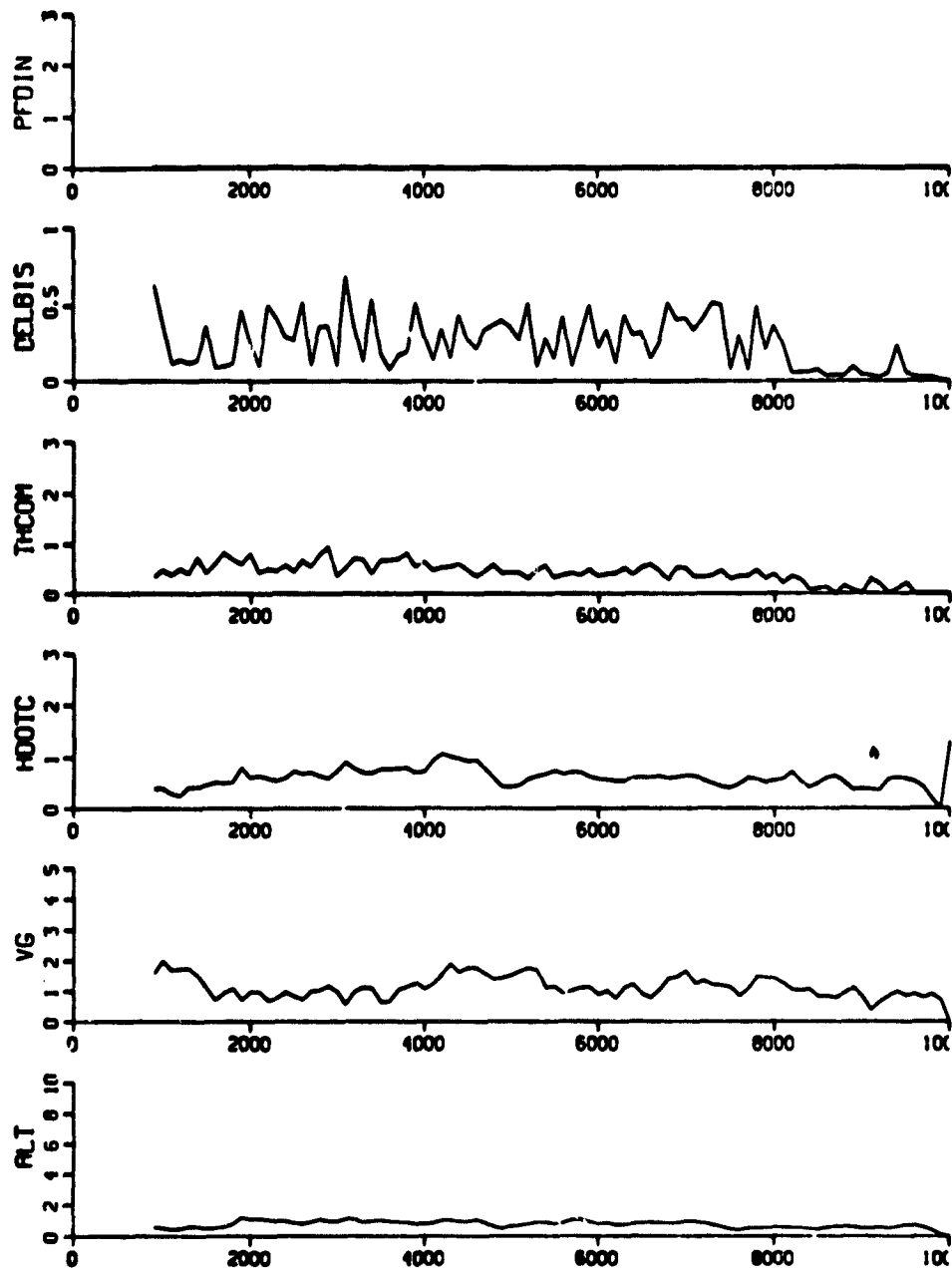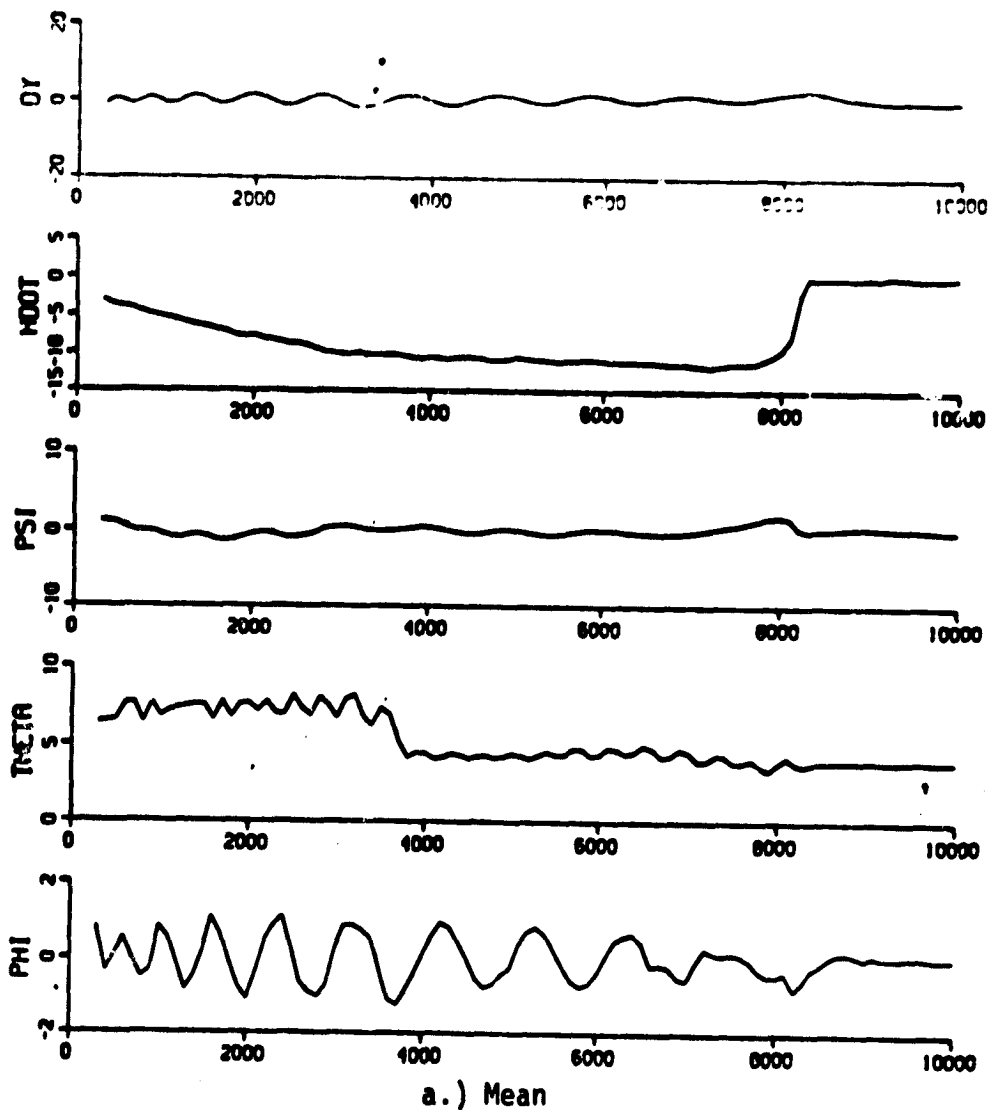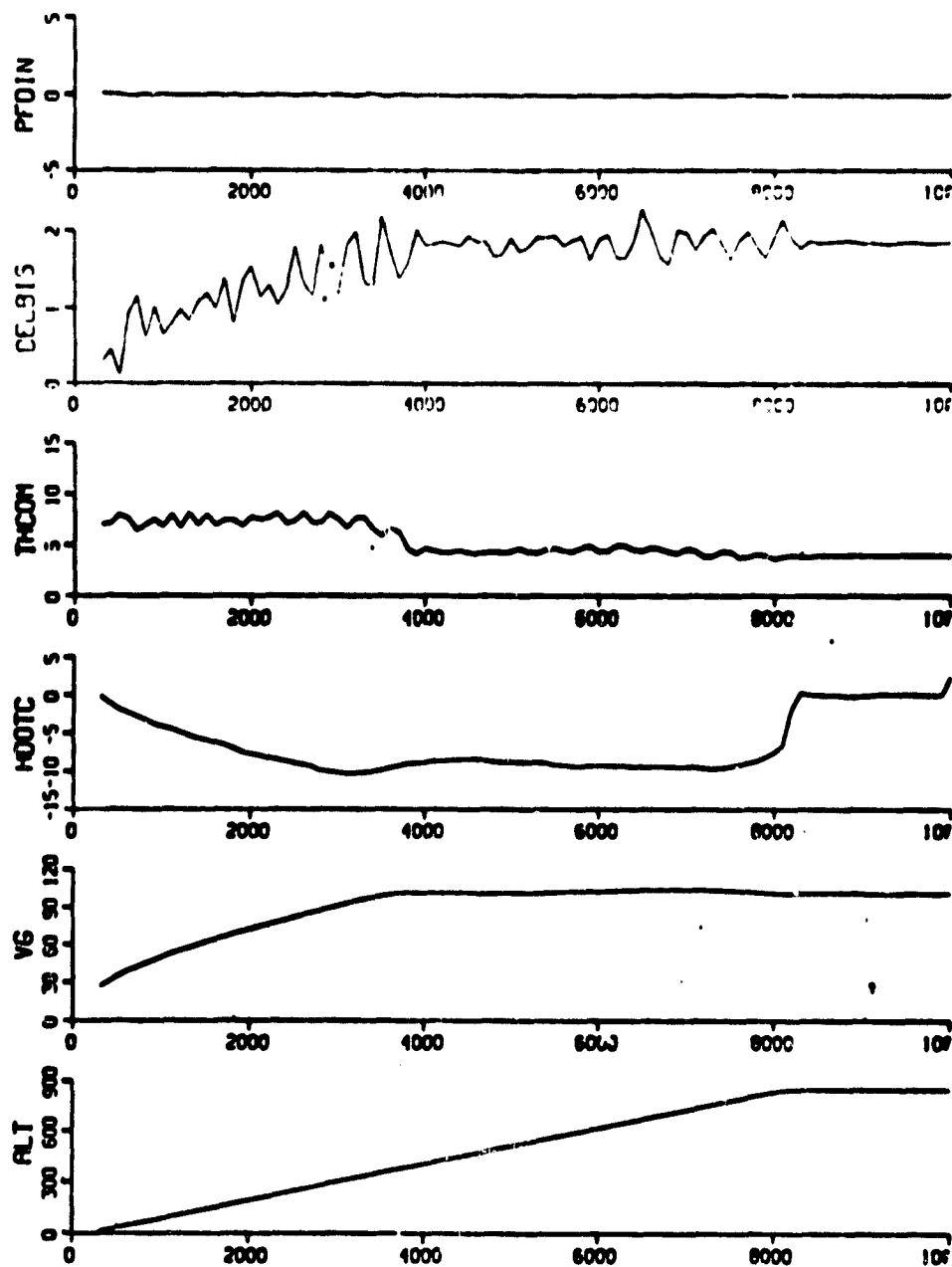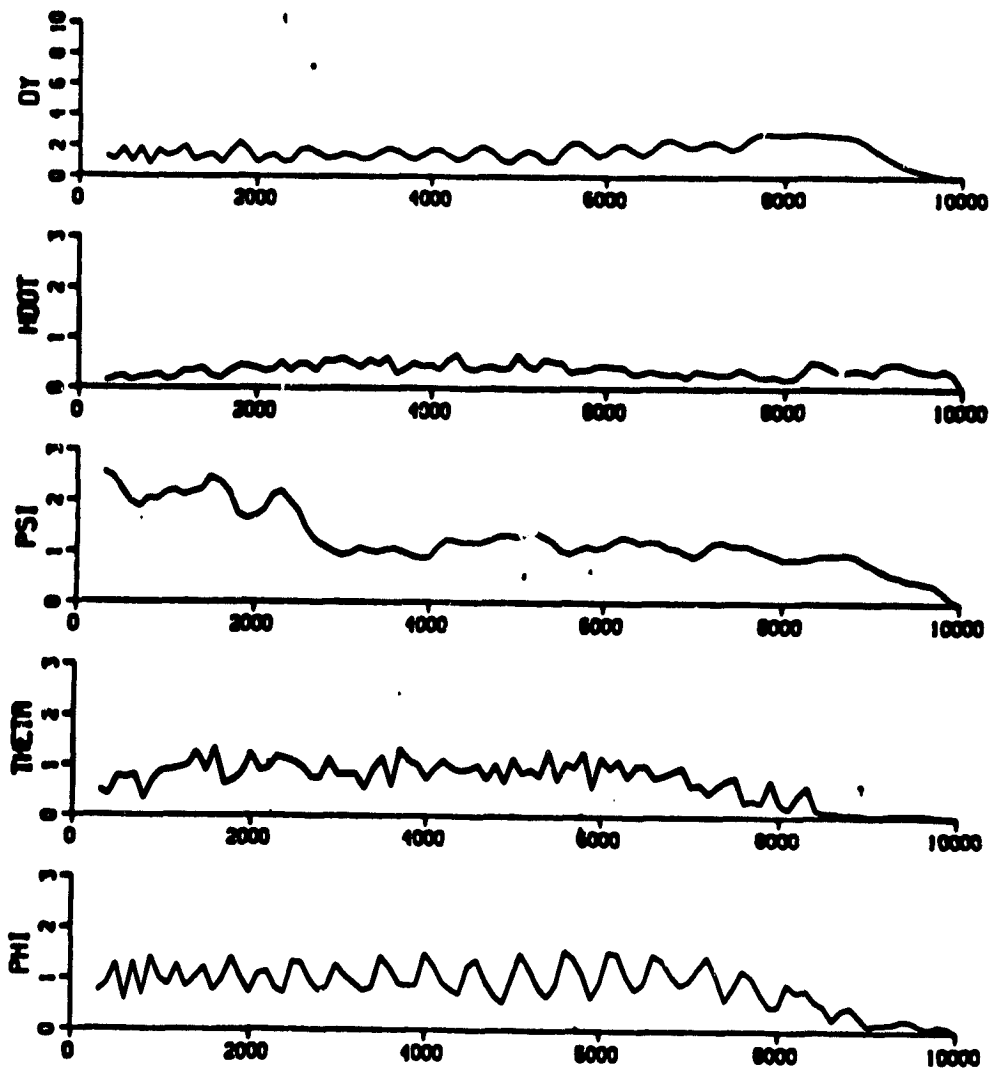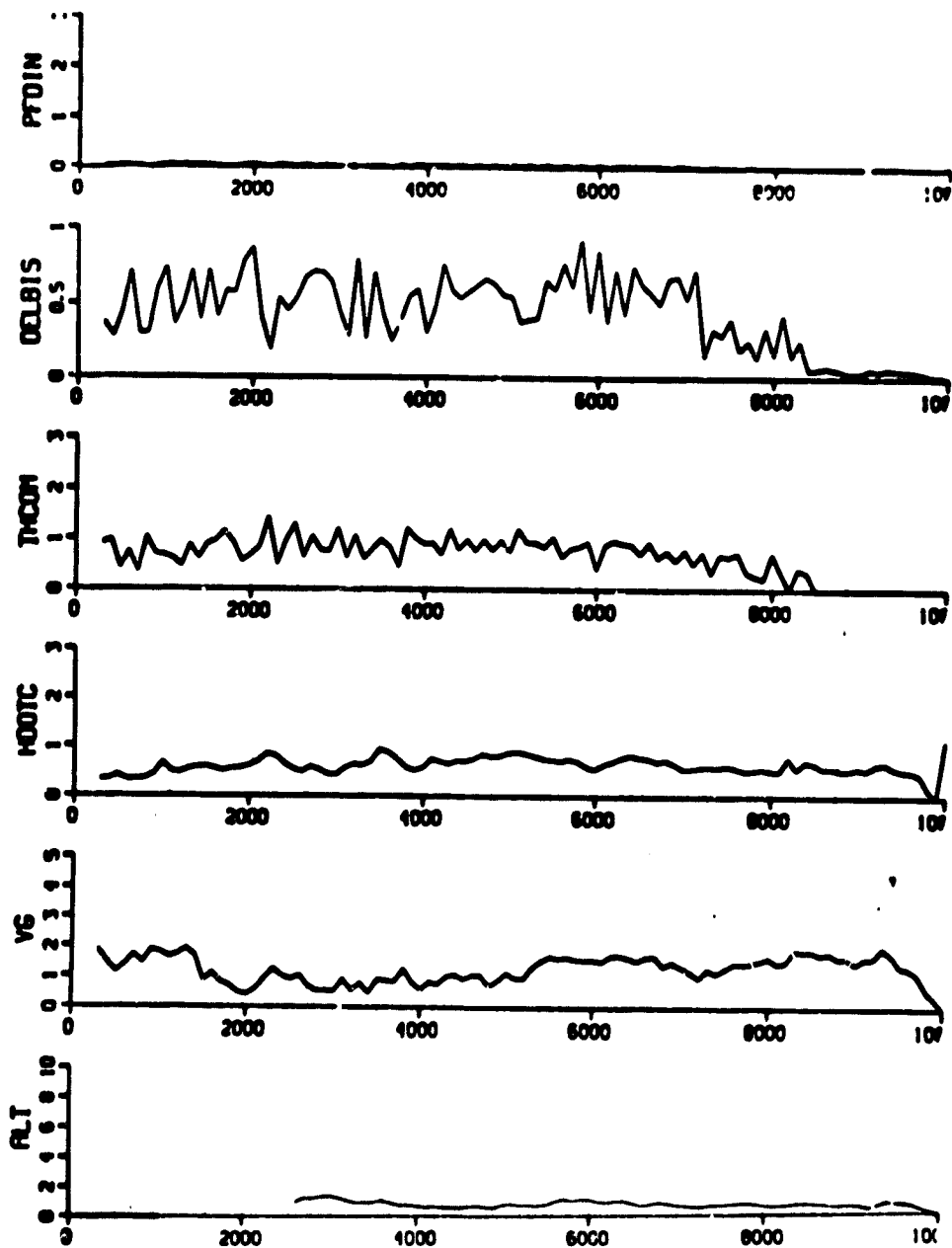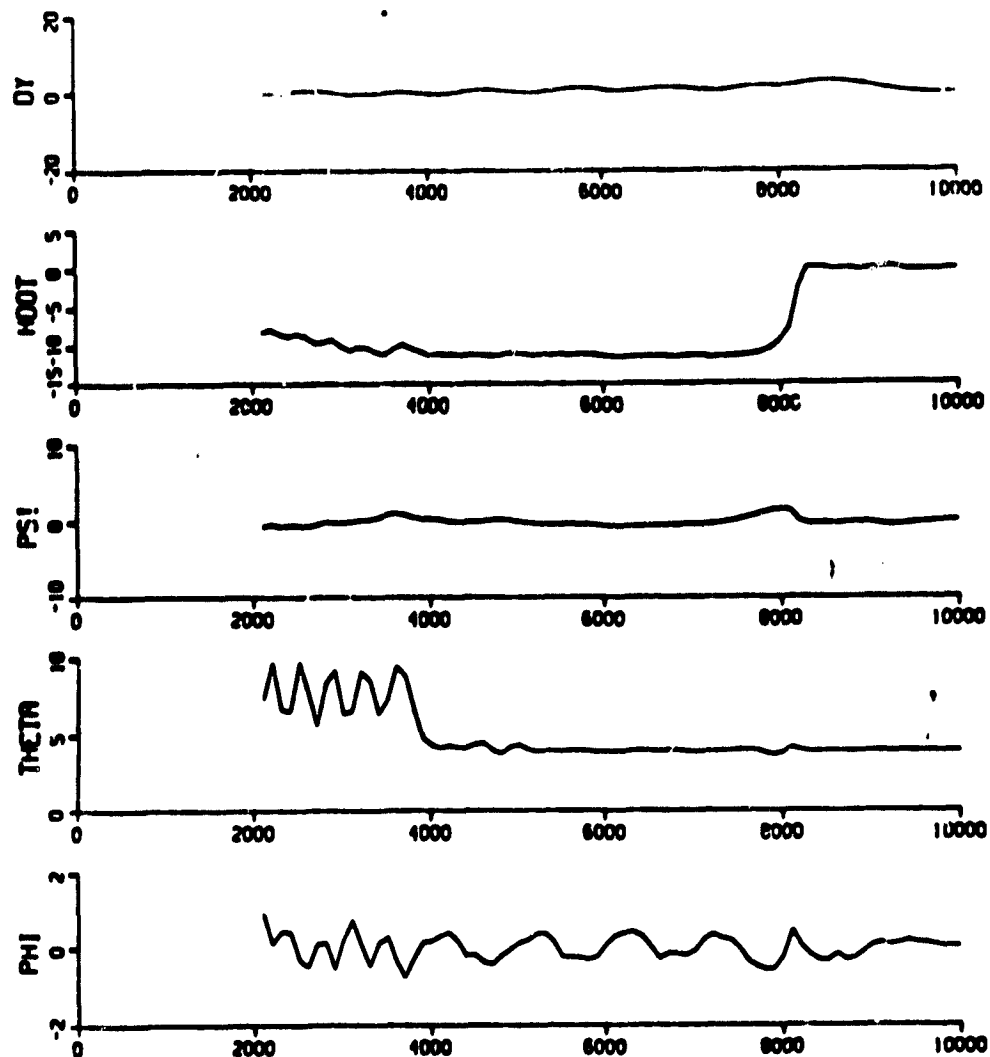ULIM(3) = 0.05 in (= 1 ft/s)

d.) Standard Deviation

Figure 29. NCC Program Simulation Results: CSS/FD/WIND/DH = 0 ft

105
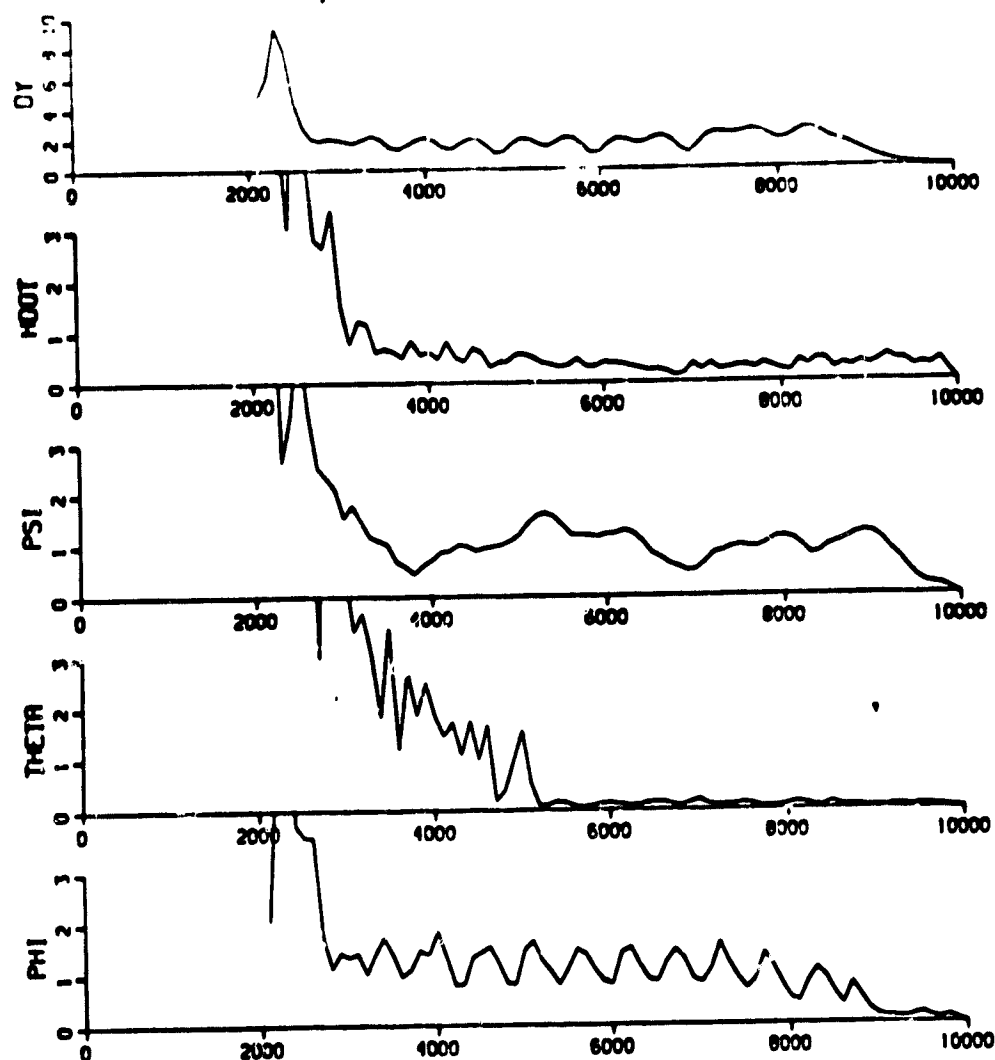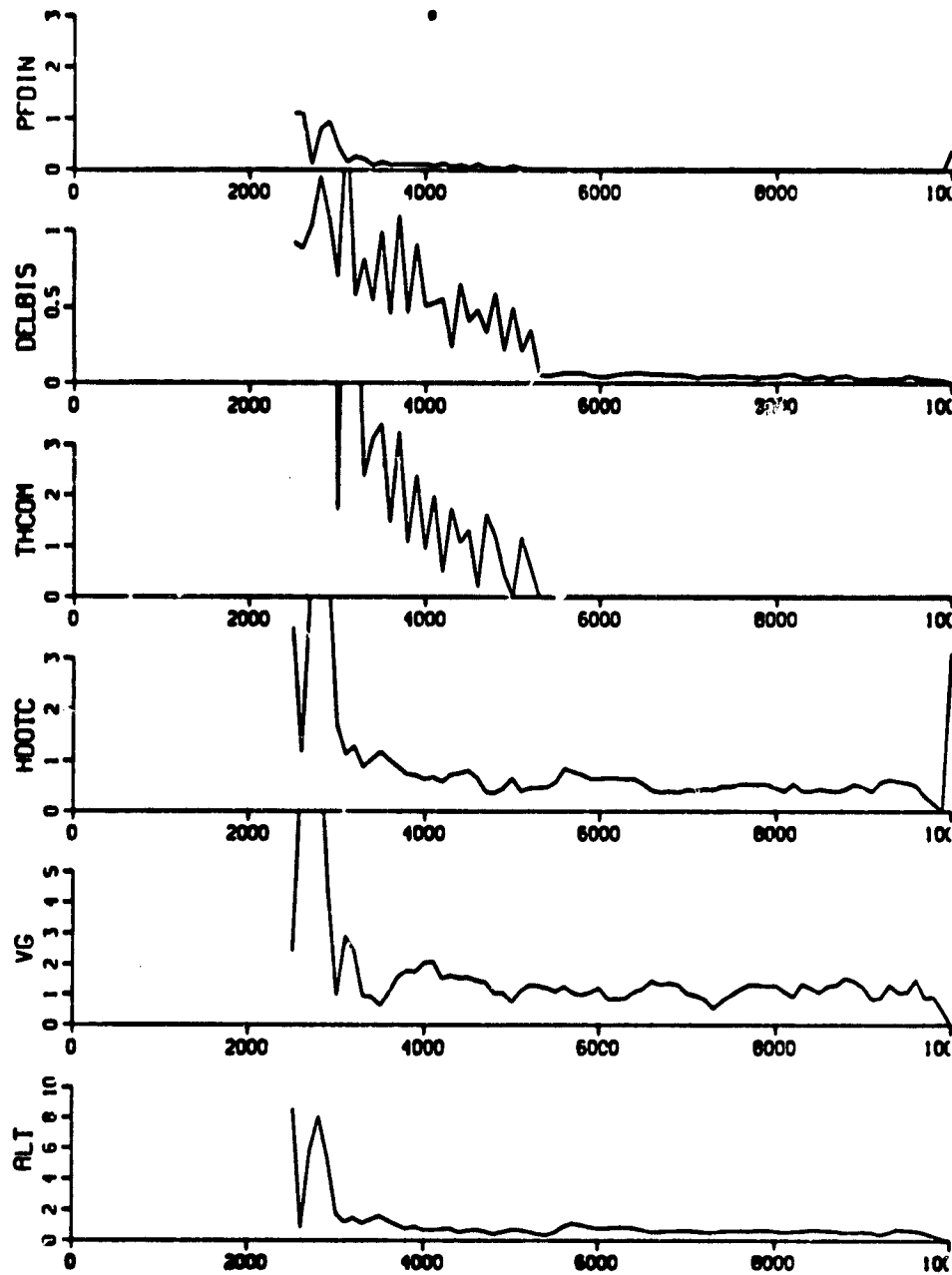
15° pitch = 66° roll = 20 ft/s collective flight director signal) were
investigated. Results show that the overall system in this mode goes
unstable in the first 30 seconds of flight. However, it would be pre-
mature to rule out this operating strategy on the basis of this limited
evaluation. Perhaps the α's need to be made adaptive to the nature of
the specific phase of the approach to hover task.

Determination of Pilot Acceptance

The results above demonstrate the feasibility of using the parameters
of a suitable pilot model as measures or metrics for relative task diffi-
culty and hence pilot workload. Thus for the option 0 strategy, the maxi-
mum permissible values for the control sampling intervals INPTCH, INROLL,
INCOLL in the pitch, roll and collective axis while maintaining acceptable
performance are shown to be 7, 15 and 20 seconds, respectively. Analysis
of this type must be carried out for the other competing configurations
to determine the maximum permissible values for INPTCH, INROLL and .)LL
for the same fixed level of acceptable system performance. These three
numbers may then be compared individually or in some aggregate form (such
as the weighted sum of the sampling frequencies) to arrive at some measure
of pilot preference or opinion rating.

More work needs to be done on the problems associated with aggregating
components of a workload vector metric into a scalar workload measure.

CONCLUDING REMARKS

A systematic approach towards the development of an analytical methodology for determining the level of pilot acceptance for a given system configuration is formulated. A general computer program (NCC) incorporating a nonlinear model for the UH-1H helicopter and a generic, homomophic, dynamic model for the human pilots information acquisition, processing and control strategy was developed.

The study points out that the weakest elements in the successful implementation of the overall approach are the particular structure of the generic pilot model and the nature of the off-line simulation scheme for evaluating pilot-aircraft system performance. Specifically, the results of this investigation show that a generic pilot model capable of describing the human information processing, decision making and control strategies peculiar to the helicopter decelerating approach to a hover task is necessary. In addition, an off-line pilot-aircraft simulation, incorporating realistic models for the aircraft and the human pilot is essential for a systematic analysis of system performance and pilot workload factors and their impact on overall level of pilot acceptance.

The UH-1H approach to a hover task is dominated by flight segments such as glide slope capture and deceleration to a hover that require explicit deterministic pilot control responses to discrete step changes in the commanded flight conditions. As a result, a pilot model with the ability to describe predominantly transient response behavior as opposed to tracking perturbations about a nominal must be considered. Thus approaches which hypothesize the partioning of the pilot response into a nominal and a perturbation control strategy are inappropriate.

Finally, the study recommends the inclusion of reasonably accurate aircraft nonlinear equations of motion in the off-line simulation, and

the use of Monte Carlo methodology for obtaining approach path dispersions (i.e., ensemble means and standard deviations) of key system variables with range (distance-to-go from the helipad) as the independent variable. Linear, time varying covariance propagation methods are not recommended for tasks, such as decelerated approach to a hover, where the dominant response is the deterministic nominal component, which must be obtained through a fully nonlinear simulation (note that the nominal response history cannot be obtained by stringing together a sequence of dynamic trim outputs).

In summary, a structured approach towards evaluating the tradeoff between system performance and pilot workload and their relationship to overall pilot acceptance as expressed by a pilot opinion rating has been outlined. Further analytical and experimental efforts aimed towards the identification of these reciprocal relationships and the development and validation of aggregated, scalar, performance and workload measures from truly multiattribute vector quantities are recommended.

REFERENCES

1. Astronautics and Aeronautics, Special Section on Civil Helicopter Outlook, Nov. 1979.

2. Moen, G.C.; Di Carlo, D.J.; and Yenni, Y R.: "A Parametric Analysis of Visual Approaches for Helicopters", NASA TN D-8275, Dec. 1976.

3. Phatak, A.V.; et al: "A Piloted Simulator Investigation of Helicopter Precision Decelerating Approaches to Hover to Determine Single-Pilot IFR (SPIFR) Requirements, 1979 AIAA Guidance and Control Conference, Boulder, Co., AIAA Paper No. 79-1886, Aug. 1979.

4. Cooper, G.E.: "Understanding and Interpreting Pilot Opinion, Aeronautical Engineering Review, Vol 16, No. 3, March 1957, pp. 47-52.

5. Cooper G.E.; and Harper, R.P., Jr.: " The Use of Pilot Rating in the Evaluation of Aircraft Handling Qualities, NASA TN D-5153, April 1969.

6. Baker, F.A., et al: "V/STOLAND Avionics System Flight Test Data on a UH-1H Helicopter, NASA TM

7. Talbot, P.D.; and Corliss, L.D.: "A Mathematical Force and Moment Model of a UH-1H Helicopter for Flight Dynamics Simulations, NASA TM-73,254; Nov. 1977.

8. Kelly, J.R. et al: "Flight Investigation of Manual and Automatic VTOL Decelerating Instrument Approaches and Landings", NASA TND-7524, July 1974.

9. Anderson, R.O.: "A New Approach to Specification and Evaluation of Flying Qualities, AFFDL TR 69-120", May 1970.

10. Teper, G.L.: " An Assessment of the 'Paper Pilot' - An Analytical Approach to the Specification and Evaluation of Flying Qualities", AFFDL TR-71=174, June 1972.

11. Levison, W.H.: "A Model Based Technique for Predicting Pilot Opinion Ratings for Large Commercial TransportsSymposium/Workshop on Flying Qualities Design Criteria", WPAFB- Ohio, Oct. 1979.

12. Levison, W.H., Elkind, J.I. and Ward, J.L.: "Studies of Multivariable Manual Control Systems: A Model for Task Interference", NASA CR-1746, May 1971.

13. Hess, R.A.: "A Method for Generating Numerical Pilot Opinion Ratings Using the Optimal Pilot Model", NASA TMX 73,101, February 1976.

14. Wanner, J.C.: "General Guidance for the Design of Manned Aerospace Vehicles", Automation on Manned Aerospace Systems, AGARD Conference Proceedings No. 114, 1973.

15. Cavalli, D.: "Discrete Time Pilot Model", Fourteenth Annual Conference on Manual Control, NASA Conf. Publication No. 2060, Nov. 1978.

16. Onstott, E.D. and Faulkner, W.H.: "Prediction, Evaluation, and Specification of Closed-Loop and Multiaxis Flying Qualities", AFFDL-TR-78-3, Feb. 1978.

17. Senders, J.W.: "The Human Operator as a Monitor and Controller of Multi-Degree of Freedom Systems", IEEE Trans. on Human Factors in Electronics, Vol. 5, No. 1., Sept. 1964.

18. Senders, J.W. et al: "An Investigation of Visual Sampling Behavior of Human Observers", NASA CR-434, April 1966.

19. Carbonnel, J.R.: "A Queuing Model of Many Instrument Visual Sampling", IEEE Trans. on Human Factors in Electronic, Vol. 7, No. 4, Dec. 1966.

20. Baron S. and Kleinman, D.L.: "The Human as an Optimal Controller and Information Processor", NASA CR-1151, Sept. 1968.
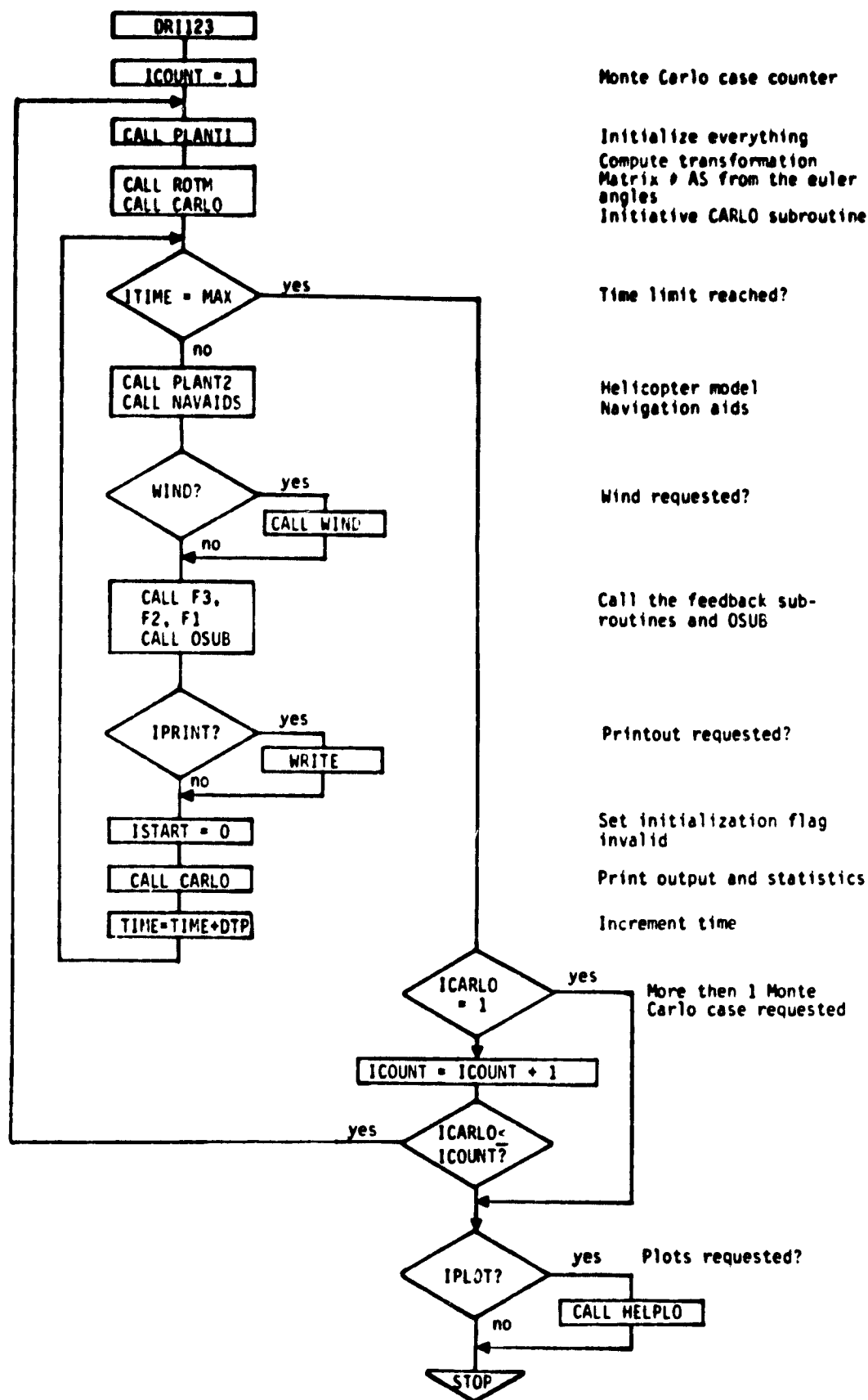
APPENDIX: Outline of NCC Program
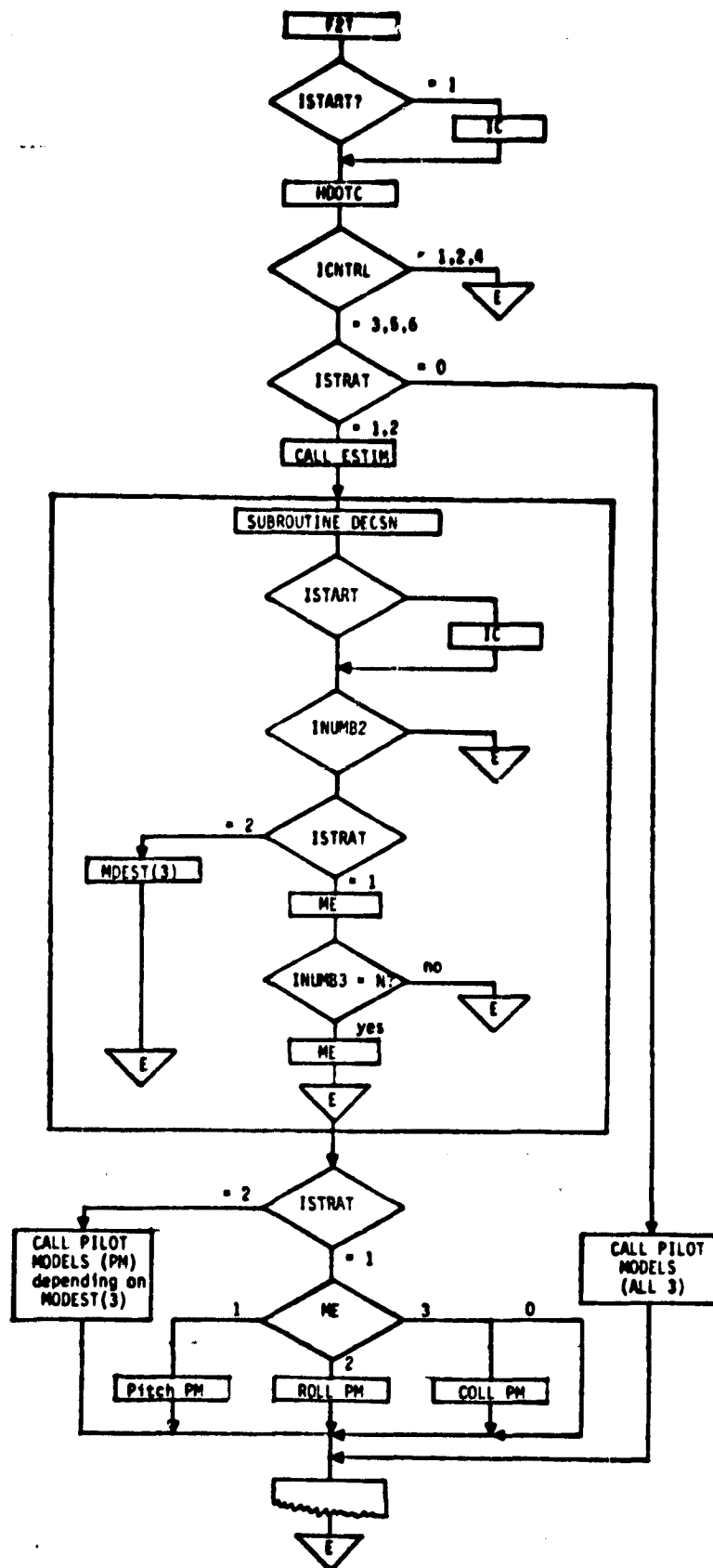
Figure A1. Flowchart for NCC

Figure A2.   Flowchart for F2

```
ZY55    .06755740 16146121

 100        SUBROUTINE F2
 200    C
 300        REAL*4 KH1,KCFD,KPH,K1,KCOL
 400        REAL*4 KTHFD,KPT,KDELTH,KC
 500        REAL*4 KPHIFD,KPPHI,KPPHI, KL
 600        REAL*4 KTHTWC,KPHIWD
 700    C
 800        DIMENSION DELP1(10),DELP2(10),DELO1(5),PDEST(3)
 900    C
1000        COMMON /F1230/ ICNTRL,PHIC,THCO4,ISTART,TIME,VG,PSIC,ISTD,ICOUNT
1100        COMMON /F1F2/ DCOL,HDOTC,DTHETI,DELPHI
1200        COMMON /F2F3/ THCCHF,PHICF
1300        COMMON /F2O/ GAMJ,HC
1400        COMMON /F2CA/ DELIN,PHIIN,DELOUT
1500        COMMON /DRIVE/ RS(3),VS(3),DVS(3),AAS(3,3),DMAA(3),DTP,FJA(3,3),
1600      •                FJA1(3,3),XLAMA,AIS,RIS,DVA(3),DDMAA(3),DTHETC,
1700      •                CELAIS,DELAIS,DTHETA,UP,VB,WP
1800        COMMON /IFDRK2/ ZCQ24,ZDQ25,ZDQ27,ZDQ32,ZDQ33,ZPQ49,ZDQ54,ZDQ55
1900        COMMON/NVAIO/ RTACR,PTACR,FMLSR,KMLSA,QMLSC,KTAISP,EULP(3)
2000      •,FSI,THETA,PHI,RPCNY
2100        COMMON /F2IC/ TCALT,KPH,BPH,APH,TDPTCH,KPT,BPT,APT,TDROLL,
2200      A KPPHI,AP,BP,IP,IREP,ISTRAT,INUMB1,INUMB2,INUMB3,INPTCH,INROLL,
2300      A INCOLL
2400        COMMON /GSTM/ XEST(3),XDEST(3)
2500    C ALTITUDE PARAMETERS
2600        DATA KCFD,KCOL,         K1, KH1/
2700      •      1.  ,7.64,        1.6,  .8  /
2800    C   DERIVATIVES DEFINED HERE:    24,  27, 28,
2900    C      29, 30, 31, 32, 33, 34,  43, 49, 50, --- 56
3000    C PITCH ATTITUDE PARAMETERS
3100        DATA KTHFD,THLIN/ .0667, 15./
3200        DATA KDELTH,TAUTH,PC  ,ZC  ,KC  /
3300      •      6.0 ,25.  ,0.  ,1.5 ,.6775/
3400    C ROLL ATTITUDE PARAMETERS
3500        DATA KPHIFD,PHIMAX / .015 ,15. /
3600        DATA KDPHI,TPHI,PL  ,7L  ,KL  /
3700      •       10.,25. ,0.,1.93,1.3817/
3800        DATA KTHTWC,KPHIWD /10., 10./
3900        DATA ALPHA /1.0/
4000    C
4100    C HEADING PARAMETERS
4200    C
4300    C ALTITUDE CONTROL
4400    C
4500        IF(ISTART .EQ. 0) GO TO 5
4600        I6 = 3
4700        IF(ICNTRL .EQ. 6) I6 = 2
4800        DELI1 = DTHETC
4900        DTHETI = 0.
5000        DELPHI = 0.
5100        DCOL = 0.
5200        DELIN = 0.
5300        DELOUT = 0.
5400        PHIIN = 0.
5500        ICOUN1 = INPTCH - 1
5600        ICOUN2 = INROLL - 1
5700        ICOUN3 = INCOLL - 1
5800    C$    PTCHWD = 0.
5900    C$    ROLLWD = 0.
6000    5 CONTINUE
6100    C  AUTOPILOT
6200        HDOTC =VG*TAN(GAMJ)+KH1*(HC+RS(3))
6300        IF(ICNTRL.EQ.3 .OR. ICNTRL.EQ.5) GO TO 8
6400        IF(ICNTRL .EQ. 6) GO TO 8
6500        RETURN
6600    C
6700    8   HDOTE = HDOTC + VS(3)
6800    C
6900        DELOUT = KCFD*HDOTE
```

Figure A3. Listing of Subroutine F2

-A3-

```
7000  C
7100        FDO32=-(2DO32+THETA1)/TAUTH
7230        THFRK=2DO32+2.*THETA
7300        DELIN=KTHFD*(THCOMF-THFRK)
7400        IF(ABS(DELIN).GT.THLIM) DELIN=THLIM*SIGN(1.,DELIN)
7530  C
7600        FCO54=-(2DO54+PHI1)/TPHI
7700        PHIIN=KPHIFD*(PHICF-2DO54-PHI)
7830        IF(ABS(PHIIN).GT.PHIMAX) PHIIN=PHIMAX*SIGN(1.,PHIIN)
7900        ICOUN1 = ICOUN1 + 1
8000        ICCUN2 = ICOUN2 + 1
8100        ICCUN3 = ICOUN3 + 1
8200        IF(ISTRAT .EQ. 0) GO TO 10
8300  C
8400        CALL ESTIM
8500  C
8600        IF(ISTRAT .EQ. 2) MF = 9
8700        CALL DECSN(MF,MDEST,16)
8800  C
8900        IF(ISTART .EQ. 1) GO TO 10
9000        WRITE(6,9601)TIME,ME,DELIN,PHIIN,DELOUT,REST,RDEST,MC,RS(1),MDEST
9100        IF(ISTRAT .EQ. 2) GO TO 9
9200        IF(ME .EQ. 0) GO TO 100
9300        IF(ME .EQ. 1) GO TO 30
9400        IF(ME .EQ. 2) GO TO 40
9500        IF(ME .EQ. 9) GO TO 10
9600  C
9700      9 CONTINUE
9800        IF(MDEST(1) .EQ. 1 .AND. INPTCH .LE. ICOUN1) CALL F2RSP1(FDO27)
9900        IF(MDEST(2) .EQ. 1 .AND. INROLL .LE. ICOUN2) CALL F2ASP1(FDO49)
10000       IF(MDEST(3) .EQ. 1 .AND. INCOLL .LE. ICOUN3) CALL F2TCP1(FDO24)
10100       GO TO 100
10200 C
10300 C    ALTITUDE CONTROL
10400 C    FLIGHT DIRECTOR
10500 C
10600    10 CONTINUE
10700       IF(IP .EQ. 1 .AND. INCOLL .LE. ICOUN3) CALL F2TCP1(FDO24)
10800       IF(IP .EQ. 2 .AND. INCOLL .LE. ICOUN3) CALL F2TCP2(FDO24)
10900       IF(ISTART .EQ. 1) GO TO 30
11000       IF(ISTRAT .EQ. 1) GO TO 100
11100 C
11200 C PITCH ATTITUDE CONTROL
11300 C
11400 C FLIGHT DIRECTOR
11500    30 CONTINUE
11600       IF(IP .EQ. 1 .AND. INPTCH .LE. ICOUN1) CALL F2RSP1(FDO27)
11700       IF(IP .EQ. 2 .AND. INPTCH .LE. ICOUN1) CALL F2HSP2(FDO27)
11800       IF(ISTART .EQ. 1) GO TO 40
11900       IF(ISTRAT .EQ. 1) GO TO 100
12000 C
12100 C ROLL ANGLE CONTROL
12200 C
12300 C FLIGHT DIRECTOR
12400 C
12500    40 CONTINUE
12600       IF(IP .EQ. 1 .AND. INROLL .LE. ICOUN2) CALL F2ASP1(FDO49)
12700       IF(IP .EQ. 2 .AND. INROLL .LE. ICOUN2) CALL F2ASP2(FDO49)
12800 C
12900   100 CONTINUE
13000       FDQ25=-K1*(2DO25-DCOL)
13100       HDOTC =KCOL*(2DQ25-DEL11)
13200 C
13300       IF(ISTRAT .EQ. 0) GO TO 150
13400       IF(ISTRAT .EQ. 2) GO TO 120
13500       IF(ME .EQ. 1) GO TO 130
13600       PTHKOD = -KTHTWD*(PTCHHD - DTHET1)
13700       DTHET1 = DTHET1 - PTCHWD
13800   130 CONTINUE
13900       IF(ME .EQ. 2) GO TO 150
```

Figure A3. (Continued)

-A4-

```
14000        ROLWOD = -KPHIWOO(ROLLWO - DELPHI)
14100        DELPHI = DELPHI - ROLLWO
14200        GO TO 150
14300    120 CONTINUE
14400        IF(MDEST(1) .EQ. 1) GO TO 125
14500 CS     PTHWOD = -KTHTWO*(PTCHWO - DTHET1)
14600 CS     DTHET1 = DTHET1 - PTCHWO
14700        DTHET1 = ALPHA*DTHET1
14800    125 CONTINUE
14900        IF(MDEST(2) .EQ. 1) GO TO 150
15000 CS     ROLWOD = -KPHIWOO(ROLLWO - DELPHI)
15100 CS     DELPHI = DELPHI - ROLLWO
15200        DELPHI = ALPHA*DELPHI
15300    150 CONTINUE
15400        FDO33=-P(*ZDO33+(ZL-P_)*KC*DTHET1
15500        DTHET2=ZDO33*KC*DTHET1
15600C       THCCW = KDELTHO*DTHET2
15700 C
15800        FDO55=-PL*ZDO55+(ZL-PL)*KL*DELPHI
15900        A9=ZDO55*KL*DELPHI
16000        PHIC = A9*KDPHI
16100        IF(INPTCH .EQ. ICOUN1) ICOUN1 = 0
16200        IF(INROLL .EQ. ICCUN2) ICOUN2 = 0
16300        IF(INCOLL .EQ. ICOUN3) ICOUN3 = 0
16400 C
16500        IF(ISTART .EQ.1) GO TO 200
16600        ZDO24 = ZDO24 + .5*(PFDO24 + FDO24)*DTP
16700        ZDO25 = ZDO25 + .5*(PFDO25 + FDO25)*DTP
16800        ZDO27 = ZDO27 + .5*(PFDO27 + FDO27)*DTP
16900        ZDO32 = ZDO32 + .5*(PFDO32 + FDO32)*DTP
17000        ZDO33 = ZDO33 + .5*(PFDO33 + FDO33)*DTP
17100        ZDO49 = ZDO49 + .5*(PFDO49 + FDO49)*DTP
17200        ZDO54 = ZDO54 + .5*(PFDO54 + FDO54)*DTP
17300        ZDO55 = ZDO55 + .5*(PFDO55 + FDO55)*DTP
17400        IF(ISTRAT .EQ. 0) GO TO 200
17500        IF(ISTRAT .EQ. 2) GO TO 185
17600        IF(ME .EQ. 1) GO TO 175
17700        PTCHWO = PTCHWO + .5*(PPTCHW + PTHWOD)*DTP
17800    175 CONTINUE
17900        IF(ME .EQ. 2) GO TO 200
18000        RCLLWO = ROLLWO + .5*(PROLLW + ROLWOD)*DTP
18100        GO TO 200
18200    185 CONTINUE
18300        IF(MDEST(1) .EQ. 1) GO TO 190
18400 CS     PTCHWO = PTCHWO + .5*(PPTCHW + PTHWOD)*DTP
18500    190 CONTINUE
18600        IF(MDEST(2) .EQ. 1) GO TO 200
18700 CS     RCLLWO = ROLLWO + .5*(PROLLW + ROLWOD)*DTP
18800    200 CONTINUE
18900        PFDO24 = FDO24
19000        PFDO25 = FDO25
19100        PFDO27 = FDO27
19200        PFDO32 = FDO32
19300        PFDO33 = FDO33
19400        PFDO49 = FDO49
19500        PFDO54 = FDO54
19600        PFDO55 = FDO55
19700        IF(ISTRAT .EQ. 0) RETURN
19800        PPTCHW = PTHWOD
19900        PROLLW = RCLWOD
20000        RETURN
20100    995 FORMAT(1H ,F5.1,12,6F10.5,7H XDEST=,3FC.3,2F10.2,3I3)
20200        END
```

Figure A3. (Concluded)

-A5-

```
  100        SUBROUTINE DECSN(MF,MDEST,IC)
  200        DIMENSION U1(3),ALPHA(3),A.TA(3),MDEST(3),ULIM(3)
  300        COMMON /BGS*N/ XEST(3),XDEST(3)
  400        COMMON /F1230/ ICNTRL,PHIC,THCOM,ISTART,TIME,VG,PSIC,ISTO,ICCUNT
  500        COMMON /F212C/ VLALY,KPM,HPM,APM,YDATCH,KDT,BPT,APT,TUMELL,
  600       A KPPHI,AP,PP,IP,IPFM,ISTRAT,INUMB1,INUMB2,INUMB3,INPTCH,INEXLL,
  700       A INCELL
  800        DATA IREAD /0/
  900        IF(ISTART .EQ. 0) GO TO 10
 1000        IF(IREAD .EQ. 1) GO TO 5
 1100        READ(5,100)(ALPHA(I),I=1,3),(ULIM(I),I=1,3)
 1200        IREAD = 1
 1300      5 CONTINUE
 1400        WRITE(6,200)(ALPHA(I),I=1,3),(ULIM(I),I=1,3)
 1500        BETA(1) = 0.
 1600        BETA(2) = 0.
 1700        BETA(3) = 0.
 1800        ICOUN2 = INUMB2 - 1
 1900        ICOUN3 = INUMB3 - 1
 2000        IPREVS = 0
 2100     10 CONTINUE
 2200        UMAX = 0.0
 2300        ICOUN2 = ICOUN2 + 1
 2400        IF(ICOUN2 .LT. INUMB2) RETURN
 2500        ICOUN2 = 0
 2600        ITEMP = 0
 2700        DO 30 I=1,16
 2800        U1(I)=ABS(ALPHA(I)*ABS(YEST(I))+BETA(I)*AMODI(I.,YEST(I))*XDEST(I))
 2900        IF(U1(I) .LT. UMAX) GO TO 20
 3000        UMAX = U1(I)
 3100        ITEMP = I
 3200     20 CONTINUE
 3300     30 CONTINUE
 3400        IF(MF .EQ. 5) GO TO 60
 3500        IF(ITEMP .EQ. IPREVS) GO TO 40
 3600        ICOUN3 = 0
 3700        MF = ITEMP
 3800        IPREVS = ITEMP
 3900        RETURN
 4000     40 CONTINUE
 4100        ICOUN3 = ICOUN3 + 1
 4200        IF(ICOUN3 .LT. INUMB3) RETURN
 4300        ICOUN3 = 0
 4400        UMAX = 0.0
 4500        DO 50 I=1,16
 4600        IF(I .EQ. ITEMP) GO TO 50
 4700        IF(U1(I) .LT. UMAX) GO TO 50
 4800        UMAX = U1(I)
 4900        MF = I
 5000     50 CONTINUE
 5100        IPREVS = MF
 5200        RETURN
 5300     60 CONTINUE
 5400        DO 70 I=1,16
 5500        MDEST(I) = 0
 5600        IF(U1(I) .GE. ULIM(I)) MDEST(I) = 1
 5700     70 CONTINUE
 5800        RETURN
 5900    100 FORMAT(6F10.3)
 6000    200 FORMAT(1X,8HALPHA'S=,3F10.3,7HULIM'S=,3F10.3)
 6100        END
```

Figure A4.   Listing of Subroutine DECSN